Doctoral Dissertation

Multi-Agent Routing Schemes Based on Travel Risk Information in Ordinary or Emergency Situations

Takanori Hara
Program of Information Science and Engineering
Graduate School of Science and Technology
Nara Institute of Science and Technology

Supervisor: Professor Shoji Kasahara
Large-Scale Systems Management Lab. (Division of Information Science)

Submitted on March 17, 2021

A Doctoral Dissertation
submitted to Graduate School of Science and Technology,
Nara Institute of Science and Technology
in partial fulfillment of the requirements for the degree of
Doctor of Engineering

Takanori Hara

Thesis Committee:

Professor Shoji Kasahara
(Supervisor, Division of Information Science)
Professor Keiichi Yasumoto
(Co-supervisor, Division of Information Science)
Associate Professor Masahiro Sasabe
(Co-supervisor, Division of Information Science)

Multi-Agent Routing Schemes Based on Travel Risk Information in Ordinary or Emergency Situations*

Takanori Hara

Abstract

With the proliferation of navigation systems and smartphones, navigation services have infiltrated various aspects of our daily life. They can provide users with not only travel routes from their current locations to destinations but also travel risk information (e.g., travel time, traffic congestion, and road conditions). In this thesis, we focus on how the travel risk information affects user behavior in ordinary or emergency situations. In ordinary situations, we consider the travel congestion caused by individual selfish routing. On the other hand, as for emergency situations, we consider the travel risk of encounters with roads blocked by collapsed buildings under disaster situations (e.g., earthquakes). To tackle these issues, we address multi-agent routing schemes leveraging the travel risk information to achieve the optimal crowd guidance under ordinary and emergency situations, respectively. We first propose selfish yet optimal routing for ordinary situations, which is inspired by Nudge theory and achieves social optimum even under the rational decision making of individuals by internalizing the marginal cost into their perceiving information. Through numerical results, we show that (1) the selfish yet optimal routing exhibits almost the same performance as the optimal routing. (2) the selfish yet optimal routing decreases the individual travel time of 82% (resp. 67%) users compared with the notification of the actual travel information in case of the grid-like network (resp. local-level real road network in Nagoya city, Japan). The selfish yet optimal routing assumes that the roads in a

*Doctoral Dissertation, Graduate School of Science and Technology, Nara Institute of Science and Technology, March 17, 2021.

selected route are simultaneously and constantly used by the corresponding agent, which is the same assumption of conventional congestion game. Since the roads in the selected route tend to be sequentially used by the agent, we further propose multi-agent distributed route selection considering such time-varying road usage among agents under the ordinary situations. Through simulation results, we demonstrate that the proposed scheme can improve the actual travel time by 5.1% compared with the existing scheme while keeping the exponential convergence property. Next, focusing on the evacuation under a large-scale disaster, we further propose two kinds of schemes: 1) a geographical risk analysis based path selection scheme for the existing automatic evacuation guidance and 2) a capacitated refuge assignment scheme to achieve the speedy and reliable evacuation. Through simulation experiments using the local-level real road network in Nagoya city, Japan, we show that 1) the path selection scheme can improve the evacuation safety while keeping the evacuation speediness compared with the shortest path selection and 2) the refuge assignment scheme can improve the average route reliability by 13.6% while suppressing the increase of the average route length by 7.3% and satisfying the refuge capacity constraints, compared with the distance-based refuge assignment scheme.

Keywords:

Multi-agent routing, travel risk information, selfish yet optimal routing, evacuation guidance, capacitated refuge assignment, ordinary and emergency situation.

Contents

List of Figures

List of Tables

Chapter 1

Introduction

1.1. Background

Thanks to the proliferation of information communication technology (ICT) and communication infrastructures (e.g., 5G networks), intelligent transportation systems (ITSs) (e.g., navigation services), can collect past and current traffic information from users' devices (e.g., smartphones and vehicle navigation systems) and provide them with useful travel information to achieve comfortable travel by mitigating various types of travel risks (e.g., undesirable traffic congestion and encounters with accidents) [4, 5].

The travel information provided to users can be categorized into the following three types of information: experiential information (EI), descriptive information (DI), and prescriptive information (PI) [6–9]. EI is the knowledge that users acquired from his/her own experience during the past decision. DI presents the information about the traffic condition provided by the system either before or during the travel. PI is the information for direct suggestion and guidance (e.g., a recommended route), which is also provided by the system. To manage the road network appropriately, the system should provide users with appropriate traffic information by considering how the provided traffic information will affect the decision making of individuals.

The travel risk will also change depending on situations. In this thesis, we focus on ordinary situations and emergency situations. In the ordinary situations, the travel risk includes traffic accidents and/or road congestion caused by

individuals' selfish routing [10]. On the other hand, in the emergency situations (e.g., large scale disasters), the travel risk could be encounters with roads blocked by collapsed buildings as well as the road congestion caused by individuals' selfish behavior [10–12]. Such travel risk can be mitigated by notifying users of travel risk information, which can be categorized into two kinds of information, i.e., reactive information and proactive information [13]. The reactive travel risk information will be dynamically acquired from environments (e.g., traffic congestion and road states) while the proactive travel risk information is statistical or empirical data (e.g., probability that a road would be blocked under disaster situations), which are computed/analyzed in advance under certain assumptions. Since it is hard for the proactive information to consider all possible situations in advance, the reactive information can compensate for the mismatch between the assumptions and actual situations.

With the proliferation of navigation systems and smartphones, most people can enjoy navigation services (e.g., vehicle navigation systems and Google maps [14]), which are one of the fundamental services of ITSs [15–19]. Given the user request, the navigation service should provide the user with the appropriate route and/or the travel risk information according to the context. In this thesis, we focus on how the travel risk information affects the individual route selection from the viewpoint of travel time and route reliability in different contexts (i.e., ordinary situations and emergency ones).

1.2. Contribution

In this thesis, we propose multi-agent routing schemes leveraging both proactive and reactive travel risk information to achieve the optimal crowd guidance under the ordinary and emergency situations, respectively. Fig. 1.1 illustrates the overview of proposed schemes in terms of the information type and the situations. In case of the ordinary situations, we first propose *selfish yet optimal routing* inspired by Nudge theory [20, 21], which can achieve social optimum even under the rational decision making of individuals by internalizing the marginal cost into the travel risk information. This approach relies on the existing distributed route selection algorithm based on congestion game [22], which implicitly assumes that

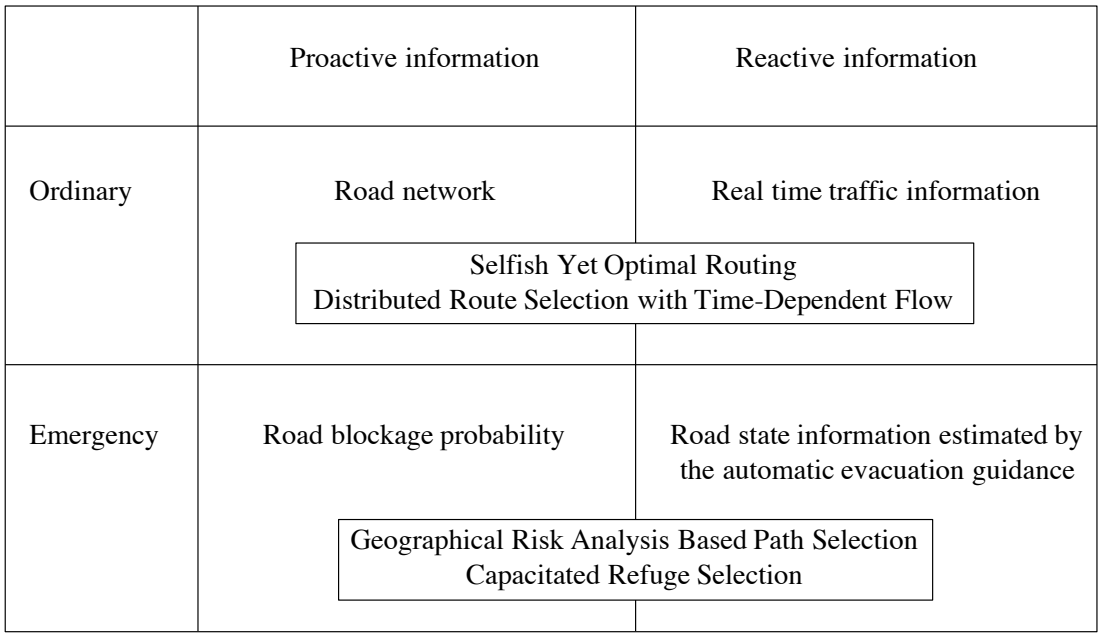

Figure 1.1. Overview of Proposed Schemes.

roads in a selected route is simultaneously and constantly used by the corresponding agent. In actual situations, the roads in a selected route will be sequentially used by the agent, and thus we further propose a distributed route selection scheme under the consideration of such time-varying road usage among agents.

Next, focusing on the evacuation under a large-scale disaster, i.e., an earthquake, we further propose a geographical risk analysis based path selection scheme, which leverages the road blockage probabilities [23] as a kind of proactive information and updates them with the help of the automatic evacuation guidance [24] to achieve speedy and safety evacuation. Furthermore, selecting the nearest refuge may cause the overflow of the refuge and/or force evacuees to pass through high risk regions, we also propose a capacitated refuge assignment scheme for the speedy and reliable evacuation.

In this thesis, we separately propose schemes for the ordinary situations and emergency ones but the proposed schemes for the ordinary situations are also applicable for the emergency ones. For instance, the selfish yet optimal routing will be more effective under the emergency situations because the selfish routing tends to arise under evacuation situations where the evacuees try to move to the

safe areas as soon as possible.

The main contributions of the thesis are as follows:

1. Inspired by the concept of Nudge, we propose selfish yet optimal routing, which achieves the social optimum even under the rational/selfish decision making of individual users by internalizing the marginal cost into the traffic information. In contrast to the standard pricing scheme where the link level tolls are homogeneous for all users, the internalized traffic information can be viewed as the personalized pricing that considers heterogeneity in user behavior. Through numerical results, we demonstrate that (1) the selfish yet optimal routing exhibits almost the same performance as the optimal routing, (2) the selfish yet optimal routing decreases the individual travel time of 82% (resp. 67%) users compared with the notification of the actual travel time in case of the grid-like network (resp. local-level real road network in Nagoya city, Japan).

2. To address the time-varying road congestion, we propose the multi-agent route selection considering the time-dependency among agents' road usage in a distributed manner. Through the numerical and simulation results, we show that the proposed scheme can achieve the low relative estimation error of travel time, i.e., 0.0036. We also confirm that the proposed scheme can improve the actual travel time by 5.1% compared with the existing scheme [22] while keeping the exponential convergence property.

3. We propose the geographical risk analysis based path selection scheme for the evacuation guidance, which is a proactive approach and can be combined with the existing reactive approach of automatic evacuation guiding. Through simulation results using the actual data of Arako district of Nagoya city, in Japan, we reveal how the proactive information contributes to the evacuation movements. Specifically, we confirm that the proposed scheme can improve the evacuation safety by 28.2% while keeping the evacuation time even under severe communication environments, compared with the shortest path selection. In addition, we demonstrate how the information collection and diffusion affects the evacuation movement under various communication environments to reveal the contribution of the reactive in-

formation. The evacuation safety improves with increase of the coverage area of communication infrastructure and the performance improvement is almost saturated when the coverage ratio is only 30%.

4. We propose the capacitated refuge assignment scheme for the speedy and safety evacuation, which is formulated as an integer linear program (ILP). Through numerical results using the Nagoya city's actual data, we demonstrate that the proposed scheme can improve the average route reliability by 13.6% while suppressing the increase of the average route length by 7.3% and satisfying the refuge capacity constraints, compared with the distance-based refuge assignment scheme. The proposed scheme also reveals the potential risks of mismatch between the geographical population distribution and the locations and capacities of refuges in Arako district of Nagoya city, in Japan.

1.3. Thesis Outline

The rest of the thesis is organized as follows. In Chapter 2, we present the selfish yet optimal routing for the ordinary situations. Chapter 3 provides the distributed route selection considering the time-dependency among agents' road usage in ordinary situations. Chapter 4 gives the geographical risk analysis based speedy and reliable path selection scheme for evacuation and Chapter 5 provides the capacitated refuge assignment scheme for the speedy and reliable evacuation. We summarize the thesis in Chapter 6.

Chapter 2

Selfish yet Optimal Routing by Adjusting Nudging Traffic Information in Ordinary Situation

2.1. Introduction

Traffic congestion in urban areas has been one of the serious problems all over the world because it causes both economic and time loss. It has been reported that 12 trillion yen of economic loss per year and 30 hours of time loss per person occur in Japan, due to traffic congestion [25]. In addition, it has been forecasted that traffic congestion will also increase total costs of the four advanced economies i.e., UK, France, Germany, and the USA, by 46% from 2013 to 2030 [26].

Such a traffic congestion problem can be modeled as a congestion game in game theory [27]. Route selection by a certain user corresponds to the usage of roads included in the selected route. When all users select their own routes, the degree of congestion of each road is determined, and thus we can estimate the travel time of both roads and routes. It is rational for each user to select a route that seems to have the minimum travel time. Such route selection is called *selfish routing* and results in a *Wardrop equilibrium* where each user cannot reduce its

travel time by changing the route [28,29]. In the Wardrop equilibrium, there is no incentive for any user to change its own route, which means the system reaches the steady state. However, in general, the average travel time among users in the Wardrop equilibrium may be far from *social optimum*, where the average travel time is minimized [10, 30].

In [10], Roughgarden pointed out three kinds of ways to overcome selfish routing: (1) increasing the road capacity, (2) routing (part of) users in a central manner, i.e., Stackelberg routing, and (3) internalizing the externalities by introducing taxes, i.e., congestion pricing. Coorperative routing [22, 31] and Stackelberg routing [32–36] cannot achieve social optimum under the users' rational decision making because these approaches fully or partly rely on the users' cooperation. Congestion pricing can alleviate traffic congestion by internalizing the externalities [37–44], however, it also has political and economic issues for the introduction [45, 46].

Since the selfish routing comes from users' rational decision making, it is difficult to prohibit the selfish routing itself. In this thesis, we aim at achieving the social optimum routing even under such users' rational (selfish) route selection by appropriately adjusting their perceived traffic information. Our approach is inspired by the Nudge theory [20]. In behavioral science, the concept of "Nudge" has been attracting many researchers to make decision making of individuals leading to desirable situations by means of indirect suggestions [21]. The Nudge concept is similar to the idea of internalizing the externalities in the congestion pricing but our approach uses the traffic information perceived by each user as the nudging information. Furthermore, the nudging traffic information is personalized per user, which is also different point compared with the standard congestion pricing. Since most of the current vehicle navigation systems and navigation software of smartphones (e.g., Google Maps [14]) have the function of notifying users about the actual traffic information, our approach can be easily introduced by replacing the advertised traffic information with the nudging traffic information. Compared with the conventional congestion pricing, our approach can be deployed anytime and anywhere.

Navigation services have become one of the most fundamental services of intelligent transportation systems (ITSs) [15–19]. Users can acquire not only

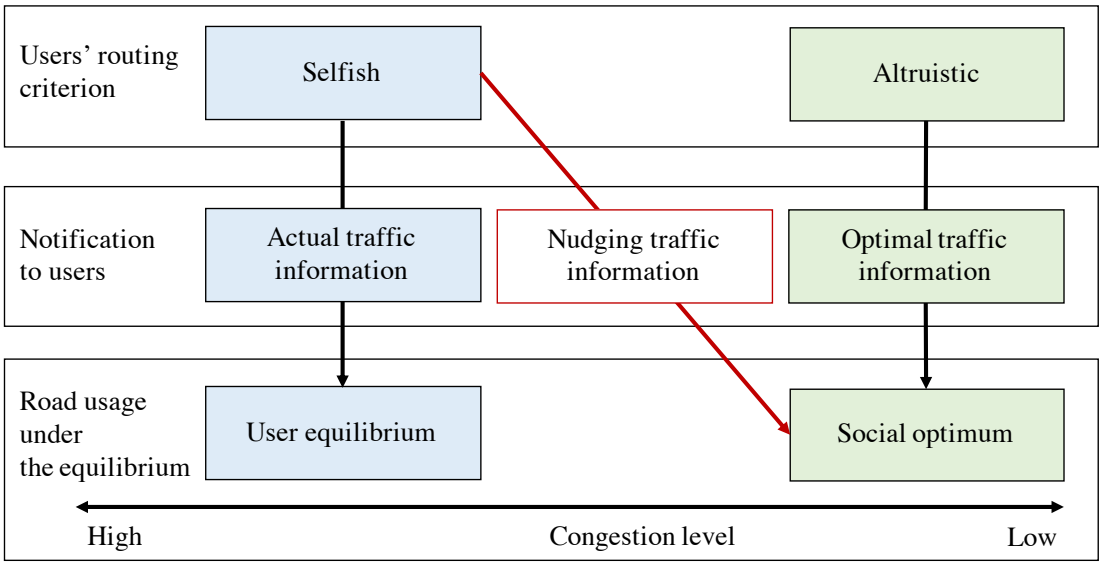

Figure 2.1. Relationship among user criteria, traffic information perceived by a user, and road usage.

the routes from their current locations to destinations but also the current traffic conditions from the navigation software. Since the navigation software is an agent for the corresponding user, its route selection also tends to be selfish routing. In what follows, the terms users and agents will be used interchangeably.

Even if all users rationally aim to minimize their own travel time, their behavior may change depending on their perceived traffic information. Fig. 2.1 illustrates the relationship among users' routing criterion, traffic information perceived by users, and road usage. The usage of each road will converge to user equilibrium (UE), which is a Wardrop equilibrium under the selfish routing criterion, when each user is selfish and receives the actual traffic information based on selfish route selection by others. On the other hand, when each user is altruistic and receives the optimal traffic information based on altruistic route selection by others, it will converge to social optimum (SO), which is also a Wardrop equilibrium under the altruistic routing criterion.

The proposed scheme, which leads selfish routing to social optimum, can be achieved by combining the following two functions. First one is the distributed route selection scheme [22], which can achieve either Wardrop equilibrium based

on users' selfish criterion, i.e., user equilibrium, or that based on users' altruistic criterion, i.e., social optimum. Second one is the distribution of the nudging traffic information from the server to each user, which affects the users' perception of traffic congestion and leads their selfish routing to social optimum as shown in Fig. 2.1. We assume the current navigation software and/or traffic support systems (e.g., vehicle information and communication system (VICS) in Japan [15]) can provides users with the nudging traffic information instead of the actual traffic information.

Someone might think that users doubt whether the perceived traffic information is tweaked and defect the proposed system. Unfortunately, the proposed scheme cannot prohibit such (selfish) behavior. This might come from the dissatisfaction with the actual (experienced) travel time compared to the pre-expected travel time based on the nudging traffic information. There are several studies on dealing with such phenomena [6–9]. In [9], the information affecting travelers' route choices is categorized into the three types of information: experiential information (EI), descriptive information (DI), and prescriptive information (PI). Without any external information, it is assumed that a traveler will choose the route based on EI, which is the knowledge acquired from his/her own experience during the past choices. DI presents the information about the travel condition (e.g., expected travel time) notified by systems either before or during the travel. PI is the information for direct suggestion and guidance (e.g., a recommended route), which is provided by systems. In our case, the nudging traffic information and the resulting expected travel time can be regarded as DI.

The impact of the three kinds of information (i.e., EI, DI, and PI) and their combinations on the travelers' route choices have been studied from the aspects of both the short-term and long-term behavior [6–8, 47]. In this thesis, we assume that all users follow the proposed scheme, in order to focus on the concept of the nudging traffic information itself. The precise modeling of users' satisfaction with their own travel time and the behavior modification based on the degree of satisfaction are possible future directions.

The main contributions of this thesis are given as follows:

1. Inspired by the Nudge theory, we propose "selfish yet optimal routing," which can achieve social optimum even under the rational (selfish) decision

making of users by internalizing the marginal cost into the traffic information, i.e., perceived travel time. In contrast to the existing approaches (e.g., cooperative routing, centralized routing, and congestion pricing), the proposed scheme does not rely on the users' cooperative behavior and can be introduced anytime and anywhere.

2. In contrast to the standard cost pricing where the link level tolls are identical for all users, the provision of the link-level nudging traffic information in the proposed scheme can be viewed as the personalized pricing that considers heterogeneity in user behavior.

3. We demonstrate the fundamental characteristics of the proposed scheme through numerical experiments under a grid-like road network. Some of the main results are as follows: (1) the proposed scheme can achieve almost the same performance compared with the optimal routing as we expected and (2) the proposed scheme can decrease individual travel time of 82% users compared with the notification of actual (user-equilibrium) traffic information.

4. Furthermore, we also evaluate the practicality and scalability of the proposed scheme through numerical experiments under two kinds of real road networks (i.e., local-level and city-level road networks of Nagoya city, Japan). In particular, we find that the proposed scheme can improve the average travel time by 19.1% (resp. 7.4%), compared with the notification of the actual traffic information, in case of the local-level (resp. city-level) road network with 1,197 (resp. 10,004) users.

The remaining of this chapter is given as follows. Section 2.2 gives related work. In Section 2.3, we explain the existing distributed route selection scheme [22]. After describing the proposed scheme in Section 2.4, we demonstrate numerical results in Section 2.5. Finally, Section 2.6 provides conclusions.

2.2. Related Work

Roughgarden first studied the traffic congestion problem from the viewpoint of selfish routing [10]. He revealed each user's selfish routing results in a Wardrop

equilibrium and focused on the performance ratio of travel time based on selfish routing to that of optimal routing, i.e., Price of Anarchy (PoA) [30], in game theory. PoA can be equal to or greater than one and smaller PoA indicates that selfish routing can achieve shorter travel time, which is competitive with that of the optimal routing. For example, PoA becomes 4/3 if the travel time of a road linearly increases with the flow over the road. Wang et al. revealed that selfish rerouting against unpredictable trouble, e.g., traffic accidents, also had a negative impact on traffic congestion [48]. In [10], Roughgarden pointed out three ways to overcome the selfish routing: (1) increasing the road capacity, (2) routing (part of) users in a centralized manner, i.e., cooperative routing and Stackelberg routing, and (3) internalizing the externalities, i.e., congestion pricing.

From the viewpoint of system, it is desirable to achieve the social optimum routing that relies on cooperative route selection among all users. In [22], Lim and Rus proposed a distributed route selection scheme that can achieve either user equilibrium or social optimum according to users' routing criterion, i.e., selfish or altruistic, which will be introduced in Section 2.3. In [31], Aslam et al. evaluated the performance of the distributed route selection scheme by using a congestion model learned from the actual traffic data of taxis. They found that the scheme could reduce the travel time by 15% compared with greedy optimal planning. However, it may be difficult to obtain cooperative support by all users, due to the potential selfishness of individuals. In particular, the selfish routing of the individual user tends to be prioritized in an emergency situation, i.e., evacuation, because evacuees want to move to a refuge as fast as possible.

If the system can obtain cooperative support by part of users, Stackelberg routing is one of the promising approaches to cope with the selfish routing problem [32–36]. Korilis et al. proposed Stackelberg strategies to improve the whole system performance, i.e., average travel time among users [33]. In [33], cooperative users first act as leaders by selecting routes that can lead the route selection of selfish users to good Nash (Wardrop) equilibria. Then, the selfish users, called followers, conduct selfish routing under the environment yielded by the leaders' decision, which will result in the expected Nash equilibria. Roughgarden showed that the derivation of the optimal Stackelberg strategy to minimize PoA was NP-hard and proposed three heuristic Stackelberg strategies [34]. Yang et al. also

proposed a Stackelberg routing game and formulated a mixed behavior equilibrium model as variational inequalities which described players' routing behavior aiming at user equilibrium, social optimum, and Cournot-Nash equilibrium, respectively [35]. In [36], Groot et al. proposed a game-theoretic approach in order to maximize traffic throughput on a freeway network by introducing a reverse Stackelberg routing [49] with a monetary incentive [50]. Our selfish yet optimal routing is similar to the idea of Stackelberg routing, where a server acts as a leader by notifying the nudging traffic information to users, and then the users act as followers by conducting selfish routing with the perceived information.

To mitigate a negative impact of selfish routing, there are also several studies on indirect control by internalizing the externalities: congestion pricing [37–44] and gate control [51]. Congestion pricing imposes taxes on the road usage according to the congestion level. Cole et al. showed that the selfish routing could result in the optimal routing by appropriately introducing congestion pricing [38]. In actual, congestion pricing has been introduced to many cities and showed good results to mitigate urban congestion [39–41]. On the other hand, it was also pointed out that the congestion pricing had political and economic issues [45, 46]. Bazzan and Junges studied the route selection to achieve the social optimum by internalizing the route congestion into the congestion tolls. [44]. In this work, a control center provides the users with the congestion tolls based on (imperfect) traffic information about the number of users selecting the corresponding route. The users select the corresponding route with the probability based on the congetion toll. Bu et al. showed that gate control could improve the crowd evacuation under emergent situations [51]. These indirect control schemes are also similar to the concept of "Nudge," which aims to lead individuals to desirable decision making through indirect suggestions [20, 21]. The main difference of the proposed scheme from the congestion pricing is the internalization of the marginal cost into traffic information, i.e., perceived travel time. In the proposed scheme, users' selfish routing unconsciously results in the optimal routing by leveraging the nudging traffic information without the user cooperation [22, 32–36] and the payment of congestion fees [37–43].

The difference of optimality between the individual users and the system, i.e., user equilibrium and social optimum, stems from the different goals among

them. There are several studies to fill this gap [52–54]. Angelelli et al. proposed a proactive route guiding scheme to avoid traffic congestion, which considered not only the system performance to suppress traffic congestion but also the user performance to suppress the increase of individual travel time [54]. In [52, 53], they balance the individual user and the system objectives by deriving system optimal flows under the user constraints.

With the proliferation of vehicle navigation systems and smartphones, each individual can easily acquire the traffic information, which would affect the route selection [47, 55–58]. Essen et al. insisted that considering both the user behavior and the system performance was important to evaluate how the traffic information notified to users would affect the traffic congestion [55]. To alleviate congestion, Hassan et al. proposed a distributed traffic coordination scheme based on the travel information exchanged through the driver's social network [56]. In [58], Ramos et al. proposed a route selection scheme based on regret minimization [59], where each agent estimated the regret of route choice based on the local information obtained by its own experience and global information provided by a mobile navigation application, and then selected the route with the smallest estimated regret. The proposed scheme is compatible with the conventional navigation systems by replacing the advertising traffic information with the nudging one.

2.3. Distributed Route Selection Scheme

In this section, we describe the details of the existing distributed route selection scheme [22], which will be used in part of the proposed scheme in Section 2.4.

2.3.1 Overview

Table 2.1 presents the symbols and the notations used throughout the paper. $G = (\mathcal{V}, \mathcal{E})$ denotes a graph representing the internal structure of a road network, where $\mathcal{V}$ is a set of vertices, i.e., intersections, and $\mathcal{E}$ is a set of edges, i.e., roads, in the road network. There are $N > 0$ users, e.g., vehicles or persons, in the road network and $\mathcal{A} = \{1, 2, \ldots, N\}$ denotes a set of users.

In the distributed route selection scheme, each user $i \in \mathcal{A}$ first calculates $K_i > 0$ route candidates $\boldsymbol{\pi}_i = \{\pi_{i1}, \pi_{i2}, \ldots, \pi_{iK_i}\}$, where π_{ik} is the k-th route

Table 2.1. Notations.

Symbol	Description
G	Directed graph of the road network
$\mathcal{V}$	Set of vertices (road intersections)
$\mathcal{E}$	Set of edges (roads)
e	Road
$\mathcal{A}$	Set of all users in the road network
N	The number of all users, $(N = \lvert\mathcal{A}\rvert)$
$\boldsymbol{\pi}_i$	Set of route candidates for user i
$\boldsymbol{p}_i$	Vector of route choice probabilities for user i
$\mathcal{K}_i$	Set of route indices for user i
K_i	The number of route candidates, $\boldsymbol{\pi}_i$, $(K_i = \lvert\mathcal{K}_i\rvert)$
π_{ik}	User i's k-th route
p_{ik}	Probability that user i selects route π_{ik}
$\mathcal{C}_i$	Set of users j whose routes $\boldsymbol{\pi}_j$ (partly) conflict with $\boldsymbol{\pi}_i$
$\boldsymbol{p}_{\mathcal{C}_i}$	Vector of $\boldsymbol{p}_j$ for $j \in \mathcal{C}_i$
$f_e(\cdot)$	Flow of road e
$\mathbb{I}(\cdot)$	Indicator function
$t_e(\cdot)$	Travel time of road e
$c_e(\cdot)$	Cost of road e
$c_e^{(\mathrm{UE})}(\cdot)$	User-equilibrium based cost of road e
$c_e^{(\mathrm{SO})}(\cdot)$	Social-optimum based cost of road e
$c_{ik}(\cdot)$	Cost of route π_{ik}
d_i	Index of the route with minimum cost among $\boldsymbol{\pi}_i$
$V_i(\cdot)$	Local cost of user i
$V(\cdot)$	Global cost
m	Navigation server
G_i	Directed graph of the road network consisting of $\boldsymbol{\pi}_i$
$\mathcal{V}_i$	Set of vertices (road intersections) consisting of $\boldsymbol{\pi}_i$
$\mathcal{E}_i$	Set of edges (roads) consisting of $\boldsymbol{\pi}_i$
$\boldsymbol{p}_i^{(m)}$	Vector of social-optimum based route choice probability for user i
$\boldsymbol{p}_i^{(i)}$	Vector of selfish route choice probability for user i
$\boldsymbol{p}_{\mathcal{C}_i}^{(m)}$	Vector of $\boldsymbol{p}_j^{(m)}$ for $j \in \mathcal{C}_i$
$\boldsymbol{f}_i^{(m)}$	Nudging traffic information for user i
$f_e^{(m)}$	Nudging traffic information of road e, $f_e^{(m)} \in \boldsymbol{f}_i^{(m)}$
$c_e^{(\mathrm{UE})-1}(\cdot)$	Inverse function of $c_e^{(\mathrm{UE})}(\cdot)$
ϵ	Error tolerance
$T_i(\cdot)$	Travel time for user i

candidate that is a set of edges in the corresponding route. Let $\mathcal{K}_i = \{1, 2, \ldots, K_i\}$ be a set of route indices for user i. Next, each user autonomously calculates route choice probabilities $\boldsymbol{p}_i = (p_{i1}, p_{i2}, \ldots, p_{iK_i})$ by using a gradient descent method [22]. Here, p_{ik} is the probability that user i selects k-th route, where p_{ik} ranges $[0, 1]$ and $\sum_{k \in \mathcal{K}_i} p_{ik} = 1$. Note that $\boldsymbol{p}_i$ can be regarded as the mixed strategy in game theory [59]. In the route selection, each peer i considers $\boldsymbol{p}_i$ and $\boldsymbol{p}_j$ for all competitors $j \in \mathcal{C}_i$, where $\mathcal{C}_i$ denotes the set of users j whose route candidates $\boldsymbol{\pi}_j$ (partly) conflict with user i's route candidates $\boldsymbol{\pi}_i$. Please note that small increase/decrease of p_{ik} may change the congestion level of the roads in the route π_{ik}, which affects not only the travel time of user i but also that of i's competitors. The relationship between the route choice probabilities and resulting travel time will be described later. In addition, the route choice probabilities are controlled by each user in a distributed manner, with the help of the gradient descent method. Please see the detail mechanism in [22, Section 3.3].

This scheme assumes that the number of users in the road network is large enough such that each user's route choice probability can be regarded as a fractional flow [60–63]. As a result, the flow of a road can also be regarded as the probabilistic occupation by users. In addition, this scheme also assumes that the user's probabilistic occupation of a road is static during the whole time horizon of the user's travel as in [62–65]. With these assumptions, flow $f_e(\boldsymbol{p}_i, \boldsymbol{p}_{\mathcal{C}_i})$ of road $e \in \mathcal{E}$ can be expressed as the sum of the probabilities that user i and competitors $\mathcal{C}_i$ use road e, where $\boldsymbol{p}_{\mathcal{C}_i}$ denotes the vector of $\boldsymbol{p}_j$ for $j \in \mathcal{C}_i$:

$$f_e(\boldsymbol{p}_i, \boldsymbol{p}_{\mathcal{C}_i}) = \sum_{j \in \{i\} \cup \mathcal{C}_i} \sum_{k \in \mathcal{K}_j} \mathbb{I}(e \in \pi_{jk}) \cdot p_{jk}, \tag{2.1}$$

where $\mathbb{I}(\cdot)$ denotes an indicator function. The cost of route π_{ik} of user i is a routing criterion and can be expressed as the sum of the cost of each road along the route:

$$c_{ik}(\boldsymbol{p}_i, \boldsymbol{p}_{\mathcal{C}_i}) = \sum_{\forall e \in \pi_{ik}} c_e(f_e(\boldsymbol{p}_i, \boldsymbol{p}_{\mathcal{C}_i})),$$

where $c_e(f_e(\cdot))$ is the cost of road e under flow $f_e(\cdot)$, which is a differentiable non-decreasing function. One possible definition of $c_e(f_e(\cdot))$ is travel time $t_e(f_e(\cdot))$ of

road e under flow $f_e(\cdot)$. The cost function represents the user's sense of value and will be described in Section 2.3.2.

Each user i defines local cost $V_i(\boldsymbol{p}_i, \boldsymbol{p}_{\mathcal{C}_i})$ as the difference between the expected cost among all route candidates and the minimum route cost:

$$V_i(\boldsymbol{p}_i, \boldsymbol{p}_{\mathcal{C}_i}) = \sum_{k \in \mathcal{K}_i} p_{ik} c_{ik}(\boldsymbol{p}_i, \boldsymbol{p}_{\mathcal{C}_i}) - c_{d_i}(\boldsymbol{p}_i, \boldsymbol{p}_{\mathcal{C}_i}), \tag{2.2}$$

where d_i is the index of the route with the minimum cost among route candidates, i.e., $d_i = \arg\min_{k \in \mathcal{K}_i} c_{ik}$. Each user i controls route choice probabilities $\boldsymbol{p}_i$ such that V_i approaches 0. Since (2.2) can be rewritten as

$$V_i(\boldsymbol{p}_i, \boldsymbol{p}_{\mathcal{C}_i}) = \sum_{k \in \mathcal{K}_i} p_{ik} \left(c_{ik}(\boldsymbol{p}_i, \boldsymbol{p}_{\mathcal{C}_i}) - c_{d_i}(\boldsymbol{p}_i, \boldsymbol{p}_{\mathcal{C}_i}) \right), \tag{2.3}$$

$V_i = 0$ results in the two conditions of Wardrop equilibrium:

$$\begin{cases} c_{ik}(\boldsymbol{p}_i, \boldsymbol{p}_{\mathcal{C}_i}) = c_{d_i}(\boldsymbol{p}_i, \boldsymbol{p}_{\mathcal{C}_i}), & \text{if } p_{ik} > 0, \\ c_{ik}(\boldsymbol{p}_i, \boldsymbol{p}_{\mathcal{C}_i}) \geq c_{d_i}(\boldsymbol{p}_i, \boldsymbol{p}_{\mathcal{C}_i}), & \text{otherwise.} \end{cases}$$

As a result, each user i will select the minimum cost when $V_i = 0$. In addition, the global cost $V(\{\boldsymbol{p}_i\}_{i \in \mathcal{A}}, \{\mathcal{C}_i\}_{i \in \mathcal{A}})$ is defined as the sum of local cost $V_i(\cdot)$ among all users:

$$V(\{\boldsymbol{p}_i\}_{i \in \mathcal{A}}, \{\mathcal{C}_i\}_{i \in \mathcal{A}}) = \sum_{i \in \mathcal{A}} V_i(\boldsymbol{p}_i, \boldsymbol{p}_{\mathcal{C}_i}).$$

When each user i control $\boldsymbol{p}_i$ to achieve $V_i = 0$, global cost V can also converge to 0.

In [22], a distributed gradient controller is developed, in which each user i can control $\boldsymbol{p}_i$ to achieve $V_i = 0$ in a distributed manner. The distributed controller governs the time derivative of the route choice probabilities using the competitors' current route choice probabilities. Please refer to [22, Section 3.3] for the detail of the mechanism.

We should note here that equilibrium $\boldsymbol{p}_i^*$ of $\boldsymbol{p}_i$ will change depending on the shape of local cost function $c_e(\cdot)$, i.e., user equilibrium or social optimum, and the resulting $(\boldsymbol{p}_1^*, \ldots, \boldsymbol{p}_N^*)$ is the global goal with the corresponding local cost function. The detail of local cost function $c_e(\cdot)$ will be given in the next subsection.

In addition, equilibrium $\boldsymbol{p}_i^*$ can be regarded as the *stochastic user equilibrium (SUE)* [66], which is a special case of the *generalized stochastic user equilibrium (GSUE)* [67]. In [67], the author also indicated that the achievement of SUE is guaranteed under the large sample approximation theorem, which assumes the absolute demand (i.e., the product of the demand rate and time period) is sufficiently large. As for this point, we will discuss in the evaluation part (Section 2.5.1).

The uniqueness of SUE with heterogeneous users is guaranteed under some simplified settings [68,69]. However, in our case, the SUE may not be unique because there is heterogeneity in individuals' route selection from their candidates, which differ among users even for the same origin and destination pair. The random nature of route updating order among users in the distributed gradient controller would also result in multiple SUEs.

2.3.2 Routing Criteria

We assume that the routing criteria depend on the user's selfishness and its cooperativeness. From the viewpoint of user's selfish decision making, cost of each road e, $c_e^{(\mathrm{UE})}(f_e(\cdot))$, can be directly expressed as the travel time $t_e(f_e(\cdot))$ under flow $f_e(\cdot)$:

$$c_e^{(\mathrm{UE})}(f_e(\cdot)) = t_e(f_e(\cdot)). \tag{2.4}$$

On the contrary, from the viewpoint of user's social-optimum decision making, cost of each road e, $c_e^{(\mathrm{SO})}(f_e)$, can be defined as follows:

$$c_e^{(\mathrm{SO})}(f_e) = t_e(f_e(\cdot)) + f_e(\cdot)\left.\frac{\partial t_e(f)}{\partial f}\right|_{f=f_e(\cdot)}, \tag{2.5}$$

which is the marginal cost of road e, i.e., the total cost increase of all the users using road e due to a small increase of the flow on road e. The existing scheme [22] converges to Wardrop equilibrium, i.e., user equilibrium (UE), (resp. social optimum (SO)) when all users select routes based on $c_e^{(\mathrm{UE})}(\cdot)$ (resp. $c_e^{(\mathrm{SO})}(\cdot)$).

2.4. Proposed Scheme

In this section, we propose selfish yet optimal routing by adjusting the perceived traffic information. After introducing the system overview, we describe the detail of the proposed scheme.

2.4.1 System Overview

In the road network $G = (\mathcal{V}, \mathcal{E})$, each user $i \in \mathcal{A}$ first requests a route from navigation server m via its user agent. After receiving a designated route (i.e., social optimal route) from server m, altruistic user i will follow the designated route. On the other hand, selfish user i may not follow the designated route and then requests other route (i.e., selfish route) to its user agent. The user i's agent asks navigation server m for traffic information of each road in its $K_i > 0$ route candidates $\boldsymbol{\pi}_i$. Server m first calculates a vector of social optimum route choice probabilities, $\boldsymbol{p}_i^{(m)} = (p_{i1}^{(m)}, p_{i2}^{(m)}, \ldots, p_{iK_i}^{(m)})$, for each user $i \in \mathcal{A}$, with the help of the existing scheme in Section 2.3. Then, it derives nudging traffic information $\boldsymbol{f}_i^{(m)} = \{f_e^{(m)}\}_{e \in \mathcal{E}_i}$, which is a vector of nudging traffic for each road included in $\mathcal{E}_i$ and required to lead the user's selfish routing to the optimal routing, where $\mathcal{E}_i$ denotes a set of roads included in $\boldsymbol{\pi}_i$, i.e. $\mathcal{E}_i = \{e \in \cup_{k=1}^{K_i} \pi_{ik}\}$. We also define $\mathcal{V}_i$ and G_i as a set of nodes consisting of $\mathcal{E}_i$ and graph $(\mathcal{V}_i, \mathcal{E}_i)$, respectively. After retrieving $\boldsymbol{f}_i^{(m)}$ from server m, each user agent i calculates selfish route choice probability $\boldsymbol{p}_i^{(i)}$ under $\boldsymbol{f}_i^{(m)}$ with help of the existing scheme [22]. Finally, user agent i selects route π_{ik^*} from $\boldsymbol{\pi}_i$ according to $\boldsymbol{p}_i^{(i)}$. Hereafter, the user and the corresponding agent will be used interchangeably.

2.4.2 Nudging Traffic Information Achieving Selfish yet Optimal Routing

In this section, we explain how server m derives nudging traffic information for each user i, which affects the user's perception of traffic congestion and leads the user's selfish routing to the optimal routing. Recall that the routing criterion is different between selfish routing and optimal routing, i.e., UE-based routing criterion (2.4) and SO-based routing criterion (2.5). If all users follow the SO-based

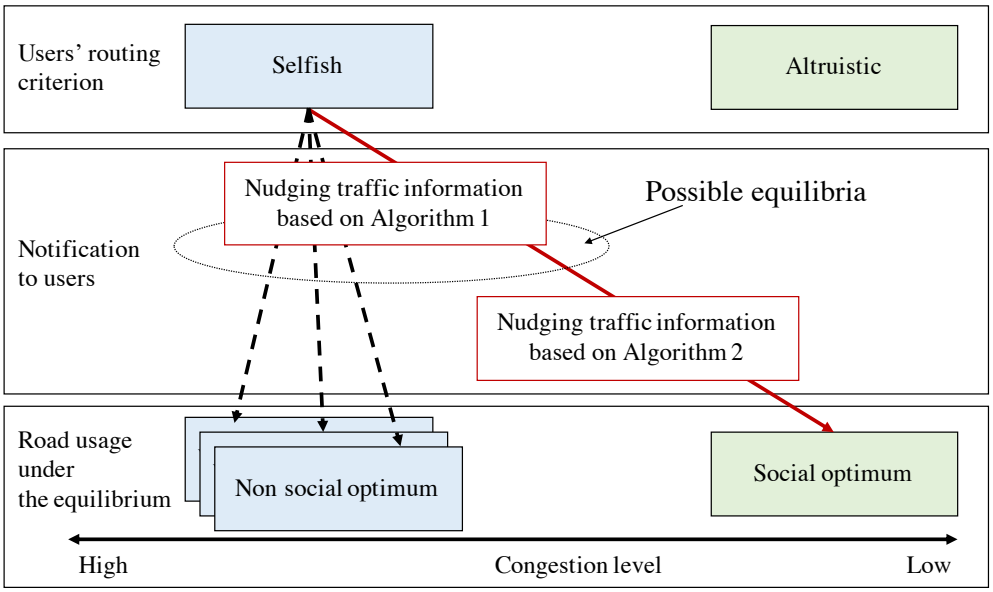

Figure 2.2. Relationship among user criteria, nudging traffic information, and road usage.

routing criterion, the optimal routing can be achieved as a Wardrop equilibrium. However, rational decisions of users tend to follow the UE-based routing criterion where they only consider their own travel time. In what follows, we aim to lead the selfish routing to the optimal routing by appropriately modifying the users' perception of traffic congestion through the nudging traffic information.

As mentioned above, server m calculates nudging traffic information $\boldsymbol{f}_i^{(m)}$ for each user $i \in \mathcal{A}$. To achieve selfish yet optimal routing, $\boldsymbol{f}_i^{(m)}$ should satisfies the following conditions:

1. The social optimum assignment for each user is equivalent to one of the Wardrop equilibria under the UE-based routing criterion, which will be satisfied by Algorithm 1.

2. Any Wardrop equilibrium for each user can be equivalent to the social optimum assignment under the UE-based criterion, which will be satisfied by Algorithm 2.

Fig. 2.2 shows the graphical implication of these conditions and the details will be given in the following.

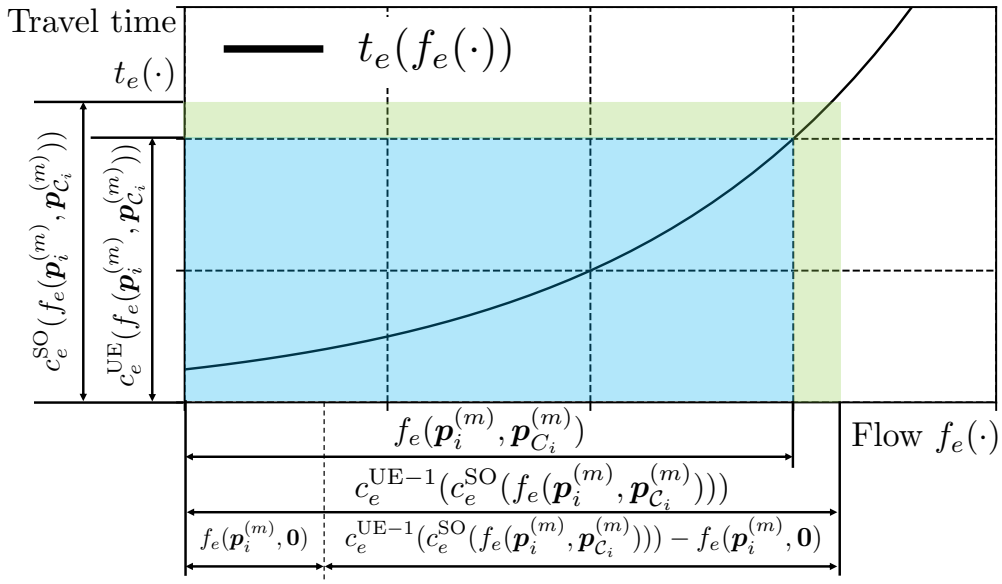

Figure 2.3. Gap between the UE-based routing criterion and SO-based routing criterion.

We first focus on the first condition. Even if all competitors $j \in \mathcal{C}_i$ of user i follow social optimum route choice probability $\boldsymbol{p}_{\mathcal{C}_i}^{(m)}$, the selfish route choice probability for user i may not be equivalent to social optimum one $\boldsymbol{p}_i^{(m)}$. This situation will come from the user i's underestimation of the traffic congestion, which is caused by the UE-based routing criterion under social optimum route assignment $(\boldsymbol{p}_i^{(m)}, \boldsymbol{p}_{\mathcal{C}_i}^{(m)})$. Recall that the usage of each road for user i is only affected by i's competitors $j \in \mathcal{C}_i$ rather than all the others.

Fig. 2.3 depicts the relationship between flow $f_e(\boldsymbol{p}_i^{(m)}, \boldsymbol{p}_{\mathcal{C}_i}^{(m)})$ on road e, travel time $t_e(f_e(\boldsymbol{p}_i^{(m)}, \boldsymbol{p}_{\mathcal{C}_i}^{(m)}))$, UE-based routing criterion $c_e^{(\mathrm{UE})}(f_e(\boldsymbol{p}_i^{(m)}, \boldsymbol{p}_{\mathcal{C}_i}^{(m)}))$, and SO-based routing criterion $c_e^{(\mathrm{SO})}(f_e(\boldsymbol{p}_i^{(m)}, \boldsymbol{p}_{\mathcal{C}_i}^{(m)}))$. Note that $t_e(f_e(\boldsymbol{p}_i^{(m)}, \boldsymbol{p}_{\mathcal{C}_i}^{(m)})) = c_e^{(\mathrm{UE})}($ $f_e(\boldsymbol{p}_i^{(m)}, \boldsymbol{p}_{\mathcal{C}_i}^{(m)}))$. We can confirm that the UE-based cost $c_e^{(\mathrm{UE})}(\cdot)$ underestimates the cost of road e as $t_e(f_e(\boldsymbol{p}_i^{(m)}, \boldsymbol{p}_{\mathcal{C}_i}^{(m)}))$, which is smaller than $c_e^{(\mathrm{SO})}(f_e(\boldsymbol{p}_i^{(m)}, \boldsymbol{p}_{\mathcal{C}_i}^{(m)}))$ by the corresponding marginal cost as in (2.5). This SO-based cost $c_e^{(\mathrm{SO})}(f_e(\boldsymbol{p}_i^{(m)},$ $\boldsymbol{p}_{\mathcal{C}_i}^{(m)}))$ can be transformed into the corresponding flow $c_e^{(\mathrm{UE})-1}(c_e^{(\mathrm{SO})}(f_e(\boldsymbol{p}_i^{(m)}, \boldsymbol{p}_{\mathcal{C}_i}^{(m)})))$ under the UE-based cost. Here, $c_e^{(\mathrm{UE})-1}(\cdot)$ is the inverse function of $c_e^{(\mathrm{UE})}(\cdot)$. Due

Algorithm 1 Nudging traffic information $\boldsymbol{f}_i^{(m)}$ for user i, which leads the social optimum assignment for user i to a Wardrop equilibrium under UE-based route criterion.

Require: $G_i = (\mathcal{V}_i, \mathcal{E}_i)$, $\boldsymbol{p}_i^{(m)}$, $\boldsymbol{p}_{\mathcal{C}_i}^{(m)}$
Ensure: $\boldsymbol{f}_i^{(m)}$

1: **for** $\forall e \in \mathcal{E}_i$ **do**
2: $f_e(\mathbf{0}, \boldsymbol{p}_{\mathcal{C}_i}^{(m)}) \leftarrow \sum_{j \in \mathcal{C}_i} \sum_{k \in \mathcal{K}_j} I(e \in \pi_{jk}) \cdot p_{jk}^{(m)}$ ▷ Calculate social optimal flow of road e among competitors $\mathcal{C}_i$
3: $f_e(\boldsymbol{p}_i^{(m)}, \boldsymbol{p}_{\mathcal{C}_i}^{(m)}) \leftarrow \sum_{k \in \mathcal{K}_i} I(e \in \pi_{ik}) \cdot p_{ik}^{(m)} + f_e(\mathbf{0}, \boldsymbol{p}_{\mathcal{C}_i}^{(m)})$ ▷ Calculate social optimal flow of road e among user i and competitors $\mathcal{C}_i$
4: $c_e^{(\mathrm{SO})}(f_e(\boldsymbol{p}_i^{(m)}, \boldsymbol{p}_{\mathcal{C}_i}^{(m)})) \leftarrow t_e(f_e(\boldsymbol{p}_i^{(m)}, \boldsymbol{p}_{\mathcal{C}_i}^{(m)})) + f_e(\boldsymbol{p}_i^{(m)}, \boldsymbol{p}_{\mathcal{C}_i}^{(m)}) \left.\frac{\partial t_e(f)}{\partial f}\right|_{f = f_e(\boldsymbol{p}_i^{(m)}, \boldsymbol{p}_{\mathcal{C}_i}^{(m)})}$ ▷ Calculate SO-based cost of road e
5: $f_e^{(m)} \leftarrow c_e^{(\mathrm{UE})-1}(c_e^{(\mathrm{SO})}(f_e(\boldsymbol{p}_i^{(m)}, \boldsymbol{p}_{\mathcal{C}_i}^{(m)}))) - f_e(\boldsymbol{p}_i^{(m)}, \mathbf{0})$ ▷ Derive nudging traffic information $\boldsymbol{f}_i^{(m)}$
6: **return** $\boldsymbol{f}_i^{(m)}$

to the linearity in (2.1),

$$f_e(\boldsymbol{p}_i^{(m)}, \boldsymbol{p}_{\mathcal{C}_i}^{(m)}) = f_e(\boldsymbol{p}_i^{(m)}, \mathbf{0}) + f_e(\mathbf{0}, \boldsymbol{p}_{\mathcal{C}_i}^{(m)}) \tag{2.6}$$

is satisfied. To make $\boldsymbol{p}_i^{(m)}$ to be the optimal usage of each road even under the UE-based routing criterion, user i should perceive traffic information $f_e^{(m)}$ ($e \in \mathcal{E}_i$), which satisfies the following:

$$f_e^{(m)} = c_e^{(\mathrm{UE})-1}(c_e^{(\mathrm{SO})}(f_e(\boldsymbol{p}_i^{(m)}, \boldsymbol{p}_{\mathcal{C}_i}^{(m)}))) - f_e(\boldsymbol{p}_i^{(m)}, \mathbf{0}). \tag{2.7}$$

Algorithm 1 presents the calculation of nudging traffic information $\boldsymbol{f}_i^{(m)}$ for user i, which satisfies the first condition. Given road network $G_i = (\mathcal{V}_i, \mathcal{E}_i)$, social optimum route choice probability of user i, $\boldsymbol{p}_i^{(m)}$, and that of user i's competitors, $\boldsymbol{p}_{\mathcal{C}_i}^{(m)}$, system m first calculates social optimal flow of road e among competitors $\mathcal{C}_i$, i.e., $f_e(\mathbf{0}, \boldsymbol{p}_{\mathcal{C}_i}^{(m)})$, and that among user i and competitors $\mathcal{C}_i$, i.e., $f_e(\boldsymbol{p}_i^{(m)}, \boldsymbol{p}_{\mathcal{C}_i}^{(m)})$, (lines 2–3). Next, it also calculates the SO-based cost of road e, i.e., sum of the travel time and marginal cost, from (2.5) (line 4). Finally, it derives the nudging traffic information of road e using (2.7) (line 5).

Algorithm 2 Nudging traffic information $\boldsymbol{f}_i^{(m)}$ for user i, which leads any Wardrop equilibrium for user i to the social optimum route assignment under UE-based route criterion.

Require: $G_i = (\mathcal{V}_i, \mathcal{E}_i)$, $\boldsymbol{p}_i^{(m)}$, $\boldsymbol{p}_{\mathcal{C}_i}^{(m)}$, $\boldsymbol{f}_i^{(m)}$, ϵ
Ensure: $\boldsymbol{f}_i^{(m)}$
1: **do**
2: $\quad \boldsymbol{p}_i^{(i)} \leftarrow$ `calc_selfish_route_prob`$(\boldsymbol{f}_i^{(m)})$ ▷ Obtain the selfish route choice probability for user i
3: $\quad$ **for** $\forall e \in \mathcal{E}_i$ **do**
4: $\quad\quad f_e(\boldsymbol{p}_i^{(i)}, \mathbf{0}) \leftarrow \sum_{k \in \mathcal{K}_i} I(e \in \pi_{ik}) \cdot p_{ik}^{(i)}$
5: $\quad\quad f_e(\boldsymbol{p}_i^{(m)}, \mathbf{0}) \leftarrow \sum_{k \in \mathcal{K}_i} I(e \in \pi_{ik}) \cdot p_{ik}^{(m)}$
6: $\quad\quad f_e^{(m)} \leftarrow f_e^{(m)} + f_e(\boldsymbol{p}_i^{(i)}, \mathbf{0}) - f_e(\boldsymbol{p}_i^{(m)}, \mathbf{0})$ ▷ Update the nudging traffic information
7: $\quad RMSE \leftarrow \sqrt{K_i^{-1} \sum_{i \in \mathcal{K}_i} (p_{ik}^{(i)} - p_{ik}^{(m)})^2}$
8: **while** $\epsilon < RMSE$
9: **return** $\boldsymbol{f}_i^{(m)}$

If the first condition is satisfied by Algorithm 1, the social optimum can be one of the Wardrop equilibria under the UE-based routing criterion. (Remind that the Wardrop equilibrium (SUE) may not be unique, as mentioned in Section 2.3.) However, it cannot guarantee that any Wardrop equilibrium under the UE-based routing criterion is equivalent to the social optimum as shown in Fig. 2.2, and thus the second condition will be required. To achieve the second condition, server m iteratively searches for selfish route choice probability $p_i^{(i)}$ of user i under nudging traffic $\boldsymbol{f}_i^{(m)}$ given by (2.7), and updates $\boldsymbol{f}_i^{(m)}$ such that the selfish flow will reach the social optimum flow. The details are given in Algorithm 2.

Given road network $G_i = (\mathcal{V}_i, \mathcal{E}_i)$, social optimum route choice probability of user i, $\boldsymbol{p}_i^{(m)}$, that of user i's competitors, $\boldsymbol{p}_{\mathcal{C}_i}^{(m)}$, nudging traffic information obtained from Algorithm 1, $\boldsymbol{f}_i^{(m)}$, and error tolerance $\epsilon \geq 0$, server m first obtains user i's selfish route choice probability $\boldsymbol{p}_i^{(i)}$ under the fictitio traffic information $\boldsymbol{f}_i^{(m)}$ using `calc_selfish_route_prob`$(\cdot)$ function (line 2). Here, `calc_selfish_route_prob`$(\cdot)$ function can be achieved by the existing scheme with UE-based routing criterion in Section 2.3. Next, in lines 3–6, it calculates

the flow of road e, which is caused by both selfish route choice probability $\boldsymbol{p}_i^{(i)}$ and latest nudging traffic information $\boldsymbol{f}_i^{(m)}$, and then updates nudging traffic information of each road $e \in \mathcal{E}_i$ as follows:

$$f_e^{(m)} \leftarrow f_e^{(m)} + f_e(\boldsymbol{p}_i^{(i)}, \mathbf{0}) - f_e(\boldsymbol{p}_i^{(m)}, \mathbf{0}). \tag{2.8}$$

The second and third terms of the right-hand side indicate the flow difference between user i's selfish flow and social optimum flow. If $f_e(\boldsymbol{p}_i^{(i)}, \mathbf{0}) - f_e(\boldsymbol{p}_i^{(m)}, \mathbf{0}) > 0$, the usage of road e under the selfish route choice probability is higher than that under the social optimum route choice probability. Therefore, server m increases nudging traffic $f_e^{(m)}$ such that user i reduces the usage probability of road e. Otherwise, it decreases $f_e^{(m)}$ to increase the usage of road e by user i. Next, it calculates root mean square error (RMSE) between $\boldsymbol{p}_i^{(i)}$ and $\boldsymbol{p}_i^{(m)}$ (line 7). These processes (line 2–7) are repeated until the selfish yet social optimum routing is almost achieved, i.e., $RMSE \leq \epsilon$. Since the update rule of $f_e^{(m)}$ given by (2.8) aims to satisfy $f_e(\boldsymbol{p}_i^{(i)}, \mathbf{0}) = f_e(\boldsymbol{p}_i^{(m)}, \mathbf{0})$, we can expect $\boldsymbol{p}_i^{(i)}$ eventually approaches $\boldsymbol{p}_i^{(m)}$.

After conducting Algorithm 2, server m sends $\boldsymbol{p}_i^{(m)}$ and $\boldsymbol{f}_i^{(m)}$ to user i. Then, user i also calculates selfish route assignment $\boldsymbol{p}_i^{(i)}$ using these information and the gradient descent method [22] (Please refer to [22, Section 3.3] for the detail of the gradient descent method). Since `calc_selfish_route_prob`$(\cdot)$ function is deterministic [22], $\boldsymbol{p}_i^{(i)}$ will be the almost same as $\boldsymbol{p}_i^{(m)}$, which is the selfish yet optimal routing as shown in Fig. 2.2. Note that the proposed scheme can achieve the selfish yet optimal routing under the situation where the altruistic users even exist because the nudging traffic information for each user is adjusted based on the social optimum assignment for each user.

2.5. Numerical Results

In this section, we first demonstrate fundamental characteristics of the proposed scheme through numerical experiments using a grid-like network: (1) convergence property and (2) degree of optimality in terms of average travel time. Next, we also evaluate the practicality of the proposed scheme through numerical experiments using the local/city level real road networks of Nagoya city in Japan.

2.5.1 Evaluation Model

To evaluate the fundamental characteristics of the proposed scheme, we first use a grid road network consisting of 50×50 nodes (intersections). There are 50 users ($\mathcal{A} = \{1, \ldots, 50\}$). Each user $i \in \mathcal{A}$ travels from $(i, 1)$-st node to $(i, 50)$-th node. We assume the travel time of each road $e \in \mathcal{E}$ follows Bureau of Public Roads (BPR) function $t_e(f_e) = \underline{t}_e(1 + \alpha(f_e/c_e)^\beta)$ [70]. $\underline{t}_e$ denotes the travel time without road congestion, which is proportional to the ratio of length to speed limit of road e. c_e denotes the capacity of road e, which is proportional to the ratio of road e's size, i.e., road width, to the size of a user. α and β represent the degree of road congestion. We set these four parameters by considering those used in [70]: $\underline{t}_e = [1, 5]$, $c_e = [3, 5]$, $\alpha = 0.15$, and $\beta = 4$.

As we will see later, the time period considered in the following evaluations may not be large enough to satisfy the large sample approximation. Since the BPR function with $\beta = 4$ is 4 times differentiable, the GSUE of order 4, i.e., GSUE(4), gives the most accurate mean flow at the expense of computing higher order moments. In [67, Section 6], the author illustrates the relationship between the time period τ and mean flow of GSUE(n) under a simple two-road network where the demand rate is 20 [vehicles/hour], the cost function of one road e_1 is 4 times differentiable function of $(f_{e_1}/10)^4$, and that of another road e_2 is 10. This result shows that the approximation error of the mean flow between the GSUE(4) and the GSUE(1) (i.e., SUE) actually exists in case of finite τ but it quickly decreases with increase of τ. In particular, the error is about 14% ($\tau = 0.1$ [hour]) and 7% ($\tau = 0.2$ [hour]). In this thesis, considering the tradeoff between accuracy and complexity, we adopt SUE.

Each user $i \in \mathcal{A}$ obtains K_i ($K_i \geq 1$) route candidates $\boldsymbol{\pi}_i$ as exclusively as possible so as to alleviate the route competition with others. Since it is hard to obtain the comprehensive route candidates due to the computational complexity [71], we obtain the route candidates according to the following heuristic approach, which is used in [22]. Each user $i \in \mathcal{A}$ first calculates the shortest route from the source, i.g., $(i, 1)$-st node to the destination, i.e., $(i, 50)$-th node, when the flow of user i only exists, i.e., $t_e(1) = \underline{t}_e(1 + \alpha(1/c)^\beta)$. Next, it obtains the next route candidate by calculating the shortest route from the source to destination under the assumption that a predefined number of road segments, i.e.,

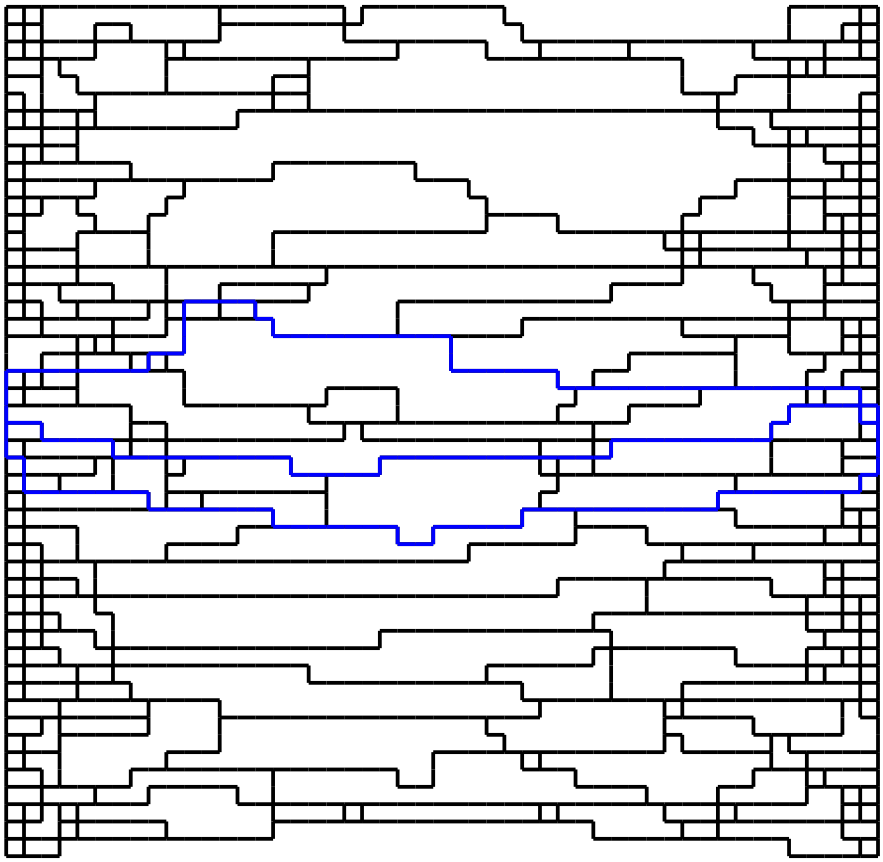

Figure 2.4. An example of route candidates for a certain user $i = 25$, $\boldsymbol{\pi}_i$, (blue lines) and those for all users, $\{\boldsymbol{\pi}_j\}_{\forall j \in \mathcal{A}}$ (black lines).

30, in the first shortest route are randomly chosen and set to be unavailable. By repeating this procedure, each user $i \in \mathcal{A}$ obtains K_i route candidates, $\boldsymbol{\pi}_i$, which are exclusive to each other as much as possible. Note that the route candidates of all users for a given origin-destination pair are not necessarily identical because the heuristic approach includes the randomness. We also evaluate the impact of K_i on the system performance in Section 2.5.2. Fig. 2.4 illustrates an example of route candidates for all users and those for user 25 are highlighted by blue color.

We evaluate the system performance in terms of the average travel time, T_{avg}, which is the mean of expected travel time among all users under route assignment

Table 2.2. Schemes for evaluation.

Scheme	Notification of traffic information	User i's criterion
Notification of $\boldsymbol{p}_{\mathcal{C}_i}^{(i)}$	user equilibrium $\boldsymbol{p}_{\mathcal{C}_i}^{(i)}$	Selfish
Notification of $\boldsymbol{p}_{\mathcal{C}_i}^{(m)}$	social optimum $\boldsymbol{p}_{\mathcal{C}_i}^{(m)}$	Selfish
Proposed scheme	nudging traffic information $\boldsymbol{f}_i^{(m)}$	Selfish
Optimal routing	social optimum $\boldsymbol{p}_{\mathcal{C}_i}^{(m)}$	Altruistic

$(\boldsymbol{p}_i^{(i)}, \boldsymbol{p}_{\mathcal{A}\setminus\{i\}}^{(i)})$:

$$\begin{aligned} T_{\text{avg}} &= N^{-1} \sum_{i\in\mathcal{A}} T_i(\boldsymbol{p}_i^{(i)}, \boldsymbol{p}_{\mathcal{A}\setminus\{i\}}^{(i)}) \\ &= N^{-1} \sum_{i\in\mathcal{A}} T_i(\boldsymbol{p}_i^{(i)}, \boldsymbol{p}_{\mathcal{C}_i}^{(i)}), \end{aligned} \tag{2.9}$$

where $T_i(\cdot)$ is given as follows:

$$T_i(\boldsymbol{p}_i^{(i)}, \boldsymbol{p}_{\mathcal{C}_i}^{(i)}) = \sum_{k\in\mathcal{K}_i} p_{ik}^{(i)} \sum_{e\in\pi_{ik}} t_e(f_e(\boldsymbol{p}_i^{(i)}, \boldsymbol{p}_{\mathcal{C}_i}^{(i)})), \tag{2.10}$$

where $f_e(\boldsymbol{p}_i, \boldsymbol{f}_i)$ is given by

$$f_e(\boldsymbol{p}_i^{(i)}, \boldsymbol{f}_i) = \sum_{j\in\{i\}\cup\mathcal{C}_i} \sum_{k\in\mathcal{K}_j} I(e \in \pi_{jk}) \cdot p_{jk}^{(j)}.$$

The proposed scheme is composed of the notification of the nudging traffic information and the route selection based on the user's selfish criterion. For comparison purpose, we also use the following three schemes depending on the combination of traffic notification and user's criterion, as shown in Table 2.2.

- *Notification of user equilibrium route choice probabilities* $\boldsymbol{p}_{\mathcal{C}_i}^{(i)}$: Server m notifies each user $i \in \mathcal{A}$ of traffic information under the assumption that all user i's competitors $\mathcal{C}_i$ follow user equilibrium route choice probabilities $\boldsymbol{p}_{\mathcal{C}_i}^{(i)}$. Each user agent $i \in \mathcal{A}$ calculates selfish route choice probability $\boldsymbol{p}_i^{(i)}$ under $\boldsymbol{p}_{\mathcal{C}_i}^{(i)}$. As a result, this scheme results in the user equilibrium but may not be social optimum.

- *Notification of social optimum route choice probabilities* $\boldsymbol{p}_{\mathcal{C}_i}^{(m)}$: Server m first notifies each user $i \in \mathcal{A}$ of traffic information under the assumption that

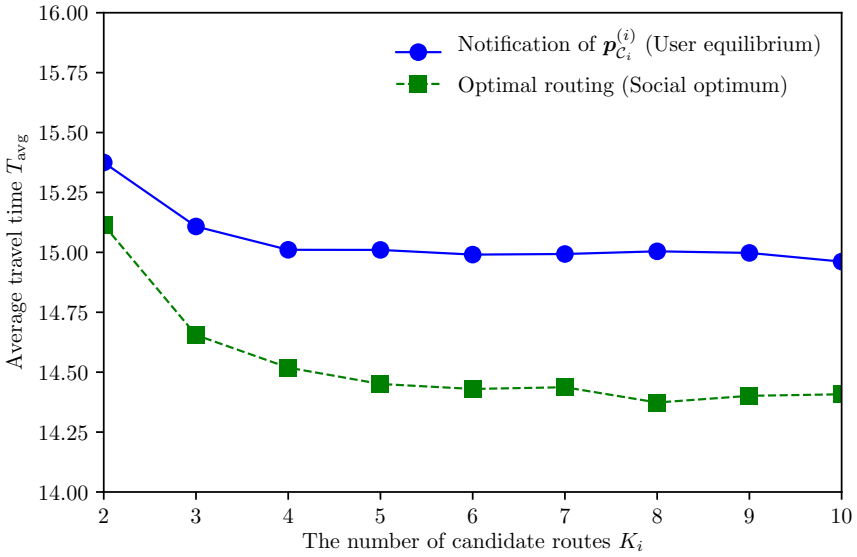

Figure 2.5. Impact of the number of route candidates K_i on the average travel time T_{avg} (grid-like network case).

all user i's competitors $\mathcal{C}_i$ follow social optimum route choice probabilities $\boldsymbol{p}_{\mathcal{C}_i}^{(m)}$. Next, each user agent $i \in \mathcal{A}$ calculates route choice probability $\boldsymbol{p}_i^{(i)}$ under the selfish criterion with the social optimum traffic information $\boldsymbol{p}_{\mathcal{C}_i}^{(m)}$. This scheme may increase traffic congestion because each user $i \in \mathcal{A}$ tends to underestimate the congestion level under the assumption that others behave cooperatively.

- *Optimal routing*: The optimal routing is achieved when all users select the route with the probability $\boldsymbol{p}_i^{(m)}$ under the altruistic criterion with the social optimum traffic information $\boldsymbol{p}_{\mathcal{C}_i}^{(m)}$ obtained from the server.

We use the server with Intel Xeon E7-8895v3 (18 cores and 2.60 GHz) and 2 TB memory to obtain the following results.

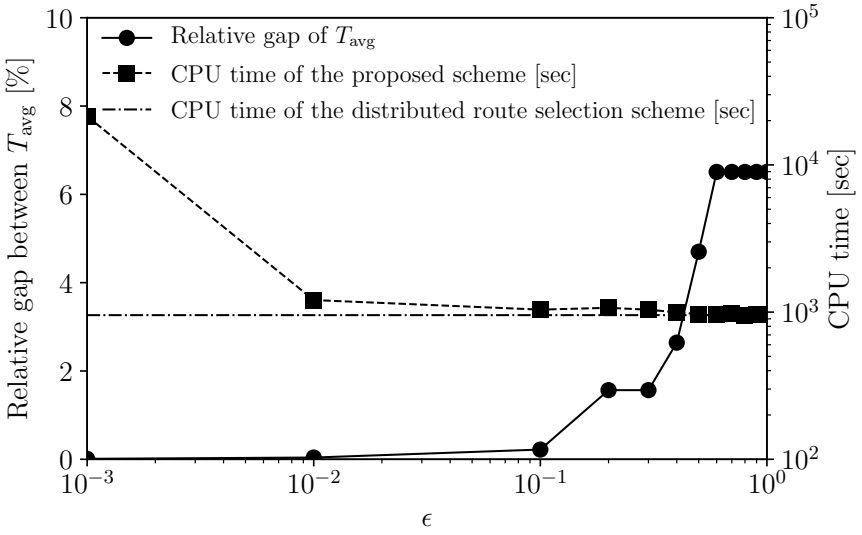

Figure 2.6. Impact of ϵ on convergence time and achievement level of selfish yet optimal routing (grid-like network case).

2.5.2 Evaluation under a Grid-like Network

2.5.2.1 Impact of Number of Route Candidates on Travel Time

We first investigate the impact of the number K_i of route candidates on the average travel time. Fig. 2.5 depicts how the average travel time of two schemes (i.e., notification of $\boldsymbol{p}_{\mathcal{C}_i}^{(i)}$ and optimal routing) changes according to the number of route candidates, K_i. We observe that T_{avg} of both schemes decreases with K_i and almost converges in case of $K_i \geq 5$, due to lack of exclusive route candidates. In what follows, we use $K_i = 5$. There are also several studies on generating the route candidates [72–74].

2.5.2.2 Convergence Property

We first focus on the convergence property of the proposed scheme consisting of the distributed route selection scheme [22], Algorithms 1, and 2. The convergence property of the distributed route selection scheme was already discussed in [22]. Since Algorithm 1 calculates nudging traffic $f_e^{(m)}$ for each road $e \in \mathcal{E}_i$ at once, it obviously converges. On the other hand, Algorithm 2 repeatedly updates $f_e^{(m)}$

Table 2.3. Average travel time T_{avg} and maximum travel time $T_{\max}$ (grid-like network case).

Scheme	T_{avg} [min]	$T_{\max}$ [min]
Notification of $\boldsymbol{p}_{\mathcal{C}_i}^{(i)}$ (User equilibrium)	15.0	16.3
Notification of $\boldsymbol{p}_{\mathcal{C}_i}^{(m)}$	18.6	27.4
Proposed scheme	14.5	16.5
Optimal routing (Social optimum)	14.5	16.5

($e \in \mathcal{E}_i$) until the selfish yet optimal routing is almost achieved, i.e., $RMSE \leq \epsilon$. ϵ controls the balance between convergence time and achievement level of selfish yet optimal routing. Fig. 2.6 illustrates how ϵ affects the convergence time, i.e., CPU time, and the achievement level, i.e., the relative gap between T_{avg} of the proposed scheme and that of optimal routing. We first observe that the relative gap of average travel time can be suppressed by appropriately adjusting ϵ. For example, $\epsilon = 0.01$ results in only 0.04% relative gap, which achieves almost the selfish yet optimal routing. On the contrary, the CPU time of the proposed scheme increases with a decrease of ϵ. To clarify which part of the proposed scheme contributes to the CPU time, we also show the CPU time of the distributed route selection scheme. Since the CPU time of Algorithm 1 is negligible, the difference between the CPU time of the proposed scheme and that of the distributed route selection scheme can be regarded as that of Algorithm 2. We can observe that the overhead of Algorithm 2 is much smaller than that of the distributed route selection scheme when $\epsilon \geq 0.01$. As a result, $\epsilon = 0.01$ can achieve selfish yet optimal routing while keeping the CPU time competitive with the distributed route selection scheme. In what follows, we use $\epsilon = 0.01$.

2.5.2.3 Average and Maximum Travel Time among Users

Table 2.3 presents average travel time T_{avg} and maximum travel time $T_{\max}$ of the four schemes. We first focus on the results of comparison schemes. We observe that T_{avg} (resp. $T_{\max}$) of the notification of $\boldsymbol{p}_{\mathcal{C}_i}^{(m)}$ increases by 3.6 [min] (24%) (resp. 11.1 [min] (68%)) compared with that of the notification of $\boldsymbol{p}_{\mathcal{C}_i}^{(i)}$. This is because the notification of $\boldsymbol{p}_{\mathcal{C}_i}^{(m)}$ results in underestimating traffic congestion, due to lack

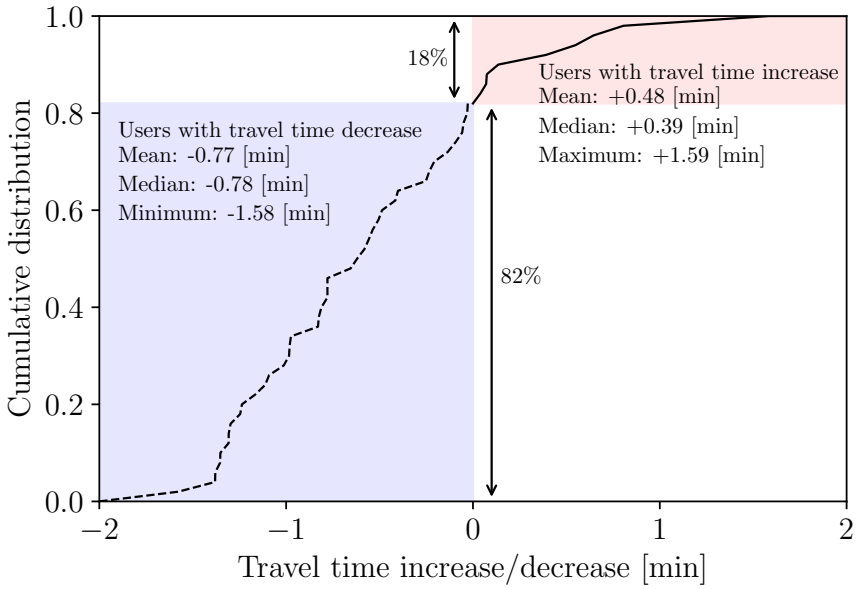

Figure 2.7. Cumulative distribution of users with travel time increase/decrease (grid-like network case).

of considering other users' selfish route selection. In addition, we also observe that the notification of $\boldsymbol{p}_{\mathcal{C}_i}^{(i)}$ increases T_{avg}, i.e., 0.5 [min] (3.4%), compared with the optimal routing.

Next, we focus on the result of the proposed scheme. We confirm that the proposed scheme achieves almost the same T_{avg} compared with the optimal routing. As a result, the proposed scheme can reduce T_{avg} by 3.6 [min] and 0.5 [min] compared with the notification of $\boldsymbol{p}_{\mathcal{C}_i}^{(m)}$ and the notification of $\boldsymbol{p}_{\mathcal{C}_i}^{(i)}$, respectively. In addition, the PoA becomes 1.03, 1.28, and 1.00, in case of notification of $\boldsymbol{p}_{\mathcal{C}_i}^{(i)}$, notification of $\boldsymbol{p}_{\mathcal{C}_i}^{(m)}$, and proposed scheme, respectively. In Section 2.5.3, we will show this improvement can become larger in the real road network.

2.5.2.4 Individual Travel Time Increase/Decrease

The proposed scheme can improve the average travel time compared with the notification of $\boldsymbol{p}_{\mathcal{C}_i}^{(i)}$, however, it may also increase the travel time for some users. Fig. 2.7 illustrates the cumulative distribution of users with travel time increase/decrease, i.e., the difference between $T_i(\cdot)$ of the proposed scheme and that of the

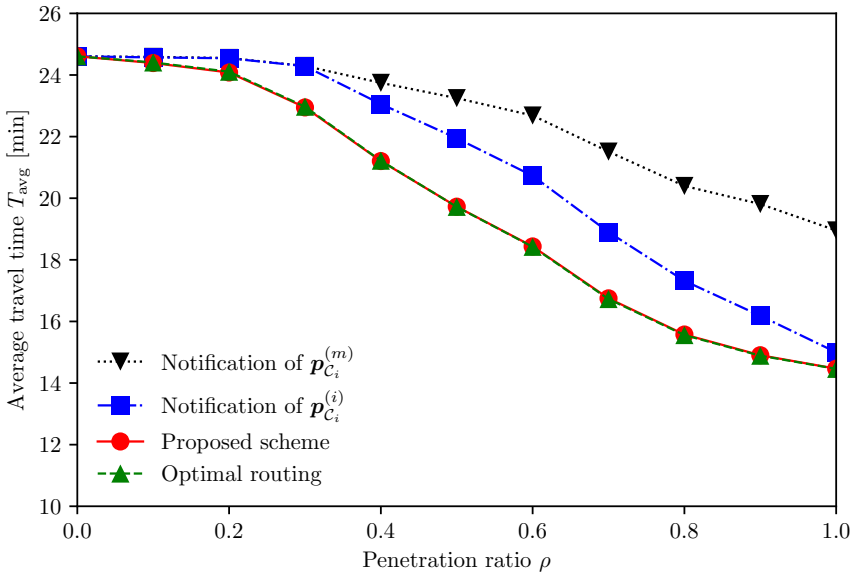

Figure 2.8. Impact of penetration ratio ρ on average travel time among all users, T_{avg}, (grid-like network case).

notification of $\boldsymbol{p}_{\mathcal{C}_i}^{(i)}$. We observe that most of the users, i.e., 82% users, experiences 0.77 [min] (5.1%) travel time decrease in average, with help of the proposed scheme. In addition, the remaining 18% users can also suppress the average travel time increase by 0.48 [min] (3.2%).

2.5.2.5 Impact of Penetration Ratio of Proposed Scheme

In actual situations, the penetration of the proposed scheme may require a certain time and the resulting insufficient penetration may cause the performance degradation, due to the selfish routing of the legacy users. We assume that a certain ratio ρ ($0 \leq \rho \leq 1$) of users adopts the proposed scheme and the remaining users follow the selfish routing without traffic notification. As a result, ρ can be regarded as the penetration ratio of the proposed scheme. Fig. 2.8 depicts the impact of the penetration ratio ρ of the proposed scheme on the average travel time among all users, T_{avg}. For comparison purpose, we also show the results for the three schemes, i.e., notification of $\boldsymbol{p}_{\mathcal{C}_i}^{(i)}$, notification of $\boldsymbol{p}_{\mathcal{C}_i}^{(m)}$, and optimal routing in a similar way. We show the average of 20 independent experiments,

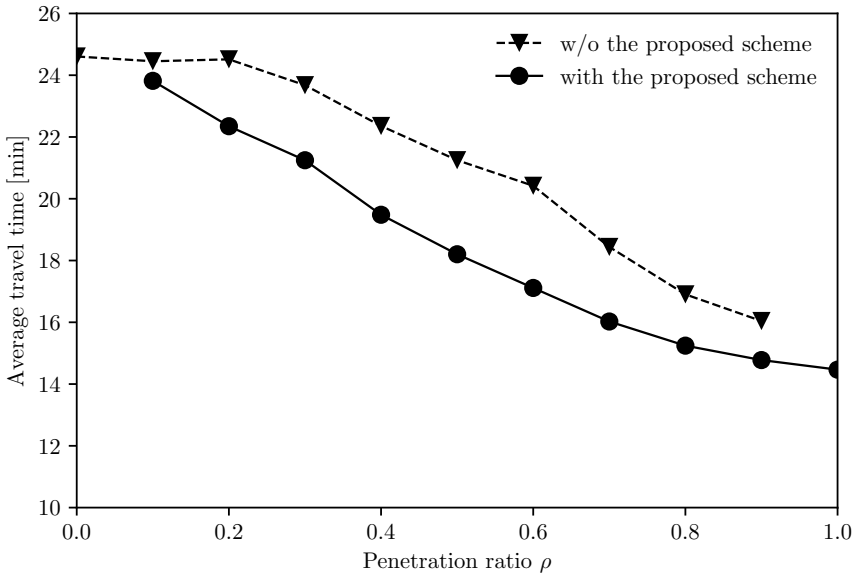

Figure 2.9. Impact of penetration ratio ρ on average travel time among the users with/without the proposed scheme (grid-like network case).

each of which has different allocation of users to the corresponding schemes.

We first observe that T_{avg} of the four schemes degrades with decrease of ρ. Note that we observe that the proposed scheme exhibits the same performance as the optimal routing, regardless of ρ, because it can appropriately notify users of nudging information in response to the background traffic generated by the legacy users' selfish routing. As a result, we confirm that the proposed scheme improves T_{avg} up to 11.3% (resp. 24.8%), compared with the notification of $\boldsymbol{p}_{\mathcal{C}_i}^{(i)}$ (resp. the notification of $\boldsymbol{p}_{\mathcal{C}_i}^{(m)}$).

Next, we focus on the breakdown of the average travel time T_{avg} of the proposed scheme: Average travel time among ρN users with the proposed scheme, $T_{\mathrm{avg}}^{(\rho)}$, and that among the remaining $(1-\rho)N$ users without the proposed scheme, $T_{\mathrm{avg}}^{(1-\rho)}$. Fig. 2.9 illustrates the impact of the penetration ratio ρ on $T_{\mathrm{avg}}^{(\rho)}$ and $T_{\mathrm{avg}}^{(1-\rho)}$. We find that $T_{\mathrm{avg}}^{(\rho)}$ can improve by up to 3.3 [min] (16.2%) compared with $T_{\mathrm{avg}}^{(1-\rho)}$ in the range of $0.1 \leq \rho \leq 0.9$. This performance improvement can be the motivation for users to follow the proposed scheme, which will contributes to its rapid penetration.

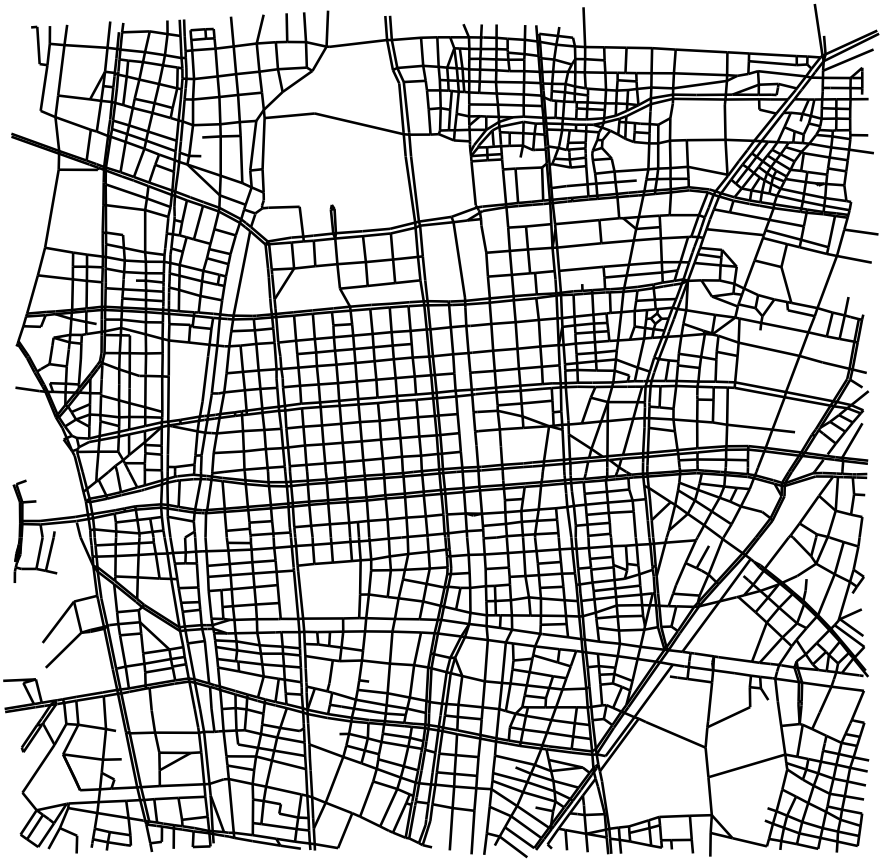

Figure 2.10. 4.7 [km] × 4.5 [km] east area of Nagoya station in Japan [1].

2.5.3 Evaluation under a Local-Level Real Road Network

In this section, we present the performance of the proposed scheme under the local-level real road network, i.e., the central part of Nagoya city, Japan.

2.5.3.1 Evaluation Model

Fig. 2.10 illustrates the target area of 4.7 [km] × 4.5 [km] east area of Nagoya station in Japan. We use the digital road map provided by Japan Digital Road Map Association [1], in which the internal graph structure is composed of 3,173 vertices and 5,013 edges. This map also has important attribute information of each road, i.e., road length, the number of lanes, and speed limit, which can be used for parameters ($\underline{t}_e$ and c_e) of the BPR function $t_e(f_e) = \underline{t}_e(1 + \alpha(f_e/c_e)^\beta)$.

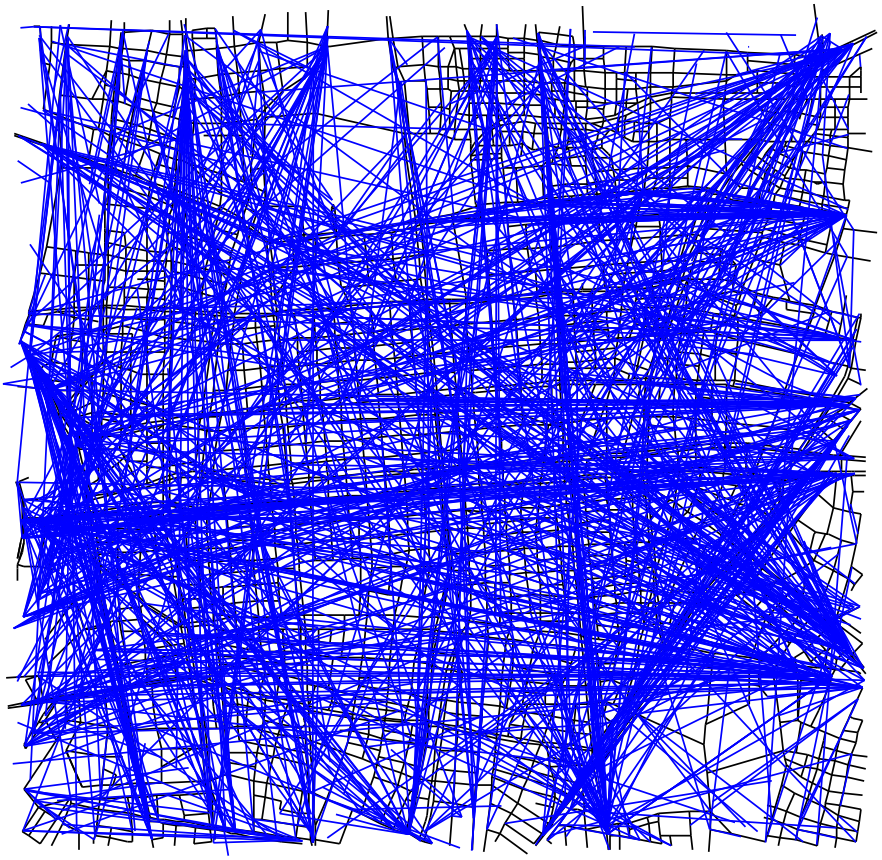

Figure 2.11. The pairs of origin and destination for each user based on the people flow data [2, 3].

Table 2.4. T_{avg} and $T_{\max}$ (real road network case).

Scheme	T_{avg} [min]	$T_{\max}$ [min]
Notification of $\boldsymbol{p}_{\mathcal{C}_i}^{(i)}$ (User equilibrium)	6.13	70.4
Notification of $\boldsymbol{p}_{\mathcal{C}_i}^{(m)}$	12.5	174
Proposed scheme	4.96	68.5
Optimal routing (Social optimum)	4.93	68.5

We set $\underline{t}_e$ by considering the road length and the speed limit, and c_e based on the number of lanes. As for α and β, we use the same settings, i.e., $\alpha = 0.15$ and $\beta = 4$.

To make the evaluation scenario more realistic, we also use the ordinary flow of people in the target area. In case of Nagoya city, Japan, we can also obtain such data called people flow data [2, 3], which describe the flow of people in a certain area during one day. The people flow data presents the number of people in the target road network and each person's origin and destination with its transportation method at a certain interval, e.g., an hour. In what follows, we focus on the start of office hours, i.e., 8:00–8:59, where 1,197 vehicle users exist in the road network. Fig. 2.11 illustrates the corresponding origin and destination pairs as blue lines.

2.5.3.2 Average and Maximum Travel Time among Users

Table 2.4 presents average (resp. maximum) travel time among all users, T_{avg} (resp. $T_{\max}$), among four schemes, i.e., the proposed scheme, Notification of $\boldsymbol{p}_{\mathcal{C}_i}^{(i)}$, Notification of $\boldsymbol{p}_{\mathcal{C}_i}^{(m)}$, and optimal routing. We first observe that the proposed scheme can improve T_{avg} and $T_{\max}$ by 1.17 [min] (19.1%) and 1.9 [min] (2.7%), compared with the notification of $\boldsymbol{p}_{\mathcal{C}_i}^{(i)}$, respectively. We also observe that the PoA of each scheme becomes 1.24, 2.54, and 1.01, in case of notification of $\boldsymbol{p}_{\mathcal{C}_i}^{(i)}$, notification of $\boldsymbol{p}_{\mathcal{C}_i}^{(m)}$, and proposed scheme, respectively. The real road network case does not have a more complex graph structure but also have biased traffic demand, i.e., the origin and destination of users, compared with the grid-like network case. The proposed scheme can effectively distribute the traffic load as in the optimal routing, and thus the improvement ratio is larger than that of the

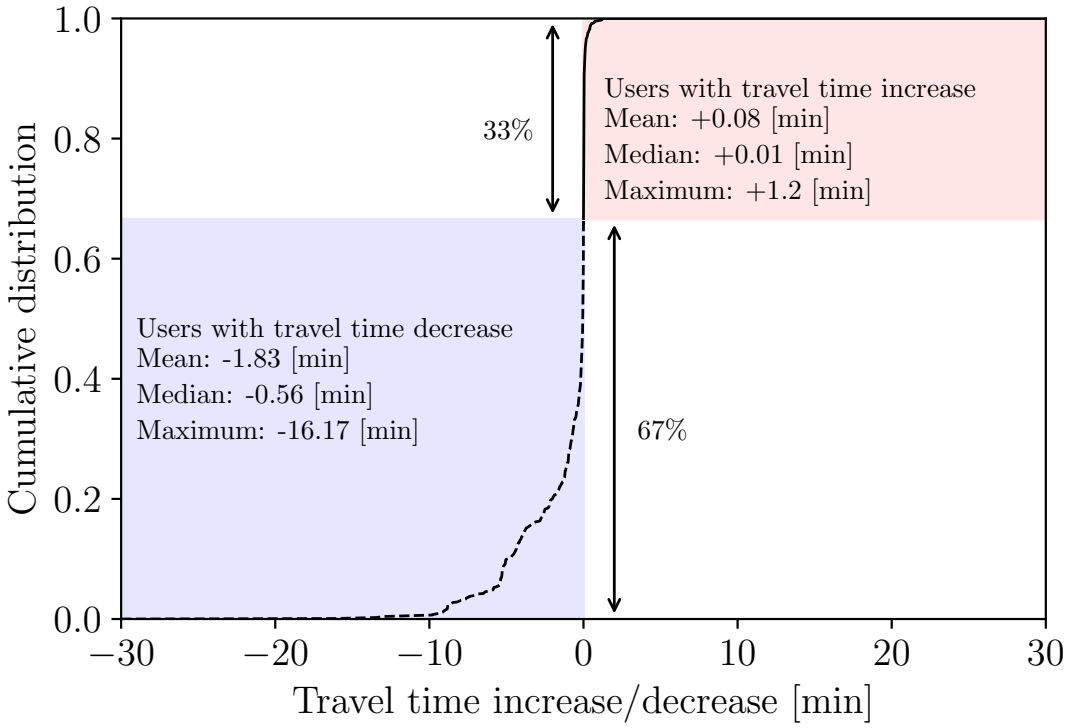

Figure 2.12. Cumulative distribution of users with travel time increase/decrease (real road network case).

grid-like network.

2.5.3.3 Individual Travel Time Increase/Decrease

Next, we focus on the degree of optimality in terms of the travel time for each user in case of the proposed scheme. Fig. 2.12 illustrates the cumulative distribution of users with travel time increase/decrease, i.e., the difference between $T_i(\cdot)$ of the proposed scheme and that of the notification of $\boldsymbol{p}_{\mathcal{C}_i}^{(i)}$. We observe that the proposed scheme can reduce the travel time among 67% users with average (resp. maximum) travel time decrease of 1.83 [min] (23.1%) (resp. 16.17 [min]), compared with the notification of $\boldsymbol{p}_{\mathcal{C}_i}^{(i)}$. On the other hand, as for the remaining 33% users, we observe that the average (resp. maximum) travel time increase is limited, 0.08 [min] (2.9%) (resp. 1.2 [min]). The above-mentioned results show that the proposed scheme can improve the travel time for most users with a slight

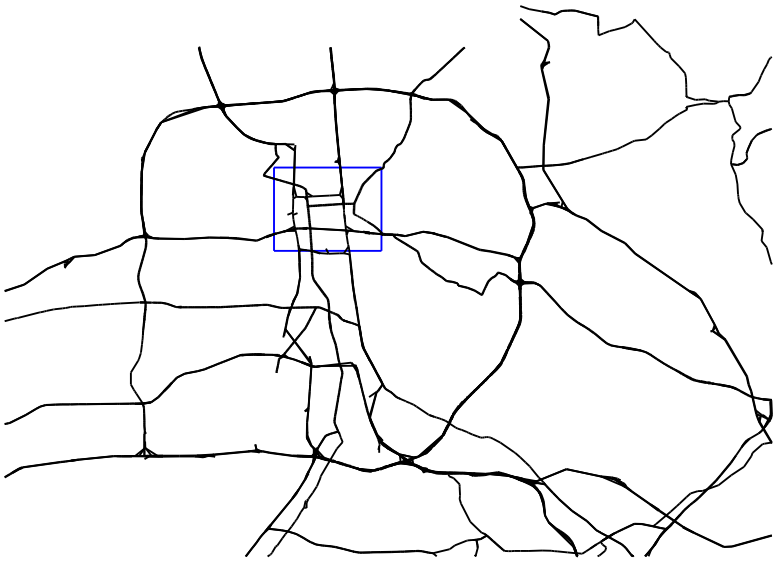

Figure 2.13. 33.9 [km] × 29.7 [km] area of Nagoya city in Japan [1].

increase of that for the remaining users.

2.5.4 Evaluation under a City-Level Real Road Network

In this section, we present the performance of the proposed scheme under the city-level real road network, i.e., the whole area of Nagoya city, Japan.

2.5.4.1 Evaluation Model

Fig. 2.13 depicts the target area of 33.9 [km] × 29.7 [km] area of Nagoya city in Japan, which is provided by Japan Digital Road Map Association [1]. The blue rectangle in Fig. 2.13 corresponds to the east area of Nagoya station in Fig. 2.10. The internal graph with 5,070 vertices and 6,332 edges consists of the major arterial roads in Nagoya city. As with the evaluation scenario at the local level, we also use the people flow data [2,3] in the target area. In what follows, we also focus on the relatively crowded time period, i.e., start of office hours (8:00–8:59), where 10,004 vehicle users exist in the road network.

Table 2.5. T_{avg} and $T_{\max}$ (real road network case).

Scheme	T_{avg} [min]	$T_{\max}$ [min]
Notification of $\boldsymbol{p}_{\mathcal{C}_i}^{(i)}$ (User equilibrium)	9.98	88.5
Notification of $\boldsymbol{p}_{\mathcal{C}_i}^{(m)}$	11.6	124.9
Proposed scheme	9.24	70.7
Optimal routing (Social optimum)	9.21	70.1

2.5.4.2 Average and Maximum Travel Time among Users

Table 2.5 presents average (resp. maximum) travel time among all users, T_{avg} (resp. $T_{\max}$), among four schemes, i.e., the proposed scheme, Notification of $\boldsymbol{p}_{\mathcal{C}_i}^{(i)}$, Notification of $\boldsymbol{p}_{\mathcal{C}_i}^{(m)}$, and optimal routing. We observe that the proposed scheme improves T_{avg} and $T_{\max}$ by 0.74 [min] (7.4%) and 17.8 [min] (20.1%), compared with the notification of $\boldsymbol{p}_{\mathcal{C}_i}^{(i)}$, respectively. We also observe that the proposed scheme has almost the same performance as the optimal routing. We confirm that the PoA of each scheme becomes 1.08, 1.26, and 1.00, in case of notification of $\boldsymbol{p}_{\mathcal{C}_i}^{(i)}$, notification of $\boldsymbol{p}_{\mathcal{C}_i}^{(m)}$, and proposed scheme, respectively.

2.5.4.3 Individual Travel Time Increase/Decrease

Fig. 2.14 depicts the cumulative distribution of users with travel time increase/ decrease, i.e., the difference between $T_i(\cdot)$ of the proposed scheme and that of the notification of $\boldsymbol{p}_{\mathcal{C}_i}^{(i)}$. We observe that the proposed scheme reduces the travel time among 40% users with the average (resp. maximum) travel time decrease of 2.01 [min] (14.7%) (resp. 40.8 [min]), compared with the notification of $\boldsymbol{p}_{\mathcal{C}_i}^{(m)}$. On the other hand, the average (resp. maximum) travel time increase is limited, 0.1 [min] (1.3%) (resp. 2.1 [min]).

2.6. Summary

Traffic congestion in urban areas is mainly caused by selfish routing of users and results in considerable economic and time loss. In this thesis, we have proposed a scheme to achieve selfish yet optimal routing by adjusting the perceived traffic information, which is inspired by the concept of "Nudge." Selfish yet optimal

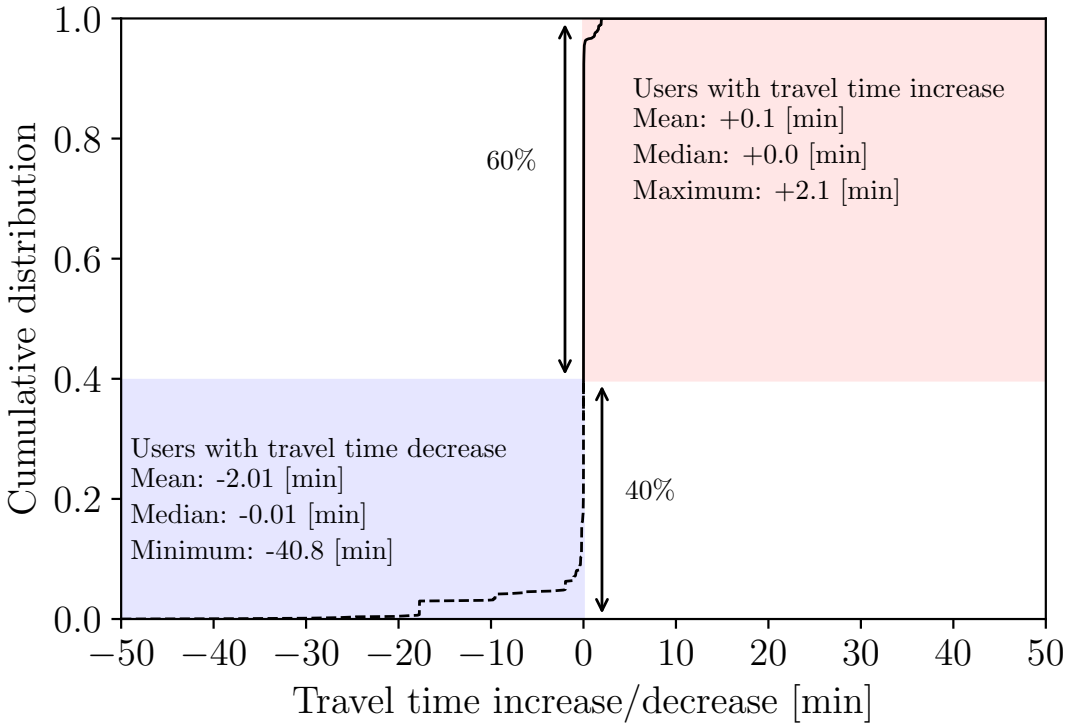

Figure 2.14. Cumulative distribution of users with travel time increase/decrease (real road network case).

routing internalizes the marginal cost into the perceived traffic information. In the proposed scheme, the server first calculates the social optimum route choice probability for each user. Then, it derives the nudging traffic information, which leads the selfish routing to the social optimum routing, and notifies it to each user. After retrieving the nudging traffic information, each user finds the selfish route choice probability under the perceived traffic information.

Through the numerical experiments under the grid-like road network, we have evaluated the following fundamental characteristics of the proposed scheme: (1) the proposed scheme achieves almost the same performance as the optimal routing and (2) it can improve the travel time of 82% users with the average travel time decrease of 0.77 [min], compared with the notification of $\boldsymbol{p}_{\mathcal{C}_i}^{(i)}$.

Furthermore, we have also evaluated the practicality and scalability of the proposed scheme under the local-level and city-level road networks of Nagoya

city. We have observed that the proposed scheme can improve the average travel time by 19.1% (resp. 7.4%), compared with the notification of $\boldsymbol{p}_{\mathcal{C}_i}^{(i)}$, in case of the local-level (resp. city-level) road network with 1,197 (resp. 10,004) users. From the viewpoint of individual travel time under the local-level (resp. city-level) road network, the proposed scheme can reduce the travel time among 67% (resp. 40%) users with the average travel time decrease of 1.83 [min] (resp. 2.01 [min]) while suppressing the average travel time increase among the remaining users by 0.08 [min] (resp. 0.1 [min]).

Chapter 3

Distributed Route Selection under Consideration of Time Dependency among Agents' Road Usage in Ordinary Situations

3.1. Introduction

It has been well-known that the traffic congestion problem can be modeled as a congestion game in game theory by regarding roads as resources. Since the route selection of one agent results in the use of roads composing the corresponding route, the route selection of all agents determines the assignment of agents to roads, which will finally determine the travel time of each agent. It is rational for each agent to select a route that seems to have the minimum travel time from its route candidates. Such route selection is called selfish routing and results in a Wardrop equilibrium where each agent cannot reduce its travel time by changing the route [10, 28].

Since the classical congestion game assumes that each player can select one or more resources at the same time, its straightforward extension to the traffic congestion problems also assumes the static flow where each agent simultaneously uses the roads composing of its route during the whole time horizon of its

travel [10, 75]. However, in case of the road networks, each agent moves along with the route, which indicates that the agent will sequentially use the roads in the route.

Ford and Fulkerson introduced the concept of flow over time to deal with the congestion over time [76, 77]. They also proposed a time-expanded network that contains one copy of the static network for each discrete time step. The time-expanded network enables us to use the algorithms designed for the static flow assumption at the expense of the enormous network size.

Lim and Rus proposed a distributed route selection scheme for each agent under the assumption of the classical congestion game [22]. In [22], each agent in the road network autonomously calculates the route choice probabilities for its route candidates by using a gradient descent method such that its expected travel time is minimized. This scheme regards the route choice probability of each agent as the fractional flow under the assumption that the number of agents on the road network is sufficiently large. As a result, the flow on a road can be expressed by the probabilistic occupation for agents [62, 64, 65].

In this paper, we propose a multi-agent distributed route selection scheme considering the time dependency among agents' road usage for vehicular networks. The proposed scheme comprises of the following two procedures. First one is the estimation of the time-dependent competitive relationship among agents considering a time dependency among agents' road usage. Second one is the distributed route selection based on a gradient descent method with the time-dependent flow information, which is an expanded version of the existing scheme in [22].

The main contributions of the manuscript are as follows:

1. We propose the multi-agent route selection considering the time dependency among agents' road usage in a distributed manner.

2. Through the numerical and simulation results, we show that the proposed scheme can improve the actual travel time by 5.1% compared with the existing scheme [22], with the help of the accurate estimation of the congestion levels.

3. We confirm that the proposed scheme can exponentially converge to the steady-state as in the existing scheme [22].

The rest of the manuscript is organaized as follows. Section 3.2 gives related work. We introduce the distributed route selection scheme considering the time dependency among agents' road usage in Section 3.3. Section 3.4 demonstrates the performance of the proposed scheme through the numerical and simulation results. Section 3.5 gives the conclusion and the future work.

3.2. Related Work

With the help of the classical congestion game, Lim and Rus proposed the multi-agent distributed route selection scheme under the assumption of the static flow [22]. This scheme interprets the route choice probability of each agent as the fractional flow under the assumption that the number of agents is sufficiently large. As a result, the flow on a road can be expressed by the agents' probabilistic occupation [62, 64, 65]. Each agent autonomously calculates the optimal route choice probabilities for its route candidates such that its travel time will be minimized. Note that the authors proved that each agent's rational route selection results in the Wardrop equilibrium.

Ford and Fulkerson first introduced the concept of the flow over time and the time-expanded network [76, 77]. In contrast to the static flow, the flow over time assumes that the flow on a road dynamically changes. The time-expanded network contains one copy of the static network for each discrete time step. The flow over time in the static network can be interpreted as the static flow in the time-expanded network. Such time-expanded network uses the fixed travel time of the road under the assumption that the capacity of the edge limits the flow into the edge at each time step [78]. Köhler et al. proposed a time-expanded graph for the flow-dependent transit time [79].

Some existing studies proved the existence of Nash equilibria for flow over time [80, 81]. Anshelevich and Ukkusuri showed the existence of Nash equilibria in single-source single-sink network where the traffic obeys the first-in-first-out (FIFO) policy [80]. Koch and Skutella introduced the congestion game with flow over time by using a deterministic queuing model [81]. In the deterministic queuing model, the traffic is regarded as the flow particles (infinitesimal flow units). The travel time of each road consists of the fixed transit time plus the

waiting time. The fixed transit time means the time that a flow particle needs to travel from the tail to the head of the road. If the traffic demand exceeds the road capacity, flow particles queue up at the end of the road in the FIFO manner. In [82–84], the authors studied the complexity properties under the competitive routing over time, Braess's paradox over time, and Stackelberg strategy over time, respectively. In this paper, we consider the time-dependent competitive relationship among agents in a different way compared with the time-expanded network and the deterministic queuing model.

There were several studies on predictive traffic congestion model [85,86]. Kong et al. proposed an approach for urban traffic congestion prediction and estimation by using the floating car trajectory data [85]. Fouladgar et al. proposed an urban traffic congestion prediction scheme using a deep neural network for modeling traffic flow [86]. Such predictive traffic congestion models would help the proposed scheme to estimate the time-dependent flow more accurately.

The congestion-aware routing using traffic data was also studied [87, 88]. Afshar-Nadjafi and Afshar-Nadjafi formulated a mixed integer problem for time-dependent vehicle routing to minimize the travel cost and proposed the heuristic algorithm [87]. Rossi et al. addressed the congestion-aware routing for autonomous vehicles and proposed an optimization method to minimize the congestion by allocating empty vehicles to non-crowded routes in a capacitated road network [88].

3.3. Distributed Route Selection under Consideration of Time Dependency among Agents' Road Usage

In this section, we propose a multi-agent distributed route selection scheme considering the time dependency of the agents' road usage, which is an extended version of the existing scheme [22].

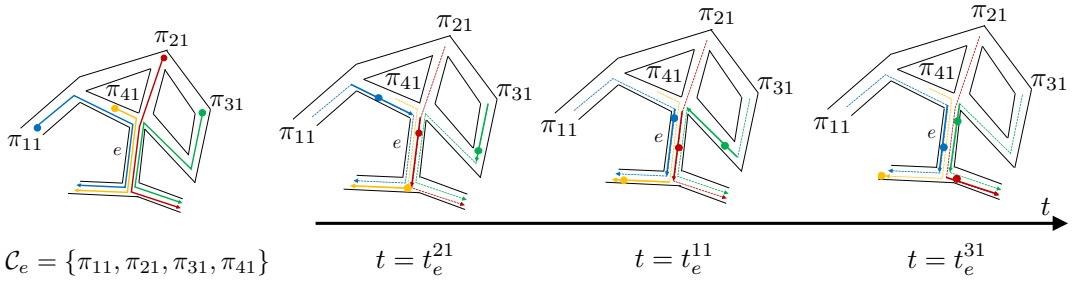

(a) Static flow case. (b) Time-dependent flow case.

Figure 3.1. Probabilistic occupation of road e by corresponding agent's routes.

Table 3.1. Notation.

Symbol	Description
G	A directed graph representing road network $G = (\mathcal{V}, \mathcal{E})$
$\mathcal{V}$	A set of vertices
$\mathcal{E}$	A set of edges
$\mathcal{N}$	A set of agents
$\boldsymbol{\pi}_i$	A vector of route candidates for agent i, $(\pi_{i1}, \ldots, \pi_{iK_i})$
$\boldsymbol{p}_i$	A vector of route choice probabilities for agent i, $(p_{i1}, \ldots, p_{iK_i})$
$\mathcal{K}_i$	A set of indices of routes for agent i, $\{1, \ldots, K_i\}$
$\mathcal{C}_e$	A set of routes that include edge e
$\mathcal{C}_e^{ik}$	A set of routes that include edge e where the probabilistic occupation by agents following that route
f_e	Flow of edge e

3.3.1 Preliminaries

$G = (\mathcal{V}, \mathcal{E})$ denotes a graph representing the internal structure of the road network, where $\mathcal{V}$ denotes a set of vertices (i.e., intersections) and $\mathcal{E}$ denotes a set of edges (i.e., roads). There are N ($N > 0$) agents (e.g., vehicles) in the road network and $\mathcal{N} = \{1, \ldots, N\}$ denotes a set of agents. Each agent $i \in \mathcal{N}$ first calculates K_i ($K_i > 0$) candidate routes $\boldsymbol{\pi}_i = (\pi_{i1}, \ldots, \pi_{iK_i})$ where route π_{ik} is the agent i's kth route candidate, which is a vector of edges composing of the corresponding route. Let $\mathcal{K}_i = \{1, \ldots, K_i\}$ be a set of the corresponding route indices.

Next, each agent $i \in \mathcal{N}$ calculates route choice probabilities $\boldsymbol{p}_i = (p_{i1}, \ldots, p_{iK_i})^\mathsf{T}$ where p_{ik} $(0 \leq p_{ik} \leq 1)$ denotes the probability that agent i selects the kth route. Note that $\sum_{k \in \mathcal{K}_i} p_{ik} = 1$ and $\boldsymbol{p}_i$ can also be regarded as the mixed strategy in game theory [59]. We assume that each agent $i \in \mathcal{N}$ collects the route choice probabilities $\boldsymbol{p}_j$ of competing agents $j \in \mathcal{N}_i$ through communication networks (e.g., cellular networks and vehicular networks). (The definition of $\mathcal{N}_i$ will be given in Section 3.3.2.) Then, each agent i calculate $\boldsymbol{p}_i$ using a gradient descent method and $\boldsymbol{p}_j$ $(j \in \mathcal{N}_i)$. Finally, each agent i selects a certain route, π_{ik^*}, according to the route choice probabilities $\boldsymbol{p}_i$. We assume that the route calculation is periodically conducted at a certain interval I_M $(I_\mathrm{M} > 0)$ to suppress the estimation error and adapt to environmental changes, e.g., new agent arrivals.

If the number of agents is large, we can regard the route choice probability p_{ik} $(i \in \mathcal{N}, k \in \mathcal{K}_i)$ as the fractional flow as in [60–62]. Therefore, the flow on a road can also be interpreted as the probabilistic occupation by the corresponding agent's route. In the classical congestion game, the probabilistic occupation of a road is assumed to be static during the whole time horizon of the agent's travel [62,64,65]. Fig 3.1 illustrates an example of the probabilistic occupation of road e by four agents' routes (i.e., $\{\pi_{11}, \pi_{21}, \pi_{31}, \pi_{41}\}$). In case of the static flow assumption, the flow on road e, f_e, is defined as the sum of the corresponding route choice probabilities:

$$f_e = \sum_{\pi_{jl} \in \mathcal{C}_e} p_{jl}, \tag{3.1}$$

where $\mathcal{C}_e$ denotes a set of each agent's route that includes road e. Table 3.1 summerizes the notations used in this paper.

3.3.2 Time Dependency among Agents' Road Usage

Since each agent travels along a route, its probabilistic occupation of each road in the route will sequentially happen as shown in Fig. 3.1b. In this case, the static flow assumption, where all the roads composing the route are simultaneously and continuously used, should be reconsidered. When the agent 1 following the route π_{11} just enters the road e at the time t_e^{11}, the agent 2 following the route π_{21} is only the leading competitor on the road e. Then, the agent 1 will have the agent

3 as its follower on the road e at its arrival on the road e at the time t_e^{31}. Note that the agent 1's movement on the road e will be affected only by its leading agent, i.e., agent 2.

As a result, we can define a set of time-dependent competitive routes of the road e for the agent i following the route π_{ik}:

$$\mathcal{C}_e^{ik} = \{\pi_{jl} \in \mathcal{C}_e \mid t_e^{jl} \leq t_e^{ik} \leq t_e^{jl} + \widetilde{t}_e\}. \tag{3.2}$$

t_e^{ik} denotes the inflow time when the agent i following π_{ik} enters road e. $\widetilde{t}_e$ denotes the estimated travel time on the road e. (The estimation method will be discussed in the next section.) $t_e^{jl} + \widetilde{t}_e$ denotes the outflow time when the agent j following π_{jl} exits the road e. The condition $t_e^{jl} \leq t_e^{ik} \leq t_e^{jl} + \widetilde{t}_e$ guarantees that the agent j following π_{jl} leads the agent i following π_{ik} on the road e, and thus becomes the competitor. Note that this model assumes that all agents obey the FIFO policy and C_e^{ik} does not change until the agent i following π_{ik} exits the road e. Using $\mathcal{C}_e^{ik}$, we can express the time-dependent flow on the road e for the agent i's route π_{ik}.

$$f_e^{ik} = \sum_{\pi_{jl} \in \mathcal{C}_e^{ik}} p_{jl}. \tag{3.3}$$

Furthermore, the competitors of the agent $i \in \mathcal{N}$ can be defined as the following set:

$$\mathcal{N}_i = \{j \in \mathcal{N} \setminus \{i\} \mid \exists l \in \mathcal{K}_j,\ \pi_{jl} \in \cup_{k \in \mathcal{K}_i} \mathcal{C}_e^{ik}\}.$$

Each agent i collects the route choice probabilities $\boldsymbol{p}_j$ of competitors $j \in \mathcal{N}_i$ through communication networks.

3.3.3 Distributed Route Selection under Consideration of Time-Dependent Road Usage

In this section, we show how the distributed route selection scheme calculates the optimal route choice probability under the consideration of the time dependency among agents.

The cost of route π_{ik} for agent i can be expressed by the sum of cost of each road along route π_{ik}.

$$c_{ik} = \sum_{\forall e \in \pi_{ik}} c_e(f_e^{ik}), \tag{3.4}$$

where $c_e(\cdot)$ denotes the cost of the road e under the flow f_e^{ik}, which is a non-decreasing function. From Eqs. (3.2) and (3.3), we should note here that $c_e(\cdot)$ depends on $\widetilde{t}_e$. This is a kind of the chicken or egg situations, and thus it is hard to obtain accurate $\widetilde{t}_e$ for each road $e \in \mathcal{E}$ before calculating the path cost c_{ik} ($i \in \mathcal{N}, k \in \mathcal{K}_i$). In this paper, we simply regard $\widetilde{t}_e$ as the lower bound of travel time on the road e, $\underline{t}_e$, which is the travel time without any congestion on the road e. In Section 3.4.2, we will show this simple assumption contributes to the congestion alleviation but we also plan to apply more sophisticated estimation methods [85, 86].

We assume that each agent $i \in \mathcal{N}$ measures the goodness of the current route choice probabilities $\boldsymbol{p}_i$ based on the local cost V_i [22]:

$$V_i = \sum_{k \in \mathcal{K}_i} p_{ik} c_{ik} - c_{id_i} = \sum_{k \in \mathcal{K}_i} p_{ik}(c_{ik} - c_{id_i}), \tag{3.5}$$

where $d_i = \arg\min_{k \in \mathcal{K}_i} c_{ik}$. Eq. (3.5) means the difference between the expected path cost under $\boldsymbol{p}_i$ and the minimum path cost. It is rational for each agent i to aim at adjusting the route choice probabilities $\boldsymbol{p}_i$ such that V_i approaches to 0. $V_i = 0$ leads to the following two conditions of Wardrop equilibrium [22]:

$$\begin{cases} c_{ik} = c_{id_i}, & \text{if } p_{ik} > 0, \\ c_{ik} \geq c_{id_i}, & \text{otherwise.} \end{cases}$$

The first condition means that each agent $i \in \mathcal{N}$ selects the minimum-cost path while the second one indicates that unselected paths have equal or larger cost than the minimum cost.

The global cost V is defined as the sum of the local cost V_i of all agents $i \in \mathcal{N}$ [22]:

$$V = \sum_{i \in \mathcal{N}} V_i. \tag{3.6}$$

When each agent i aims to adjust $\boldsymbol{p}_i$ such that V_i approaches to 0, V also converges to 0. As a result, Wardrop equilibrium is achieved among all agents.

In [22], a distributed gradient controller is proposed, in which each agent $i \in \mathcal{N}$ can control $\boldsymbol{p}_i$ such that $V_i = 0$ in a distributed manner. The distributed gradient controller governs the time derivative of the route choice probabilities using the competitors' current route choice probabilities. We propose the distributed gradient controller considering the time dependency of the agents' road usage, which is the extended version of the existing scheme [22].

We can obtain the local cost increase of the route π_{ik}, w_{ik}, by a small change in p_{ik}:

$$w_{ik} = \sum_{j \in \mathcal{N}_i} \frac{\partial V_j}{\partial p_{ik}}. \tag{3.7}$$

From Eq. (3.5), the local cost increase of agent j by the small change in p_{ik}, $\partial V_j / \partial p_{ik}$, can be expressed by

$$\begin{aligned}
\frac{\partial V_j}{\partial p_{ik}} &= \frac{\partial}{\partial p_{ik}} \sum_{\forall l \in \mathcal{K}_j \setminus \{d_j\}} p_{jl}(c_{jl} - c_{jd_j}) \\
&= \begin{cases}
\displaystyle\sum_{\forall l \in \mathcal{K}_j \setminus \{d_j\}} p_{jl} \left(\frac{\partial c_{jl}}{\partial p_{ik}} - \frac{\partial c_{jd_j}}{\partial p_{ik}} \right) & \text{if } i \neq j, \\
\displaystyle c_{ik} - c_{id_i} + \sum_{\forall l \in \mathcal{K}_i \setminus \{d_i\}} p_{il} \left(\frac{\partial c_{il}}{\partial p_{ik}} - \frac{\partial c_{id_i}}{\partial p_{ik}} \right) & \text{if } i = j.
\end{cases}
\end{aligned}$$

The cost increase of π_{jl} by the small change in p_{ik}, $\partial c_{jl} / \partial p_{ik}$, is expressed by the sum of each edge's cost increase. Since the small change in p_{ik} only affects the cost of edges shared by both π_{ik} and π_{jl}, we can express $\partial c_{jl} / \partial p_{ik}$ as follows:

$$\begin{aligned}
\frac{\partial c_{jl}}{\partial p_{ik}} = &\sum_{e \in \pi_{ik} \cap \pi_{jl}} \mathbb{I}(\pi_{ik} \in \mathcal{C}_e^{jl}) \frac{\partial c_e(f_e^{jl})}{\partial f} \\
&- \sum_{e \in \pi_{id_i} \cap \pi_{jl}} \mathbb{I}(\pi_{id_i} \in \mathcal{C}_e^{jl}) \frac{\partial c_e(f_e^{jl})}{\partial f},
\end{aligned}$$

where $\mathbb{I}(\cdot)$ denotes an indicator function. The right-hand side of the equation denotes the sum of the cost derivative in the edge level when the corresponding route is included in the set of time-dependent competitive routes of the road e

for the agent j following the route π_{jl}. Note that p_{id_i} may also change depending on the small change in p_{ik}.

As in [22], we can finally obtain the following distributed gradient controller per unit time of τ ($\tau > 0$):

$$\frac{d\boldsymbol{p}_i}{d\tau} = -\gamma V_i \frac{\boldsymbol{y}_i - (\mathbf{1}_{K_i}^{\mathsf{T}} \boldsymbol{y}_i)\boldsymbol{e}_{d_i}}{||\boldsymbol{y}_i||^2}. \tag{3.8}$$

γ ($\gamma > 0$) denotes a learning rate. $\mathbf{1}_{K_i}$ denotes a column vector of size K_i with all elements set to be 1. $\boldsymbol{e}_{d_i}$ denotes a column vector of size K_i, where d_ith element is set to be 1 and the remaining elements are set to be 0. $\boldsymbol{y}_i = (y_{i1}, \ldots, y_{iK_i})^{\mathsf{T}}$ is defined as follows for $k \neq d_i$:

$$y_{ik} = \begin{cases} 0 & \text{if } p_{ik} = 0, w_{ik} > 0 \text{ or } p_{ik} = 1, w_{ik} < 0, \\ w_{ik} & \text{otherwise.} \end{cases} \tag{3.9}$$

When each agent $i \in \mathcal{N}$ adjusts $\boldsymbol{p}_i$ according to Eq. (3.8), the global cost V reaches to zero, and thus the Wardrop equilibrium is achieved.

3.4. Simulation Results

In this section, we demonstrate the fundamental characteristic of the proposed scheme.

3.4.1 Evaluation Model

To evaluate the fundamental characteristic of the proposed scheme, we use a grid road network consisting of 50×50 nodes (intersections). There are fifty agents ($N = 50$) and each agent $i \in \mathcal{N}$ travels from node $(i, 1)$ to node $(i, 50)$. Note that $(1, 1)$ (resp. $(50, 50)$) is the left-top (resp. right-bottom) node of the grid network. We assume that travel time of each road $e \in \mathcal{E}$ follows the BPR function [70], i.e., $t_e(f_e) = \underline{t}_e(1+\alpha(f_e/c_e)^\beta)$ where $\underline{t}_e$ denotes the travel time without any congestion on the road e, and c_e denotes the capacity of the road e. α and β represent the degree of the traffic congestion. For each road e, we randomly set $\underline{t}_e$ (resp. c_e) in the range of $[0, 1]$ (resp. $[2, 4]$). We also use $\alpha = 0.15$ and $\beta = 4$.

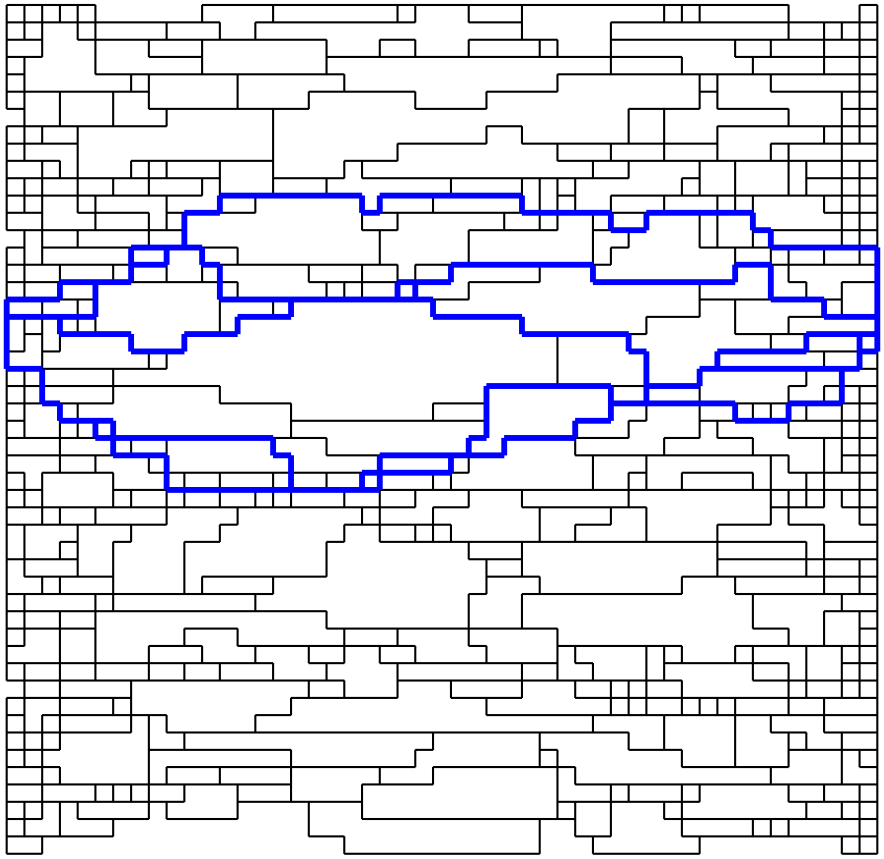

Figure 3.2. Route candidates $\boldsymbol{\pi}_{25}$ for agent 25 (blue lines) and route candidates $\{\boldsymbol{\pi}_j\}_{\forall j \in \mathcal{N}}$ for all agents (black lines).

Each agent $i \in \mathcal{N}$ obtains $K_i = 5$ route candidates $\boldsymbol{\pi}_i$ according to the following procedure. Each agent $i \in \mathcal{N}$ first calculates the shortest route from the origin, i.e., node $(i, 1)$, to the destination, i.e., node $(i, 50)$, when the flow of the agent i only exists, i.e., $t_e(1) = \underline{t}_e(1 + \alpha(1/c_e)^\beta)$. Next, it obtains the second route candidate by calculating the shortest route from the origin to the destination under the assumption that the predefined number of road segments, i.e., 30, in the shortest route are unavailable. By repeating this procedure, each agent $i \in \mathcal{N}$ obtains K_i route candidates $\boldsymbol{\pi}_i$, which are exclusive to each other as much as possible. Fig. 3.2 illustrates an example of route candidates for all agents and those for agent 25 are highlighted by blue color.

As for evaluation criteria, we use the estimated travel time and the actual

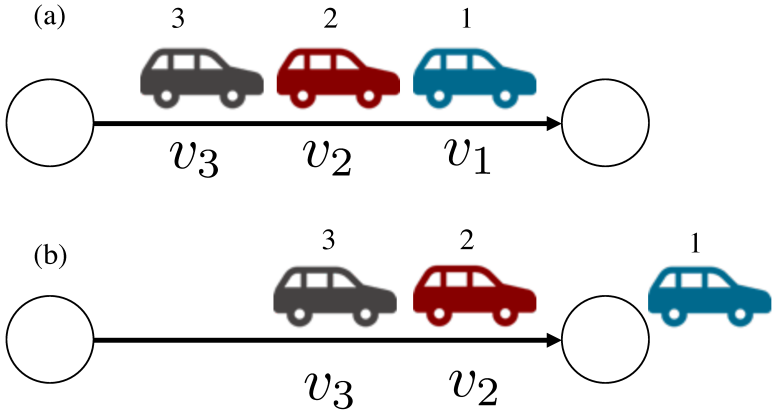

Figure 3.3. Congestion model.

one. The estimated travel time for agent i, $\widetilde{T}_i$, is defined as the weighted sum of the travel time corresponding each route π_{ik}.

$$\widetilde{T}_i = \sum_{k \in \mathcal{K}_i} p^*_{ik} \sum_{e \in \pi_{ik}} t_e(f_e^{ik}), \tag{3.10}$$

where the weights are given by $\boldsymbol{p}^*_i$, which is derived by the distributed gradient controller in Section 3.3. On the other hand, the actual travel time for each agent i, T_i, is the difference between arrival time to a destination and departure time from a origin.

To obtain the actual travel time T_i, i.e., the elapsed time between the departure from the origin and the arrival at the destination, for each agent $i \in \mathcal{N}$, we implemented a Java simulator. In what follows, we assume that the control interval I_{M} is sufficiently large and the route calculation is conducted once at the beginning of the simulation. Each agent $i \in \mathcal{N}$ first calculates the route choice probabilities $\boldsymbol{p}^*_i$, and then selects one of the candidates, k^*_i, according to $\boldsymbol{p}^*_i$. We define the deterministic version of $\boldsymbol{p}^*_i$ as $\widehat{\boldsymbol{p}}_i = (\widehat{p}_{i1}, \ldots, \widehat{p}_{iK_i})^{\mathsf{T}}$. $\widehat{\boldsymbol{p}}_i$ is a vector of size K_i where k^*_ith element is set to be 1 and the remaining elements are set to be 0.

Fig. 3.3 shows the congestion model used in the simulator. Suppose that three agents i ($i = 1, 2, 3$) selecting the route π_{i1} travel a road e in the same direction and in this order. We obtain $f_e^{11} = \widehat{p}_{11} = 1, f_e^{21} = \widehat{p}_{11} + \widehat{p}_{21} = 2$, and $f_e^{31} = \widehat{p}_{11} + \widehat{p}_{21} + \widehat{p}_{31} = 3$ from Eq. (2.1) (Fig. 3.3a). As a result, the agent i

Table 3.2. Estimated travel time and actual travel time (Proposed scheme and conventional scheme).

Scheme	$\widetilde{T}_i$ [min]			T_i [min]		
	avg.	max.	std.	avg.	max.	std.
Proposed scheme	23.1	25.1	1.32	22.3	24.2	1.05
Conventional scheme [22]	28.0	29.8	0.87	23.5	25.9	1.17

moves as the speed of $v_i = d_e/t_e(f_e^{i1})$ where d_e is the length of the road e. When the agent 1 exits the road e (Fig. 3.3b), the time-dependent flow for the agents 2 (resp. 3) is updated to $f_e^{21} = \widehat{p}_{21} = 1$ (resp. $f_e^{31} = \widehat{p}_{21} + \widehat{p}_{31} = 2$), and thus the corresponding speed also changes.

For comparison purpose, we also use the conventional scheme, which is the distributed route selection scheme based on the classical congestion game [22], i.e., $\mathcal{C}_e^{ik} = \mathcal{C}_e$. In what follows, we show the average of 100 independent experiments.

3.4.2 Fundamental Results

Table 3.2 shows the estimated travel time $\widetilde{T}_i$ and the actual one T_i for both schemes in terms of the average and maximum values. We first focus on the difference between the estimated travel time and actual one for each scheme. We observe that the proposed scheme can more accurately estimate the travel time than the conventional scheme. In particular, the relative estimation error, i.e., $(\widetilde{T}_i - T_i)/T_i$, of the proposed scheme is 0.036 (resp. 0.037) in case of the average (resp. maximum) travel time, which is much smaller than that of the conventional scheme (i.e., 0.19 (resp. 0.15) in case of the average (resp. maximum) travel time).

Next, we focus on the performance difference between the proposed scheme and the conventional scheme. We observe that the proposed scheme can improve the average (resp. maximum) actual travel time by 5.1% (resp. 6.6%) compared with the conventional scheme. The static flow assumption used in the conventional scheme considers the worst congestion case while the time-dependent flow assumption in the proposed scheme seems to succeed in estimating more possible congestion level of each road.

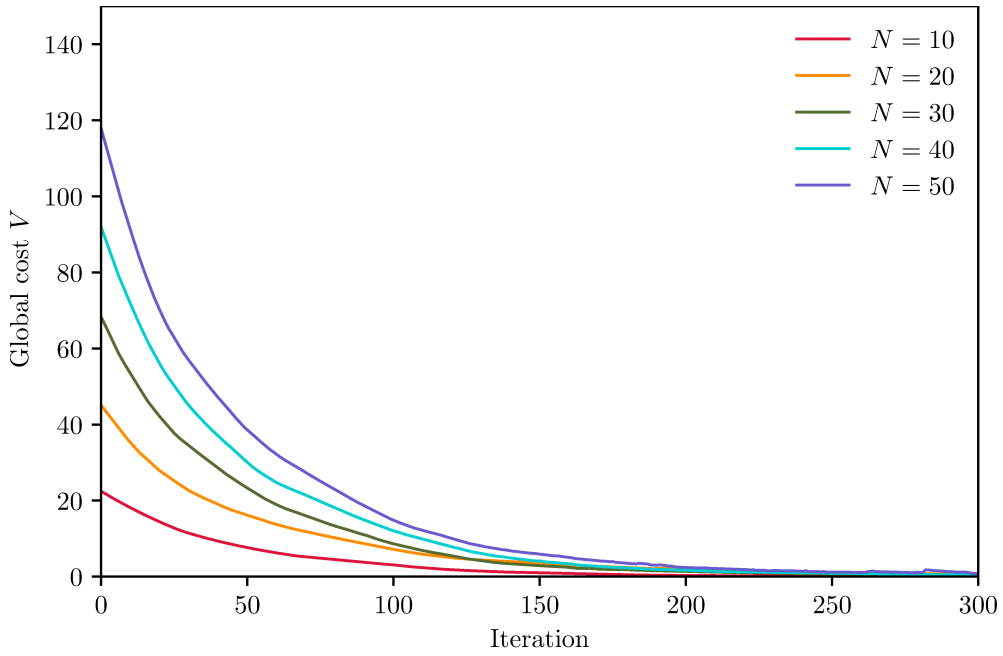

Figure 3.4. Impact of N on the convergence property ($K = 5$).

3.4.3 Convergence Property

Finally, we evaluate the convergence property of the proposed scheme. Fig. 3.4 shows the transition of the global cost V when $K = 5$ and N is set to be $10, 20, 30, 40$, and 50. In addition, Fig. 3.5 also depicts the transition of V when $N = 50$ and K is set to be $2, 3, 4$, and 5. In these figures, we first observe that the global cost V exponentially decreases with the number of iteration. We also observe that the convergence speed is in inverse proportion to both the number of agents, N, and that of candidate routes, K.

3.5. Summary

In the classical routing game, all the roads composing the route are assumed to be used simultaneously and continuously. However, this assumption should be reconsidered since the congestion level would change over time. In this paper, we have proposed a multi-agent distributed route selection scheme based on a gradient descent method considering time dependency among agents' road usage.

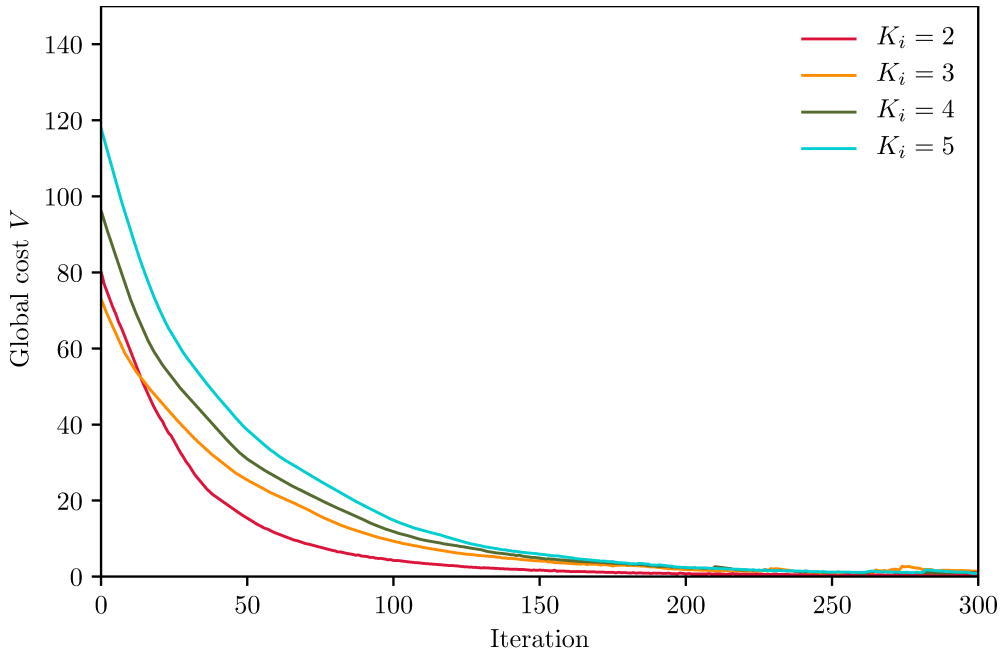

Figure 3.5. Impact of K on the convergence property ($N = 50$).

In the proposed scheme, each agents calculates the route choice probabilities by using the estimated time-dependent flow on each road in the distributed manner. Through the numerical results and the simulation results, we have shown that the proposed scheme can improve the actual travel time by 5.1%. We have also confirmed that the proposed scheme exponentially converges to the steady-state.

In future work, we plan to investigate how the proposed scheme can improve the actual travel time by controlling the interval I_{M}, which will contribute to increase the estimation accuracy at the expense of the computational complexity. In addition, we also consider to apply the existing predictive traffic congestion models to estimate the time-dependent flow more accurately. Finally, we will conduct the mathematical analysis of the convergence property.

Chapter 4

Geographical Risk Analysis Based Speedy and Reliable Path Selection in Emergency Situations

4.1. Introduction

In the 2011 Great East Japan Earthquake, both fixed and mobile communication networks have been unavailable for long time and in wide areas, due to damage of information communication infrastructures. As a result, it has been reported that there were many cases where evacuees and rescuers could not collect and distribute important information, e.g., damage information, evacuation information, and government information [89]. Evacuees quickly have to evacuate to refuges along safe routes to keep their own safety when a large-scale disaster occurs. While they can acquire static information, e.g., map and location of refuges, in usual time, they cannot grasp dynamic information, e.g., blocked road segments, until the disaster occurs.

To tackle this problem, Komatsu et al. have proposed an automatic evacuation guiding scheme based on implicit interactions between evacuees and their mobile devices [24], where communication among mobile devices is enabled by Delay

Tolerant Networks (DTNs) [90]. In this scheme, an application for evacuation guiding tries to navigate an evacuee by presenting his/her evacuation route as a recommended route using information shared between mobile devices and/or between mobile devices and cloud systems. When a large-scale disaster occurs, the application is activated automatically. Note that the application should be preinstalled into his/her mobile device in usual time. The application calculates an evacuation route from the current position to a refuge, based on the map and the location detected by Global Positioning System (GPS), and navigates the evacuee by presenting the route. In addition, the application can also grasp the actual evacuation route of the evacuee, i.e., his/her trajectory, by measuring his/her position periodically. The evacuee tries to evacuate along the recommended route. When the evacuee discovers a blocked road segment during his/her evacuation along the recommended route, he/she will take an another route by his/her own judgment. As a result of tracing his/her actual evacuation route as the trajectory, the application can detect a blocked road, which makes the difference between the recommended route and the actual evacuation route. The application can automatically estimate and record this road as a blocked road segment. We can expect that the evacuation route can be improved by sharing blocked road segments, which were discovered, when a mobile device can communicate with other mobile devices and/or the remaining communication infrastructures.

The automatic evacuation guiding scheme is a reactive approach, which can dynamically adapt to environmental changes under disaster situations. In [24], the effectiveness of the automatic evacuation guiding scheme has been evaluated in terms of the average/maximum evacuation time and the ratio of evacuees that have finished evacuating to all evacuees. They, however, do not take into account the safety of evacuation routes and the shortest path is used for the recommended route. In case of earthquakes, an evacuee has to evacuate quickly and safely by avoiding encounters with blocked road segments as much as possible. Recently, we can obtain static information to predict occurrence of blocked road segments, i.e., road blockage probability, from a certain municipality, e.g., Nagoya city in Japan [23]. (See the details in Section 4.4.1.2). We can also obtain information about geographical distribution of people in the usual time, e.g., location data collected from mobile phones and people flow data [2].

In this thesis, we propose a speedy and reliable path selection for the automatic evacuation guiding by using the geographical information about map, road blockage probabilities, and geographically population distribution in the usual time. This is a kind of proactive approach, which can be conducted before disaster occurs. We also propose a guideline of parameter determination approach for the proposed scheme to achieve both speediness and safety. Through simulation experiments, we show the validity of the proposed scheme in terms of the total number of encounters with blocked road segments and the average/maximum evacuation time. In particular, we expect that evacuation guiding with the reactive approach and proactive approach can improve evacuation movement in enormous damage environments, e.g., inferior communication environments.

The rest of this chapter is organized as follows. Section 4.2 gives related work. In Section 4.3, we explain the existing automatic evacuation guiding scheme. In Section 4.4, the proposed scheme is presented, and Section 4.5 gives simulation results. Finally, Section 4.7 provides conclusions and future work.

4.2. Related Work

There are several existing studies on evacuation guiding supported by information and communication technology (ICT) [24, 91–93]. Iizuka et al. propose an evacuation guiding scheme which presents evacuees evacuation paths and evacuation timing to avoid traffic jams, by using an ad-hoc network [91]. Fujihara and Miwa propose an evacuation guiding scheme using DTN under the situations of damage to communication infrastructures [92]. It is much difficult for an evacuee to operate his/her mobile device properly even if the communication environments can be secured. In addition, evacuees may not use an evacuation guiding application and a device for the first time without understanding the operation method. Under such a background, Komatsu et al. propose an automatic evacuation guiding scheme based on implicit interactions among evacuees and their mobile devices [24]. In the existing studies, the evacuation route is selected from the viewpoint of speedy evacuation, e.g., route length. In the evacuation, safety is important as well as speediness. In this thesis, we propose a speedy and reliable path selection for the automatic evacuation guiding, which allows evacuees to

evacuate quickly while avoiding encounters with blocked road segments as much as possible.

There are several existing studies on the risk analysis after a disaster occurs [23, 94, 95]. In Japan, a certain municipality, e.g., Nagoya city, has been evaluating the regional risks, road blockage probabilities, after occurrence of a large-scale disaster [23]. Church and Cova map evacuation risks on transportation networks using a spatial optimization model, called critical cluster model, in which the whole area is dividied into multiple small areas, and the small areas with high ratio of population to exit capacity are regarded as those with high evacuation risk [94]. Since the model in [94] is only based on pre-disaster factors, i.e., population and exit capacity, Chen et al. extend this model by adding post-disaster factors, e.g., spatial impact of disaster and potential traffic jams caused by evacuation guiding [95]. In this thesis, we improve the safety of evacuation guiding by taking into account of pre-disaster factor, i.e., road blockage probability.

The concept of path reliability, which will be explained in Section 4.4.2, is inspired by road network reliability. [96–98]. There are two kinds of definitions of road network reliability: connectivity reliability and travel time reliability [96]. Connectivity reliability is defined as a probability that there exists at least one route between a source and a destination without heavy delay or road disruption. Travel time reliability is defined as a probability that traffic on the path can reach the destination within a specified time. Iida proposes a method to analyze and to evaluate the connectivity reliability, the travel time reliability, and the reliability of the links composing the road network [96]. Chen et al. analyze a road network with traffic demands by considering the connectivity reliability, the travel time reliability, and the capacity reliability [97]. Ahuja et al. propose a method to calculate the path reliability from the reliability of each link of the path [98].

When a disaster occurs, the road network might not be able to function as usual. Thus, evacuees have to select appropriate evacuation routes by taking into account of various aspects: estimated evacuation time, traveling distance, and traffic congestion. There are several studies on a multi-objective path selection [99–101]. In [100], Yuan and Wang propose path selection models for emergency logistics management, with the help of an ant colony optimization

algorithm [102], in order to select a route that minimizes both total travel time and route complexity. In [99], Lu et al. assume that the available capacities of nodes and edges of the road network may change during evacuation. They model the node capacities and edge capacities as time-series data and propose capacity constrained routing algorithms. Saadatseresht et al. propose path selection for evacuation planning with the help of the multi-objective evolutionary algorithm, where multiple factors, i.e., the distance from refuges, the capacity of refuges, and the population, are considered [101]. In this thesis, we also tackle a kind of the multi-objective path selection, which considers the path length and path reliability.

4.3. Automatic Evacuation Guiding

In this section, we introduce the overview of automatic evacuation guiding scheme in [24]. Note that we slightly extend it by adding a function to collect information about passable road segments, which will be used to calculate the reliability of evacuation path.

4.3.1 Preliminaries

$G = (\mathcal{V}, \mathcal{E})$ denotes a graph representing the internal structure of target region, where $\mathcal{V}$ is a set of vertices, i.e., intersections, and $\mathcal{E}$ is a set of edges, i.e., roads, in the map. There are N ($N > 0$) evacuees in the region and each of them has a mobile device. $\mathcal{N} = \{1, 2, \ldots, N\}$ denotes a set of the evacuees (devices). Each device $n \in \mathcal{N}$ measures and records its own locations by using GPS at intervals of I_{M} ($I_{\mathrm{M}} > 0$) just after a disaster occurs.

4.3.2 Overview

Fig. 4.1 illustrates the flow of guiding evacuee $n \in \mathcal{N}$ to a refuge. Evacuee n has pre-installed an application for evacuation guiding into his/her mobile device before a disaster occurs. The application can obtain static information, i.e., the peripheral map of target region and the location of refuges, in advance. When a disaster occurs, the application is initiated automatically. The application first

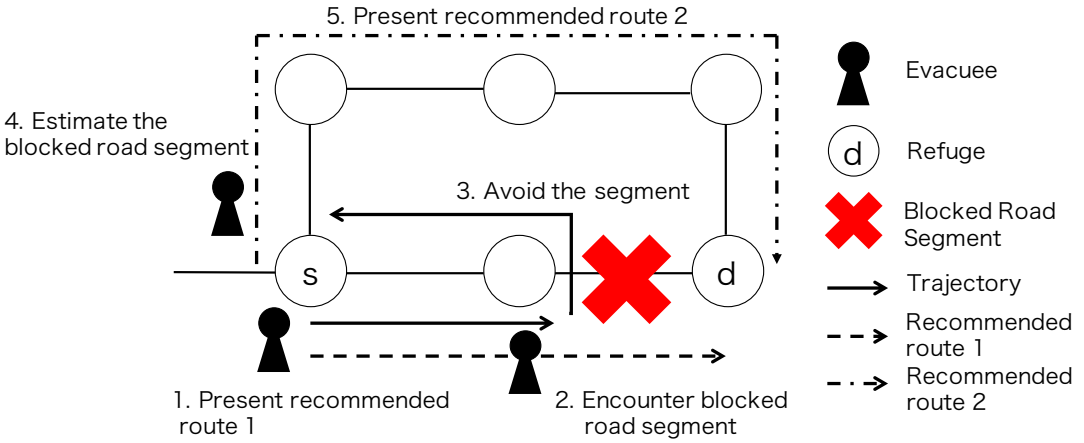

Figure 4.1. Flow of evacuation guiding.

finds out the nearest refuge $d \in \mathcal{V}$ from location $s \in \mathcal{V}$ of evacuee n. Next it calculates an evacuation route $r_{n,s,d}$ and presents him/her the route as the recommended route (Step 1 in Fig. 4.1). Recommended route $r_{n,s,d}$ between source s and destination d on map G is given by a vector of edges constructing the route. Evacuee n tries to move along recommended route $r_{n,s,d}$. When evacuee n discovers a blocked road segment during his/her evacuation along recommended route $r_{n,s,d}$ (Step 2 in Fig. 4.1), he/she will take an another route by his/her own judgement (Step 3 in Fig. 4.1). The application can trace the actual evacuation route as a trajectory by measuring his/her positions periodically, i.e., at the intervals of I_{M}. As a result, the application can detect road segment $e \in \mathcal{E}$, which makes the difference between the recommended route and the actual evacuation route. Then, the application automatically records blocked road segment e into a set of blocked road segments, $\mathcal{E}_n^{\mathrm{NG}}$ (Step 4 in Fig. 4.1). The application further recalculates a new evacuation route $r_{n,s',d}$, which does not include blocked road segments in $\mathcal{E}_n^{\mathrm{NG}}$, and presents him/her the route, from the current location s' to the nearest refuge d (Step 5 in Fig. 4.1). On the other hand, when evacuee n has passed road segment $e \in \mathcal{E}$ during his/her evacuation, the application automatically records e into a set of passable road segments, $\mathcal{E}_n^{\mathrm{OK}}$.

When the mobile device can communicate with other mobile devices and/or the remaining communication infrastructures, it tries to obtain new information about blocked road segments and passable road segments. These information will

be used to recalculate the recommended route. Evacuation guiding for evacuee n finishes when he/she reaches the refuge or the application cannot find out any evacuation route to the refuge.

4.3.3 Impact of Penetration Ratio on Evacuation Time

In actual situation, the ratio of the evacuees with the proposed application, i.e, penetration ratio ρ ($0 \leq \rho \leq 1$), might be low. In [24, Section 4.3], the authors investigated the impact of the penetration ratio of the application on the system performance in terms of the evacuation time. In this experiment, the authors assumed that the ρN evacuees with the proposed application play a role of leaders. The remaining evacuees without the proposed application first move to random destinations but follow the direction of the leaders just after encountering them. The authors showed that the average evacuation time monotonically increases with decrease of ρ but the proposed scheme is still effective even under low penetration cases. In particular, the increase of the average evacuation time when $\rho = 0.2$ can be suppressed by 14% compared with that when $\rho = 1.0$. We expect the similar tendency will be kept because the proposed scheme is based on the automatic evacuation guiding scheme [24].

4.4. Proposed Scheme

4.4.1 Geographical Information

Nowadays, we can easily use digital maps, e.g., OpenStreetMap [103] and Google Maps [14], and some of them, e.g., OpenStreetMap, can also be used even under offline environments. Moreover, we can also obtain other types of geographical information, e.g., the geographical population distribution in usual time and geographical risk, in particular areas. Evacuees can prepare these geographical information using the mobile application in advance.

4.4.1.1 Geographical Population Distribution in Usual Time

The geographical population distribution in usual time is important because it affects the initial positions of evacuations. It can be generated by location data

collected from mobile phones and/or people flow data [3]. In this thesis, we use the people flow data, which can be easily obtained. The people flow data is spatio-temporal information about movements of people, which is generated based on the person trip survey [104]. The person trip survey has been conducted for particular areas by Ministry of Land, Infrastructure and Transport and municipalities in Japan. It is a questionnaire survey that records the series of personal movements from origins to destinations, called trips. Since the person trip survey is applied to a limited number of people in the target area, an expansion factor is introduced to estimate the movement of the whole people in that area. The expansion factor of a trip means the number of people that follow that trip. Each trip is divided into one or more sub-trips such that each sub-trip has the same transportation method, e.g., walk, car, or train. Each sub-trip has some information, e.g., the origin, destination, travel time between them, and travel time. The people flow data are calculated by transforming each of sub-trip data into a series of the corresponding person's locations at a given interval, i.e., a minute. We can obtain the geographical people distribution at a certain period, e.g., one hour, by analyzing the people flow data.

4.4.1.2 Road Blockage Probability

In Japan, a municipality, e.g., Nagoya city, has been evaluating the regional risks, e.g., road blockage probabilities, which would be caused by future large-scale disasters such as Nankai Trough Earthquake [23]. Road blockage probability p_e ($0 \leq p_e \leq 1$) is an estimated probability that road segment $e \in \mathcal{E}$ is blocked due to collapse of building along the road under a certain disaster. Let $\widehat{G} = (\mathcal{V}, \mathcal{E}, g)$ denote a risk map where $g : \mathcal{E} \rightarrow \mathbb{I}$ is a real-valued function that assigns the blockage probability p_e in the closed unit interval $\mathbb{I} = [0, 1]$ to each edge $e \in \mathcal{E}$. It is calculated per road according to the three models (i.e., road model, roadside building collapse model, and road blockage model).

The road model consists of the road attributions (i.e., road length and road width) obtained from the city planning basic map. The roadside building collapse model first calculates the probability of total collapse of each building along a road according to the magnitude of an earthquake and building-related parameters (i.e., height, building year, and building type (i.e., wooden or non-wooden)).

This model assumes the worst-case scenario where all the buildings on the both roadsides would collapse and the width of road blockage (debris) caused by the building collapse would be the height of the building.

In the road blockage model, the road is considered to be blocked if the difference between the road width and height of collapsed building (i.e., the available road width) is less than $\sigma = 2$ [m], which is the minimum space for walking evacuation. More correctly, this model first divides a road e between two intersections into sections per 20 [m], which corresponds to the width of the building site, and calculates the blockage probability for each section $s \in e$, $\hat{p}_s$, according to the relationship between the road width F_e [m] and the height of the buildings on the section s's both roadsides (i.e., the height $H_{s,1}$ [m] (resp. $H_{s,2}$ [m]) of building on one (resp. another) roadside 1 (resp. 2) of the section s). Without loss of generality, $\hat{p}_s$ is defined under the assumption of $H_{s,1} \geq H_{s,2}$:

$$\hat{p}_s = \begin{cases} R_{s,1} & \text{if } F_e - H_{s,1} < \sigma \text{ and } F_e - H_{s,2} \geq \sigma, \\ 1 - (1 - R_{s,1})(1 - R_{s,2}) & \text{if } F_e - H_{s,1} < \sigma \text{ and } F_e - H_{s,2} < \sigma, \\ R_{s,1} R_{s,2} & \text{if } F_e - H_{s,1} \geq \sigma, F_e - H_{s,2} \geq \sigma, \text{ and} \\ & \quad F_e - (H_{s,1} + H_{s,2}) < \sigma, \\ 0 & \text{if } F_e - H_{s,1} \geq \sigma, F_e - H_{s,2} \geq \sigma, \text{ and} \\ & \quad F_e - (H_{s,1} + H_{s,2}) \geq \sigma, \end{cases} \tag{4.1}$$

where $R_{s,1}$ and $R_{s,2}$ denote the probability of total collapse of building on one roadside 1 and another roadside 2 of the section s, respectively. Note that $R_{s,1}$ and $R_{s,2}$ are calculated according to roadside building collapse model.

The road e is considered to be blocked when at least one section $s \in e$ is blocked according to (4.1). As a result, the road blockage probability p_e can be expressed by

$$p_e = 1 - \prod_{s \in e} (1 - \hat{p}_s).$$

Note that the longer the length of road e, d_e is, the higher the road blockage probability p_e tends to be.

4.4.2 Path Reliability

We define path reliability based on the road blockage probabilities. Since p_e is the road blockage probability, $1 - p_e$ indicates road passable probability that road segment e is passable. Path reliability can be defined as the probability that all roads $\forall e \in r$ on path r are passable. If road blockage probabilities are independent, path reliability is given by the product of road passable probabilities of all roads of the path,

$$f_{\mathrm{p}}(r) = \prod_{e \in r} (1 - p_e). \tag{4.2}$$

The path reliability takes a value in the range of $[0, 1]$ and a large (resp. small) value means high (resp. low) reliability.

We should note here that p_e of each road $e \in \mathcal{E}$ can be updated with the help of the automatic evacuation guiding [24]. In the automatic evacuation guiding, each road segment is categorized into three states: unknown, passable, and blocked. All road segments initially start from the unknown state. When a mobile device detects that road segment $e \in \mathcal{E}$ is passable (resp. blocked), p_e can be updated to zero (resp. one). These updates will contribute to selecting more reliable path selection.

4.4.3 Speedy and Reliable Path Selection

We propose a speedy and reliable path selection based on a two-step approach, where we first enumerate candidates of short paths and then select the most reliable path from the candidates. The length of path r, i.e., path length, is given by the sum of the length of all roads composing path r:

$$f_{\mathrm{d}}(r) = \sum_{e \in r} d_e,$$

where d_e denotes the length of road $e \in \mathcal{E}$. We should note here that we can also apply traveling time of road e as the road cost, instead of road length. Since the traveling time of road e increases with the number of evacuees on that road, congestion-aware path selection can be achieved [105].

Algorithm 3 presents the first step, i.e., mobile device n's enumeration of at most $k_{\max}$-shortest paths with constraint on path length, $\delta_{\max}$, which is the

Algorithm 3 Mobile device n's enumeration of at most $k_{\max}$ shortest paths with constraint on path length, $\delta_{\max}$.

Require: $\widehat{G} = (\mathcal{V}, \mathcal{E}, g), s, d, k_{\max}, \delta_{\max}$
Ensure: $\mathcal{R}_{n,s,d}^{k_{\max},\delta_{\max}}$
1: $\mathcal{R}_{n,s,d}^{k_{\max},\delta_{\max}} = \emptyset$ ▷ Initialize path candidates
2: $k = 1$
3: $r = k$-th_shortest_path$(\widehat{G}, n, s, d, k)$ ▷ Obtain shortest path
4: $d_{\min} = f_{\mathrm{d}}(r)$
5: **while** $k \leq k_{\max}$ **do** ▷ Enumerate at most $k_{\max}$ shortest paths
6: **if** $f_{\mathrm{p}}(r) == 1$ **then** ▷ If successful route for evacuation is found
7: **return** $\{r\}$
8: $\mathcal{R}_{n,s,d}^{k_{\max},\delta_{\max}} = \mathcal{R}_{n,s,d}^{k_{\max},\delta_{\max}} \cup \{r\}$
9: $k = k + 1$
10: $r = k$-th_shortest_path$(\widehat{G}, n, s, d, k)$ ▷ Obtain next candidate
11: **if** $r =$ null or $f_{\mathrm{d}}(r) - d_{\min} > \delta_{\max}$ **then** ▷ If proper next candidate is not found
12: **return** $\mathcal{R}_{n,s,d}^{k_{\max},\delta_{\max}}$
13: **return** $\mathcal{R}_{n,s,d}^{k_{\max},\delta_{\max}}$

maximum increment from the shortest path. Given risk map $\widehat{G} = (\mathcal{V}, \mathcal{E}, g)$, current location $s \in \mathcal{V}$, destination $d \in \mathcal{V}$, $k_{\max}$, and $\delta_{\max}$, mobile device $n \in \mathcal{N}$ initializes the set of path candidates, $\mathcal{R}_{n,s,d}^{k_{\max},\delta_{\max}}$, to an empty set (line 1). Next, it calculates the shortest path r using k-th_shortest_path() function with $k = 1$ and uses its path length as the lower bound of path length, $d_{\min}$ (lines 2–4). Here, k-th_shortest_path() function can be achieved by existing algorithms, e.g., Yen's algorithm [106] and Pruned Landmark Labeling based approach [107]. Then, mobile device n sequentially enumerates at most $k_{\max}$-shortest paths with constraint on path length, $\delta_{\max}$ (lines 5–12). If it finds that r is a successful route for evacuation, which consists of only passable road segments, it stops the enumeration and returns the set of the most reliable route, i.e., $\{r\}$ (lines 6–7). Otherwise, it adds r to $\mathcal{R}_{n,s,d}^{k_{\max},\delta_{\max}}$ and tries to obtain the next candidate route as r (lines 8–10). If r is not found or the path length of r violates the constraint,

it stops the enumeration and returns current candidates $\mathcal{R}_{n,s,d}^{k_{\max},\delta_{\max}}$ (lines 11–12). If there is no successful route for evacuation and no violation of path length constraint, it returns $k_{\max}$-shortest paths as $\mathcal{R}_{n,s,d}^{k_{\max},\delta_{\max}}$ (line 13). After obtaining path candidates $\mathcal{R}_{n,s,d}^{k_{\max},\delta_{\max}}$ using Algorithm 3, mobile device n selects a path with the largest path reliability as recommended route $r_{n,s,d}^{k_{\max},\delta_{\max}}$:

$$r_{n,s,d}^{k_{\max},\delta_{\max}} = \underset{r \in \mathcal{R}_{n,s,d}^{k_{\max},\delta_{\max}}}{\arg\max} \; f_{\mathrm{p}}(r).$$

We can control the balance between speediness and safety of evacuation by appropriately selecting $k_{\max}$ and $\delta_{\max}$. In case of $k_{\max} = 1$, the proposed path selection is equivalent to the shortest path selection. If $k_{\max} = \delta_{\max} = \infty$, the proposed path selection adopts the most reliable path without taking into account of path length. Basically, small (resp. large) $k_{\max}$ and/or $\delta_{\max}$ emphasize speedy (resp. safe) evacuation but these two parameters have different roles. $k_{\max}$ guarantees the quantity of candidate paths while $\delta_{\max}$ guarantees the quality of them in terms of speediness of evacuation.

The appropriate values of these two parameters highly depend on the structure of road network. In Section 4.4.4, we will tackle this problem.

4.4.4 Determination of Appropriate Parameter Settings

It is desirable for evacuees to be able to determine appropriate values $k_{\max}^*$ and $\delta_{\max}^*$ for the two parameters $k_{\max}$ and $\delta_{\max}$ before disasters occur. In this section, we propose a parameter determination approach based only on the geographical information that can be retrieved in usual time, i.e., geographical population distribution in usual time and risk map $\widehat{G} = (\mathcal{V}, \mathcal{E}, g)$. Suppose that evacuees start their evacuations from initial locations, $\mathcal{V}_{\mathrm{init}}$, which is obtained by the geographical people distribution. If the target area does not have information about the geographical people distribution, we assume that evacuee's initial locations are uniformly distributed in the area. Given $\widehat{G} = (\mathcal{V}, \mathcal{E}, g)$, $k_{\max}$, and $\delta_{\max}$, we can calculate an appropriate path $r_{s,d}^{k_{\max},\delta_{\max}}$ from each $s \in \mathcal{V}_{\mathrm{init}}$ to the nearest destination $d \in \mathcal{V}$, according to Algorithm 3. Let $\delta_{s,d}^{k_{\max},\delta_{\max}}$ denote the increment of path length from the shortest path, i.e., $f_{\mathrm{d}}(r_{s,d}^{k_{\max},\delta_{\max}}) - f_{\mathrm{d}}(r_{s,d}^{1,0})$. The average $\overline{\delta}^{k_{\max},\delta_{\max}}$ of $\delta_{s,d}^{k_{\max},\delta_{\max}}$ among all $s \in \mathcal{V}_{\mathrm{init}}$ nearest to $d \in \mathcal{V}$ can be regarded as the

goodness of $(k_{\max}, \delta_{\max})$ in terms of path length. On the other hand, the average $\overline{f}_{\mathrm{p}}^{k_{\max},\delta_{\max}}$ of $f_{\mathrm{p}}(r_{s,d}^{k_{\max},\delta_{\max}})$ among all $s \in \mathcal{V}_{\mathrm{init}}$ nearest to $d \in \mathcal{V}$ can be regarded as the goodness of $(k_{\max}, \delta_{\max})$ in terms of path reliability.

Suppose that search space $\mathbf{S}$ is given by direct product $\mathbf{K} \times \mathbf{\Delta}$, where $\mathbf{K}$ (resp. $\mathbf{\Delta}$) is the space of values that $k_{\max}$ (resp. $\delta_{\max}$) can take on. Since there is a trade-off between path length and path reliability, we introduce parameter δ_{th} to control this trade-off. We first find space $\mathbf{S}_{\delta_{\mathrm{th}}}$ in which $\overline{\delta}^{k_{\max},\delta_{\max}}$ is not more than predetermined threshold δ_{th} for each $d \in \mathcal{V}$ as follows:

$$\mathbf{S}_{\delta_{\mathrm{th}}} = \{(k_{\max}, \delta_{\max}) \in \mathbf{S} \mid \overline{\delta}^{k_{\max},\delta_{\max}} \leq \delta_{\mathrm{th}}\}.$$

We assume that each evacuee can set δ_{th} to tell the system his/her sensitivity to speediness of evacuation. Next, we obtain appropriate values $k_{\max}^*$ and $\delta_{\max}^*$, which maximize the path reliability:

$$(k_{\max}^*, \delta_{\max}^*) = \underset{(k_{\max},\delta_{\max}) \in \mathbf{S}_{\delta_{\mathrm{th}}}}{\arg\max} \overline{f}_{\mathrm{p}}^{k_{\max},\delta_{\max}}. \tag{4.3}$$

Numerical examples of parameter determination will be given in Section 4.5.2.

4.5. Simulation Results

Through simulation experiments, we evaluate the effectiveness of the proposed scheme in terms of safety and speediness of evacuation.

4.5.1 Simulation Model

We use The ONE Simulator [108]. We also use the risk map of $2,600$ [m] $\times$ $1,700$ [m] Arako area of Nagoya city in Japan, which is provided by Nagoya city (Fig. 4.2). This map's internal graph structure is composed of 939 vertices and $1,878$ directed edges. There are five refuges (d_1: Uchide nursery school, d_2: Maruike park, d_3: Arako primary school, d_4: Arako park, and d_5: Arako community center), which are presented by blue squares in Fig. 4.2. We set the simulation time to be $5,000$ [s]. When the simulation starts, a disaster occurs and the evacuees start moving from given points on the map (blue points in Fig. 4.2) to the nearest refuges at a speed of 1.11 [m/s]. Since all evacuees may require some

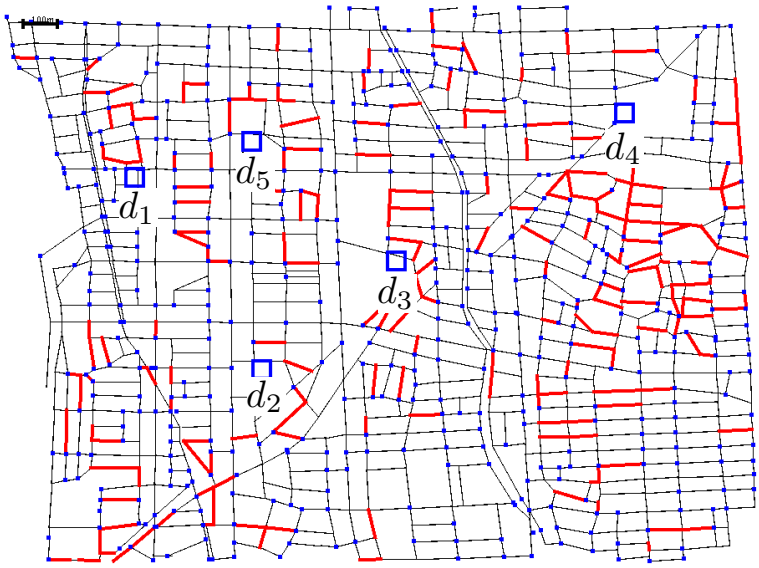

Figure 4.2. Risk map: $2,600$ [m] $\times 1,700$ [m] Arako area of Nagoya city in Japan.

time to start evacuation, the start time of each evacuation is randomly delayed from 0 to 200 seconds.

Because the initial positions of evacuees may affect the evacuation performance, we prepare different kinds of scenarios: random, commuting, and returning scenarios. In the random scenario, evacuees start evacuations from random positions. This scenario is regarded as the default scenario where the geographical population distribution in usual time cannot be obtained. To evaluate the impact on taking account of the geographical population distribution in usual time, we use the commuting and returning scenarios. In the commuting (resp. returning) scenario, the initial locations of evacuees are determined by the geographical population distribution at 8:00 (resp. 17:00), which is obtained by the people flow data of Nagoya city. People tend to move to a relatively small number of points, e.g., companies and schools, in the commuting scenario while they tend to move to various points, e.g., home and stations, in the returning scenario. The number of evacuees are set to be 2,415 (resp. 705) in the commuting (resp. returning) scenario, which is equal to the number of pedestrians in the corresponding people flow data. For comparison purpose, we prepare two kinds of random scenarios: random scenario with $N = 705$ and that with $N = 2,415$.

We set measurement interval I_M to be 50 [s]. We assume communication ranges for mobile-to-mobile direct communication, e.g., Wi-Fi Direct, to be 100 [m] and communication ranges for communication with infrastructures, e.g., wireless LAN, to be 100 [m]. To focus on the effectiveness of the proposed scheme itself, we assume that mobile devices can finish retrieving information at each contact with other mobile devices and/or communication infrastructures. One wireless LAN access point (AP) is located at the refuge, and AP's are placed in $N \times N$ grid arrangement. We define *coverage* as the ratio of the area of roads included in the transmission ranges of APs to the whole area of all roads. We can control the coverage by changing N.

As for the disaster situations, we set the blocked road segments (red lines in Fig. 4.2) according to the road blockage probability of each edge on the graph. Nagoya city in Japan provides information of the road blockage probabilities for several classes depending on the degree of damages. In what follows, we use the data of maximum class that considers the possibility of all kinds of disasters.

Since the performance of the proposed scheme depends on communication environments, we change the coverage of infrastructures in the range of $[0, 100]$. We compare the performance of the proposed scheme with the following evacuation schemes.

- Ideal evacuation: All evacuees know the information about all blocked road segments at the start of their evacuations. The ideal evacuation demonstrates the lower bound of the evacuation time of the proposed scheme.

- Shortest path selection: All evacuees follow the automatic evacuation guiding based on shortest path selection [24]. Note that this is equivalent to the proposed scheme with $k_{\max} = 1$ and $\delta_{\max} = 0$.

We use two kinds of evaluation criteria. The first one is the total number of encounters with blocked road segments of all evacuees, B, which is related to the safety of evacuation. The second one is the average (resp. maximum) evacuation time among evacuees, $\overline{T}$ (resp. $T_{\max}$), to evaluate the speediness of evacuation. Here, we define the evacuation time as the time interval from evacuation start to the evacuation completion. In what follows, simulation results are the average of 50 independent simulation experiments.

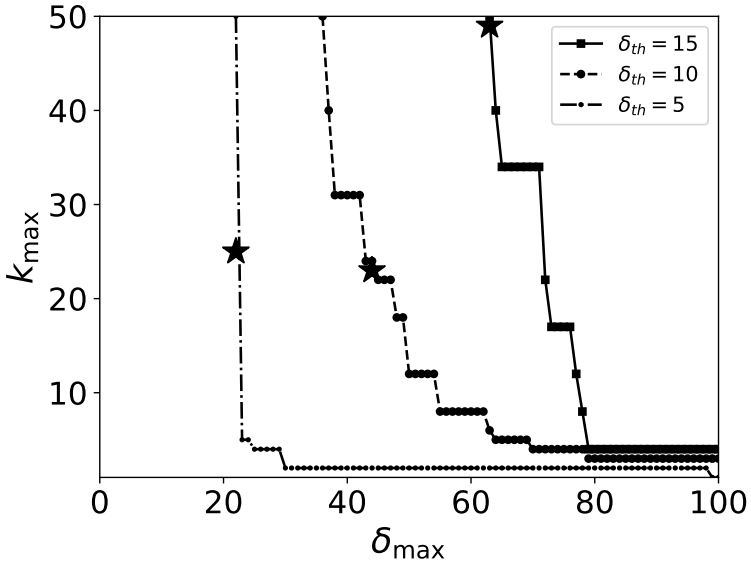

Figure 4.3. $\mathbf{S}_{\delta_{\text{th}}}$ and $(k^*_{\max}, \delta^*_{\max})$ for risk map in Fig. 4.2 ($\delta_{\text{th}} = 5$, 10, and 15).

Table 4.1. $\overline{T}(k^*_{\max}, \delta^*_{\max})$ and statistics of $\overline{T}(k_{\max}, \delta_{\max})$, i.e., minimum, mean, value of top 10%, and standard deviation.

δ_{th}	$\overline{T}(k^*_{\max}, \delta^*_{\max})$	$\overline{T}(k_{\max}, \delta_{\max})$			
		minimum	mean	top 10%	standard deviation
5	1266	1234	1299	1265	17.6
10	1262	1227	1280	1254	21.1
15	1252	1193	1272	1246	22.8

4.5.2 Validity of parameter determination approach

In this section, we examine the validity of the parameter determination approach through numerical examples. We first show the numerical examples of parameter determination approach when setting search space $\mathbf{S} = \mathbf{K} \times \mathbf{\Delta}$ to be $\mathbf{K} = (1, 2, \ldots, 50)$ and $\mathbf{\Delta} = (0, 1, \ldots, 100)$. Fig. 4.3 illustrates $\mathbf{S}_{\delta_{\text{th}}}$ and $(k^*_{\max}, \delta^*_{\max})$ for destination d_4 when δ_{th} is set to be 5, 10, and 15 in the random scenario ($N = 705$). Recall that there is a trade-off between path length and path reliability. Basically, path length (resp. path reliability) tends to become short (resp. high) in left bottom (resp. right top) area of $\mathbf{S}$. Three curves indicate

Table 4.2. $B(k^*_{\max}, \delta^*_{\max})$ and statistics of $B(k_{\max}, \delta_{\max})$, i.e., minimum, mean, value of top 10%, and standard deviation.

δ_{th}	$B(k^*_{\max}, \delta^*_{\max})$	$B(k_{\max}, \delta_{\max})$			
		minimum	mean	top 10%	standard deviation
5	1131	1075	1194	1135	46.7
10	1081	1022	1156	1085	58.8
15	1004	897	1120	1032	73.2

the boarder lines of $\mathbf{S}_{\delta_{\text{th}}}$ in case of $\delta_{\text{th}} = 5$, 10, and 15, respectively. Each curve and its left area corresponds to $\mathbf{S}_{\delta_{\text{th}}}$. We observe that $\mathbf{S}_{\delta_{\text{th}}}$ expands to the upper right area with increase of δ_{th}. We also find out that each curve shows inversely proportional relationship between $k_{\max}$ and $\delta_{\max}$, so as to avoid increase of δ_{th}. The parameter settings on each curve have the same performance of path length but may have different path reliability. A star on each curve indicates $(k^*_{\max}, \delta^*_{\max})$ given by (4.3). Since large $k_{\max}$ can provide evacuees with many candidates of evacuation routes, $(k^*_{\max}, \delta^*_{\max})$ tends to have large $k_{\max}$. In what follows, we use the case of $\delta_{\text{th}} = 15$ in the random scenario ($N = 705$).

Next, we examine the validity of obtained parameters $(k^*_{\max}, \delta^*_{\max})$ by analyzing the simulation results obtained over the same search space $\mathbf{S}$ and δ_{th}, which are used in the parameter determination approach. Note that the communication environment is offline. Through simulation experiments with parameter settings $(k_{\max}, \delta_{\max})$, we can obtain average evacuation time $\overline{T}(k_{\max}, \delta_{\max})$ and total number of encounters with blocked road segments, $B(k_{\max}, \delta_{\max})$. Table 4.1 (resp. Table 4.2) presents $\overline{T}(k^*_{\max}, \delta^*_{\max})$ (resp. $B(k^*_{\max}, \delta^*_{\max})$) and statistics of $\overline{T}(k_{\max}, \delta_{\max})$ (resp. $B(k_{\max}, \delta_{\max})$), i.e., minimum, mean, top 10%, and standard deviation. We observe that both $\overline{T}(k^*_{\max}, \delta^*_{\max})$ and $B(k^*_{\max}, \delta^*_{\max})$ cannot achieve the minimum for each δ_{th}. This is because the parameter determination approach only analyzes the risk map and cannot fully deal with the actual avoidance behavior that occurs at the encounters with blocked road segments. This limitation also causes the counterintuitive phenomenon where $\overline{T}(k^*_{\max}, \delta^*_{\max})$ decreases with increase of δ_{th}. In the parameter determination approach, we assume that the shortest path is passable but this assumption may not be true in the actual situation. Selecting more reliable path with increase of δ_{th} will also contribute to reducing the

wasteful evacuation behavior caused by encountering blocked road segments. In spite of these difficulty in analyzing, the parameter determination approach can achieve the performance that is better than the mean and is competitive with the top 10% results.

4.6. Effectiveness of Proposed Scheme

In this section, we evaluate the effectiveness of the proposed scheme with appropriate parameter settings. In what follows, we use the case of $\delta_{\text{th}} = 15$ in the random scenario ($N = 705$). Since the performance of the proposed scheme depends on communication environments, we change the coverage of infrastructures in the range of $[0, 100]$. We compare the performance of the proposed scheme with the following evacuation schemes.

- Ideal evacuation: All evacuees know the information about all blocked road segments at the start of their evacuations. The ideal evacuation demonstrates the lower bound of the evacuation time of the proposed scheme.
- Shortest path selection: All evacuees follow the automatic evacuation guiding based on shortest path selection [24]. Note that this is equivalent to the proposed scheme with $k_{\max} = 1$ and $\delta_{\max} = 0$.

4.6.1 Total Number of Encounters with Blocked Road Segments

Fig. 4.4 illustrates the transition of the number of encounters with blocked road segments when changing coverage of communication infrastructures. We show the results of proposed scheme and shortest path selection. There are two functions that contribute to safety of evacuation by reducing the number of encounters with blocked road segments. First one is sharing of information about blocked road segments among mobile devices, which is a reactive function provided by the automatic evacuation guiding. Second one is reliable path selection based on geographical risk analysis, which is a proactive function provided by the proposed scheme. Note that the proposed scheme has both functions while the automatic

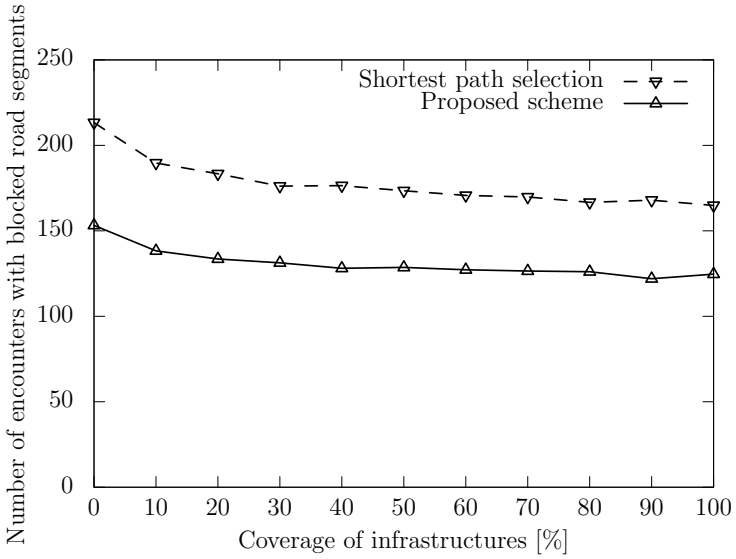

Figure 4.4. The number of encounters with blocked road segments.

evacuation guiding based on shortest path selection has only the first function of information sharing.

We can confirm the effect of reliable path selection by comparing the results of two schemes. The proposed scheme can reduce the number of encounters with blocked road segments compared with the shortest path selection, e.g., 28.2% (0% coverage) and 24.2% (100% coverage). We also evaluate both schemes in an offline case where the information sharing is unavailable due to lack of both mobile-to-mobile direct communication and communication infrastructures. In the offline case, the number of encounters with blocked road segments of the proposed scheme becomes 1235, which is much smaller than that of the shortest path selection, i.e., 1911.

Next, we focus on the impact of coverage on the evacuation safety. We observe that the number of encounters with blocked road segments monotonically decreases with coverage, regardless of schemes. In case of the proposed scheme, the performance improvement is almost saturated when the coverage is only 30%. From the above results, we can conclude that the proposed scheme is robust against the damage of communication environments.

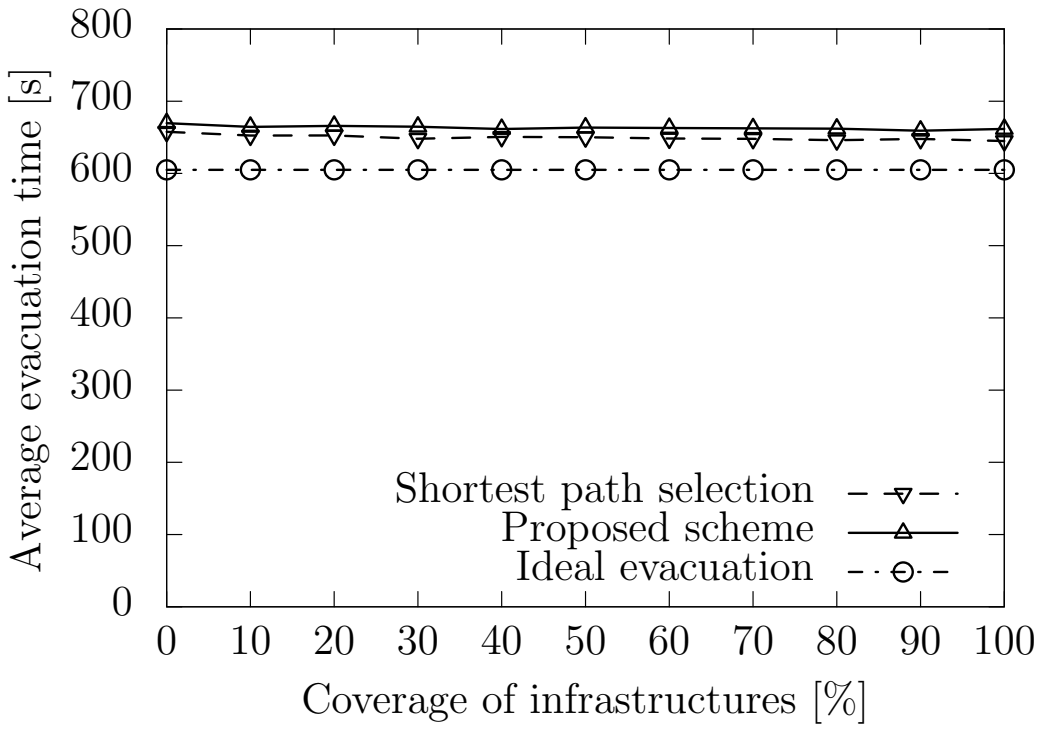

Figure 4.5. Average evacuation time.

4.6.2 Evacuation Time

In Section 4.6.1, we showed that the proposed scheme with appropriate parameters can reduce the number of encounters with blocked road segments, regardless of communication coverage. However, reliable path selection may also make evacuation routes longer with increase of $k_{\max}$ and $\delta_{\max}$. In this section, we evaluate the effectiveness of the proposed scheme in terms of average evacuation time and maximum evacuation time.

Fig. 4.5 (resp. Fig. 4.6) illustrates the transition of average (resp. maximum) evacuation time when changing coverage of communication infrastructures. We show the results of three evacuation schemes: proposed scheme, shortest path selection, and ideal evacuation. We first observe that the results of proposed scheme are competitive with those of shortest path selection, despite of selecting more reliable path, which may make the evacuation path longer. We also find that the coverage does not affect the average evacuation time but can improve the

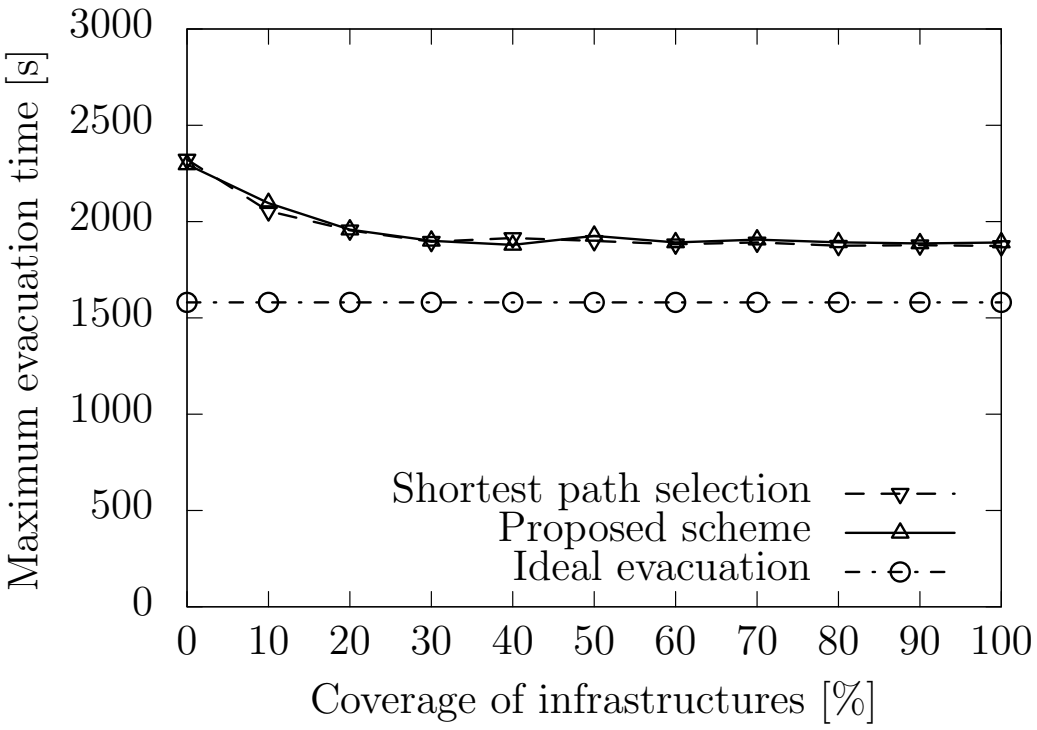

Figure 4.6. Maximum evacuation time.

maximum evacuation time. This indicates that the information sharing through communication infrastructure is still important to reduce the evacuation time, especially for evacuees that tend to be isolated from others.

In the offline case, all evacuees are isolated with each other. We find that the average evacuation time of the proposed scheme becomes 779, which is shorter than that of shortest path selection, i.e. 801. This is because the shortest path selection may cause wasteful evacuation behavior by encountering blocked road segments, which can be alleviated by the reliable path selection. These results show that the proactive approach is more effective for the evacuation under inferior communication environments.

4.6.3 Impact of Initial Locations of Evacuees

In general, the geographical population distribution temporally varies according to the human life cycle. To reveal how the initial locations of evacuees and the

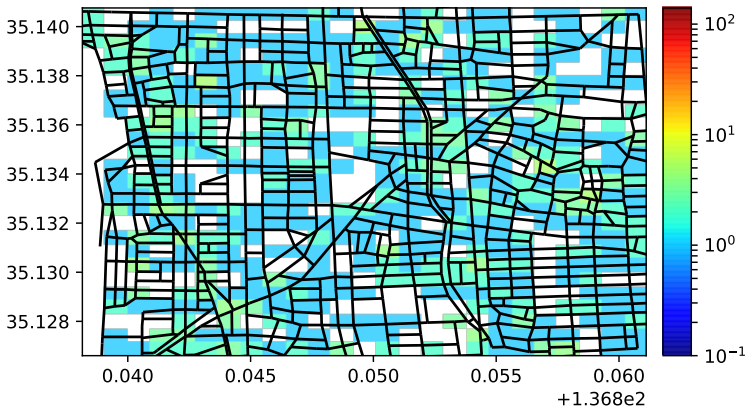

Figure 4.7. The initial locations of evacuees in the random scenario ($N = 705$).

Table 4.3. B, $\overline{T}$, and $T_{\max}$ with the proposed scheme in four scenarios (offline case).

Scenario	B	$\overline{T}$	$T_{\max}$
Random scenario ($N = 2,415$)	2919 (1.21)	726	3736
Commuting scenario ($N = 2,415$)	3078 (1.27)	628	2587
Random scenario ($N = 705$)	1235 (1.75)	779	3058
Returning scenario ($N = 705$)	338 (0.49)	782	2391

number of evacuees affect the evacuation performance, we compare the results among four scenarios: random scenario with $N = 705$ (Fig. 4.7), random scenario with $N = 2,415$ (Fig. 4.8), commuting scenario with $N = 2,415$ (Fig.4.9), and returning scenario with $N = 705$ (Fig. 4.10). In what follows, we use the case of $\delta_{\text{th}} = 15$.

The locations of evacuees have complex effects on the evacuation. From the viewpoint of the proactive approach, the difficulty of finding speedy and reliable paths may change according to locations. In terms of the reactive approach, the locations of evacuees and the number of evacuees affect not only the opportunities of information sharing through device-to-device communication but also the degree of evacuation improvement yielded by the obtained information.

First, we focus on the impact of initial evacuees' locations on the proactive approach, which can be analyzed through the evaluation under the offline case.

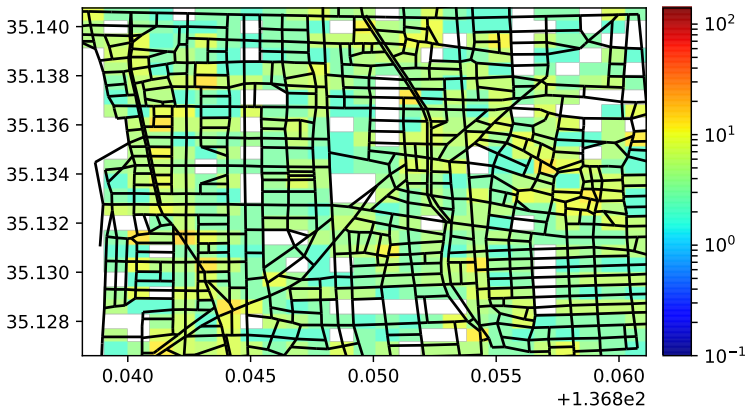

Figure 4.8. The initial locations of evacuees in the random scenario ($N = 2,415$).

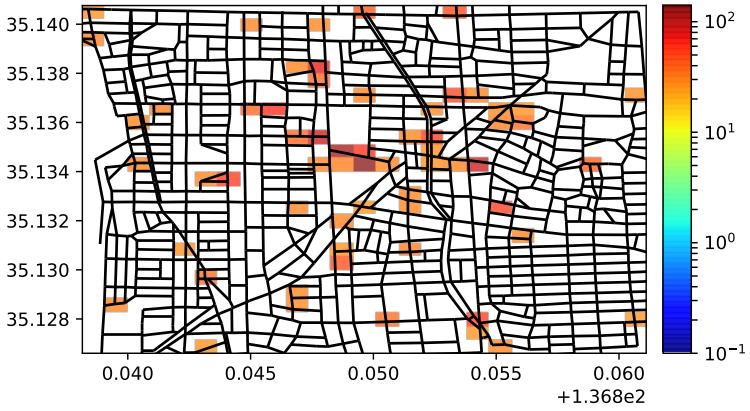

Figure 4.9. The initial locations of evacuees in the commuting scenario.

Table 4.3 illustrates the results, i.e., B, $\overline{T}$, and $T_{\max}$, in the four scenarios when the communication environment is offline. Because the number of evacuees in the commuting scenario, i.e., 2,415, is larger than that in the random and returning scenario, i.e., 705, we also give normalized B, which is the number of encounters with blocked road segments per evacuee. The results in the random scenario can be regarded as the average evacuation behavior that an evacuee starting from an arbitrary point will experience. We first observe that there is almost no difference between B in the commuting scenario and that in the random scenario ($N = 2,415$). We also find that $\overline{T}$ and $T_{\max}$ in the commuting scenario

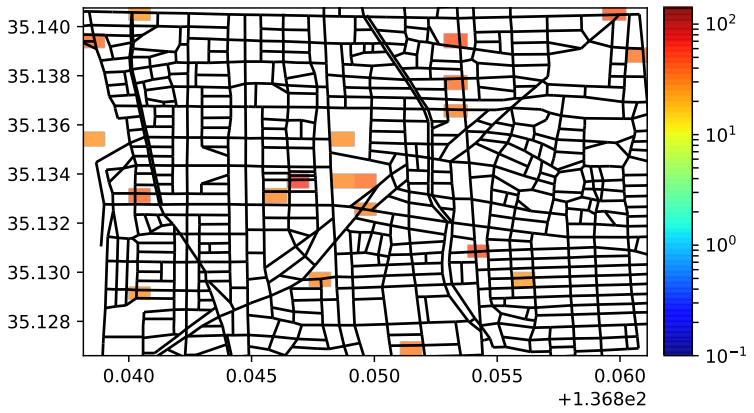

Figure 4.10. The initial locations of evacuees in the returning scenario.

Table 4.4. B, $\overline{T}$, and $T_{\max}$ with the proposed scheme in four scenarios (100% coverage case).

Scenario	B	$\overline{T}$	$T_{\max}$
Random scenario ($N = 2,415$)	260 (0.11)	632	1938
Commuting scenario ($N = 2,415$)	614 (0.25)	568	1957
Random scenario ($N = 705$)	125 (0.18)	662	1891
Returning scenario ($N = 705$)	338 (0.49)	782	2391

are less than those in the random scenario ($N = 2,415$), which indicates that evacuees in the commuting scenario are initially located at better places in terms of speediness. On the other hands, B in the returning scenario is greater than that in the random scenario ($N = 705$), which indicates that evacuees in the returning scenario are initially located at worse places in terms of safety.

Second, we focus on the impact of initial evacuees' locations on the reactive approach. We first investigate the relationship between the initial locations and improvement degree of evacuation behavior yielded by information sharing. This can be analyzed through the evaluation under the 100% coverage case where evacuees can retrieve all the dynamic information, i.e., blocked road segments and passable road segments, in a real-time manner. Table 4.4 illustrates the results, i.e., B, $\overline{T}$, and $T_{\max}$, in the four scenarios when the communication environment is 100% coverage. Comparing Table 4.4 with Table 4.3, we find that

Table 4.5. B, $\overline{T}$, and $T_{\max}$ with the proposed scheme in four scenarios (0% coverage case).

Scenario	B	$\overline{T}$	$T_{\max}$
Random scenario ($N = 2,415$)	277 (0.11)	634	1939
Commuting scenario ($N = 2,415$)	711 (0.29)	574	2245
Random scenario ($N = 705$)	153 (0.22)	670	2297
Returning scenario ($N = 705$)	419 (0.59)	798	2667

the improvement ratio of B in the 100% coverage case to that in the offline case becomes 91.1%, 80.1%, 89.9%, and 76.7%, in the random ($N = 2,415$), commuting, random ($N = 705$), and returning scenarios, respectively. Since the initial locations are well distributed over the area in the random scenarios (Figs. 4.7 and 4.8), each evacuee can easily obtain useful information from preceding evacuees. In the commuting and returning scenarios, evacuees initially tend to form groups as in Figs. 4.9 and 4.10. The improvement ratio in the commuting scenario becomes larger than that in the returning scenario because of the larger number of evacuees and the denser distribution of groups.

Next, we focus on the results in the 0% coverage case, which can reveal how the device-to-device communication improves the evacuation performance. Table 4.5 illustrates the results, i.e., B, $\overline{T}$, and $T_{\max}$, in the four scenarios when the communication environment is 0% coverage and only the device-to-device is available. Comparing the results of random scenario ($N = 705$) and those of random scenario ($N = 2,415$), we can confirm that larger N yield better results, which come from the more opportunities for device-to-device communication. We also find that the results of commuting scenario are better than those of returning scenario. This is because of not only the larger number of evacuees but also the denser distribution of evacuees. In other words, the coverage of communication infrastructure is more important when the evacuees are sparsely distributed over the area.

Table 4.6. The result of the proposed scheme used in the risk map of each class.

Risk-map class	Offline			100% coverage		
	B	$\overline{T}$	$T_{\max}$	B	$\overline{T}$	$T_{\max}$
Maximum class	542	508	1330	110	496	1279
Historical class	550	509	1323	113	496	1270

4.6.4 Impact of Risk-Map Accuracy

Recall that the road blockage probabilities in risk map depend on the magnitude of disaster. For example, Nagoya city provides the road blockage probabilities of two classes: maximum class and historical class. The maximum class considers all kinds of disaster risks while the historical class is based on the maximum disaster in recorded history. However, it may be difficult to prepare the road blockage probabilities corresponding to the actual magnitude of disaster and/or judge the actual disaster magnitude precisely at the start of evacuation. One possible way to cope with this problem is using the risk map with maximum class.

Suppose that the disaster causes the blocked road segments according to the road blockage probability of the historical class. In what follows, we show how the performance of proposed scheme changes depending on the class of risk map. We use $\delta_{\text{th}} = 15$ and the commuting scenario. Table 4.6 presents the result of the proposed scheme with the two classes of risk maps. Since the results of risk map with maximum class are similar to those of risk map with historical class, the mismatch of risk-map class does not much affect the system performance.

To reveal this reason, we show the correlation between road blockage probabilities of maximum class and those of historical class in Fig. 4.11. We observe that there is a strong correlation between them and the correlation coefficient becomes 0.949. In the proposed scheme, the application first calculates the top k-shortest route candidates and then selects the most reliable route based on path reliability (4.2). The top k-shortest route candidates is exactly the same, regardless of the risk-map class, but the path reliability will change depending on the risk-map class. The risk map with maximum class tends to suggest more reliable path than that with historical class but these two paths also tend to be similar due to the high correlation coefficient of blockage probabilities.

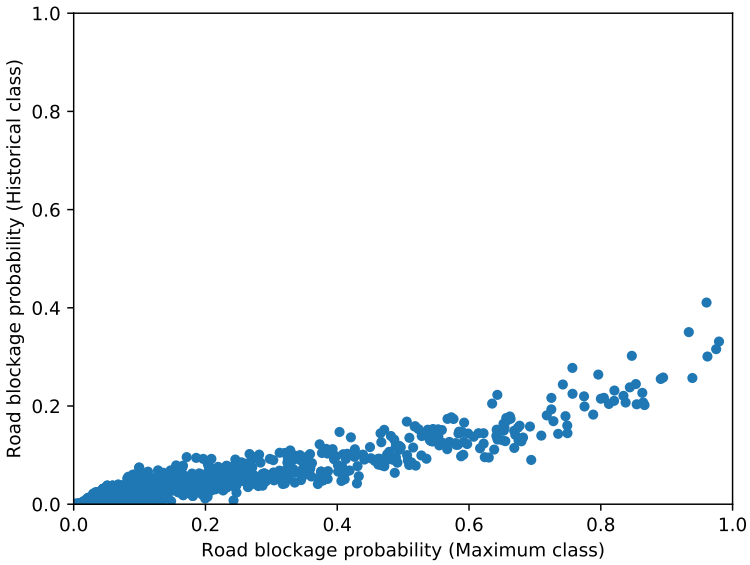

Figure 4.11. Correlation between road blockage probabilities of maximum class and those of historical class.

4.7. Summary

When a large-scale disaster occurs, evacuees have to evacuate to refuges speedily and safely. Most of the existing evacuation guiding schemes have been focusing on the speedy evacuation based on the shortest path selection. In this thesis, we proposed a geographical risk analysis based path selection for speedy and reliable evacuation guiding. The proposed scheme first enumerated multiple shortest paths from the evacuee's current location to the destination. Next, it selected the route with the highest path reliability based on geographical risk analysis from the candidates. Since the appropriate parameters of the proposed scheme depend on the structure of road network, we also proposed a parameter determination approach based on the risk map and geographical population distribution, which can be retrieved in usual time.

Through simulation experiments, we first showed the validity of parameter determination approach. Next, we found that the proposed scheme can improve the safety of evacuation in terms of the number of encounters with blocked road segments, compared with the shortest path selection, regardless of the commu-

nication environments. In addition, the proposed scheme can also improve both average and maximum evacuation times, compared with the shortest path selection under the severe communication environments. We further showed that the initial locations of evacuees affect the difficulty of finding speedy and reliable routes in terms of the proactive approach. From the viewpoint of the reactive approach, the initial locations and the number of evacuees also affect the opportunities of information sharing as well as the degree of evacuation improvement. Finally, we also found that the evacuation performance can be kept even if the evacuees cannot precisely grasp the disaster magnitude and are forced to use the risk map with the maximum class.

Chapter 5

Capaciated Refuge Assignment for Speedy and Reliable Evacuation in Emergency Situations

5.1. Introduction

When a large-scale disaster, e.g., an earthquake, occurs, each evacuee should move to an appropriate refuge in a speedy and safe manner. Such speedy and reliable evacuation can be achieved by both pre-disaster and post-disaster approaches. The pre-disaster approaches include establishment of refuges [109–114], refuge assignment [101, 115, 116], evacuation planning [99, 117, 118], and geographical risk analysis [3, 23, 119–121]. From the viewpoint of the refuge assignment, most of the existing studies basically consider the evacuation time and refuge capacity while the safety evacuation is also important.

The pre-disaster approaches can provide us with a global picture of evacuation under predefined assumptions (e.g., refuge locations, geographical population distribution, and road network risk). Since it is difficult to consider all possible disaster situations, the post-disaster approaches are also important to compensate for the mismatch between the assumptions and actual situations.

The post-disaster approaches include evacuation guiding [24, 92, 93, 122] and signage systems [123–125]. In comparison with the pre-disaster approaches, the post-disaster ones can flexibly deal with dynamic environmental changes due to the disaster for supporting the evacuees' decision making under their high-stressed situation. However, most of the post-disaster approaches implicitly assume that each evacuee selects the nearest refuge for evacuation, which might guide the evacuee to a less reliable route and/or to a filled refuge. In recent years, we can obtain the safety-related information (e.g., geographical risk information) in addition to the capacity-related information (e.g., population distribution and refuge locations and capacities) from governments and some municipalities [3, 23, 119].

In this thesis, we consider the earthquake case study and propose a refuge assignment scheme to achieve speedy and safety evacuations under the refuge capacity constraint. This is a kind of the multi-objective optimization problems, i.e., minimization of route length and maximization of route reliability. We first formulate the refuge assignment problem as a two-step integer linear program (ILP) under the input of route candidates between evacuees and their possible refuges, which can be solved by the existing solver, CPLEX [126]. As for the route candidates, we also propose a speedy and reliable path selection scheme, which is an extended version of the existing path selection scheme [122] to improve the route reliability. The proposed scheme can be viewed as either pre-disaster approach or post-disaster one, depending on the knowledge about the locations of evacuees. If the proposed scheme uses the geographical distribution of residents as their initial locations, it can be viewed as pre-disaster refuge assignment for evacuation planning. On the other hand, if it can obtain the actual locations of evacuees under the disaster situations through information and communication technologies (e.g., mobile devices, global positioning systems, and communication networks), it can also achieve post-disaster refuge assignment, which is responsive to the environmental changes.

In this thesis, we mainly focus on the pre-disaster refuge assignment under the earthquake case study using actual geographical data (i.e., road blockage probabilities, map of Nagoya city, locations and capacities of refuges, and the distribution of residents), which are provided by the Japanese government and

municipality [23, 127–129]. Through numerical results using the actual data of Arako district of Nagoya city, in Japan, we will show the effectiveness of the proposed refuge assignment scheme in terms of speediness and safety of evacuation under the refuge capacity constraints.

The rest of this chapter is organized as follows. Section 5.2 gives related work. In Section 5.3, we introduce the proposed scheme. After showing numerical results in Section 5.4, we finally give conclusions and future work in Section 5.5.

5.2. Related Work

5.2.1 Geographical Risk Analysis and Path Selection

In case of evacuation guiding, the simple shortest path may not be enough for the speedy and safety evacuation. Several studies focused on various metrics for the speedy and reliable path selection: traffic congestion [130, 131], obstructions related to the presence of debris [132, 133], and road vulnerability [23, 119, 121, 134, 135]. From the viewpoint of the evacuation speediness, the selfish behavior of evacuees (i.e., trying to move to their refuges as speedy as possible) may cause heavy congestion. To grasp such congestion caused by the selfish behavior, several studies provide pedestrian flow models [130, 131]. In [136], Bernardini analyzed the video recording the real earthquake evacuations and proposed a database for earthquake pedestrian evacuation models, which includes the step-by-step evacuation behavior as well as motion quantities (i.e., speed, acceleration, and distance from obstacles). In [137], Liu et al. proposed a path selection method based on the artificial bee colony algorithm to avoid the congestion during the evacuation in building. Kasai et al. proposed a congestion-aware route selection using collected evacuees' locations through the device to device communication [105]. For simplicity, we focus on the path length as the metric of speediness but the proposed approach can also be applied to other speediness metrics if applicable.

From the viewpoint of the evacuation safety, Coutinho-Rodrigues et al. proposed a multi-objective location-routing problem using two kinds of paths (i.e., a main path and a backup one), which aims to minimize the distance and risk during evacuations [110]. In this case study, they conducted a case study analysis

under the fire-risk assumption where Fire Risk Index Method [119] is used as a tool for assessing the fire safety in buildings. The fire risk index is a weighted sum of multiple risk parameters and ranges from 0.0 to 5.0. The high (resp. low) risk index represents the high (resp. low) level of the fire safety. There are several studies on earthquake emergencies in Italy and Japan [122, 134, 138]. Bernardini et al. considered multiple safety factors for evacuees (e.g., street vulnerability, street blockages probability, and crowding conditions along paths) and proposed a dynamic guidance tool based on Dijkstra's algorithm with the integrated safety index [138]. Santrelli et al. developed vulnerability indices for a road network under an earthquake [134]. These two studies assumed the possibility of road blockage caused by debris of collapsed buildings, which is evaluated by the road width, the height of buildings along the road, and the vulnerability of buildings [121].

In Japan, a certain municipality (e.g., Nagoya city) also provides the road blockage probability in a similar manner, which represents the probability that the corresponding road segment will be blocked after an occurrence of a certain magnitude of an earthquake. The detailed definition has been given in Section 4.4.1.2. In [122], Hara et al. proposed a geographical risk analysis based path selection scheme that provides a speedy and safe route for each evacuee with the help of the road blockage probability.

In this thesis, we extend this path selection scheme to improve the path safety and use it to obtain route candidates between evacuees and their possible refuge candidates.

5.2.2 Evacuation Guiding and Human Interactions

There have been several studies on the indirect/direct evacuation guiding systems: indirect guiding based on signage systems [123–125] and direct evacuation guiding systems [24, 92, 93, 122]. The signage system is one of the building attributions in emergencies as well as ordinary conditions, and provides evacuees with indirect suggestion about evacuation [123, 125]. However, Galea et al. demonstrated that the effectiveness of signage systems for evacuation is limited and only 38% of evacuees use the information about evacuation from the signage system [123]. To tackle this problem, the impact of interactions between people and

signages on the relationship among the perception, interpretation, and use has been investigated [124, 125].

From viewpoint of the direct evacuation guiding, Fujihara and Miwa proposed an evacuation guiding scheme that can work even when the existing communication infrastructures were highly damaged [92]. In this scheme, evacuees manually register the state information of each road (e.g., passable and blocked) to their mobile devices and share it with others through a delay tolerant network [90], which is composed of the mobile devices. Since such manual operations may be difficult under the emergent situations, Komatsu et al. proposed a mobile-edge collaborative automatic evacuation guiding scheme where the evacuees' mobile devices automatically estimate the road state information through information sharing with their evacuees [24].

In the field of psychology, it has been pointed out that a small number of leaders can lead many evacuees (e.g., follow-direction method and follow-me method) [139, 140]. In [24], the implicit interactions among evacuees through information sharing can be regarded as a kind of such leader-follower communication. Since such post-disaster approaches implicitly build the cooperative relationship caused by human interactions, it can not only improve the evacuation speediness but also contribute to avoiding roads with high risks in an adaptive manner. However, most of studies on the evacuation guiding are the post-disaster approaches and basically adopted the shortest path selection.

To improve the evacuation safety, Hara et al. proposed a geographical risk analysis based path selection for automatic evacuation guiding scheme, which provided each evacuee with a speedy and safe route by combining the pre-obtained risk information and the collected information during the evacuation [122]. This approach, however, implicitly assumes that each evacuee selects the nearest refuge, which may cause the overflow of the refuge and/or the selection of routes/refuges in high risk regions. In this thesis, we propose a refuge assignment scheme that can consider the capacity limitation as well as the speediness and safety of evacuations.

5.2.3 Refuge Assignment

There have been several studies on the refuge assignment for speedy evacuation under large-scale disasters [101, 115, 116]. Ng et al. proposed a refuge assignment scheme that considers the balance between the global refuge assignment for minimizing the total evacuation time and the individual selfish refuge selection under emergent situations [115]. Saadatseresht et al. proposed a refuge assignment scheme considering the evacuation route length, population, and refuge capacity, with the help of the multi-objective evolutionary algorithms and the geographical information system [101]. Bayram proposed a refuge assignment scheme such that the route length of each evacuee does not exceed the length of the shortest route plus a certain threshold [116]. These existing studies focus on the speedy evacuation and the refuge capacity while the safety of the evacuation is not taken account. In terms of the evacuation safety, Coutinho-rodrigues et al. proposed a multi-objective mixed integer linear programming model to minimize the distance and fire risk during evacuations [110, 111]. In this thesis, we consider the earthquake case study and address the refuge assignment for speedy and safety evacuation under the refuge capacity constraints.

5.2.4 Multi-Objective Mathematical Programming

As mentioned above, the appropriate refuge assignment has to consider the various aspects (i.e., speediness, safety, and refuge capacity), which indicates it is a kind of the multi-objective optimization problem. There have also been several studies on multi-objective optimization, e.g., weighting method [141, 142], ε-constraint method [141–143], and AUGMECON [144, 145]. Their common goal is to derive the representative subset of the Pareto set, which is the set of Pareto optimal solutions (i.e., solutions that cannot improve one objective function without deteriorating the remaining objective functions). The weighting method transforms the original objective functions into a single objective function, i.e., the weighted sum of them [141, 142]. It requires the careful design of the weighting parameters that can consider the relative importance of each objective. ε-constraint method optimizes the first objective functions under the constraints where each remaining k-th objective function is bounded by a certain threshold

ε_k [143]. The vector of ε_k should be chosen carefully by considering the trade-off among the objectives. The augmented ε-constraint method (AUGMECON) provides us with the way to determine the range of ε_k [144].

In this thesis, inspired by ε-constraint method and AUGMECON, we formulate the refuge assignment as a two-step ILP, where the first step ILP is used to determine the range of parameter and the second step ILP is formulated based on ε-constraint method.

5.3. Proposed Scheme

5.3.1 Overview of Proposed Refuge Assignment Scheme

Refuge assignment for evacuees is a kind of combinational optimization problems where we require to consider multiple important features of evacuation (i.e., speediness, safety, and capacity constraint of refuges). We first provide notations and criteria for evacuation route, i.e., speediness and reliability, in Section 5.3.2 and explain the overview of the proposed refuge assignment scheme in Section 5.3.3. Next, we formulate such refuge assignment as a two-step ILP in Section 5.3.4. We further propose an algorithm to calculate speedy and reliable route candidates between evacuees and their possible refuges in Section 5.3.5.

5.3.2 Preliminaries

Since the refuge assignment is part of the evacuation planning, we focus on the target area for the evacuation planning. In Japan, the unit of the target area is typically a school district and the mayor of municipality must determine designated emergency evacuation site for each disaster type (e.g., earthquake and flood) [146]. $G = (\mathcal{V}, \mathcal{E}, g)$ denotes the graph representing the internal structure of the target area, where $\mathcal{V}$ is a set of vertices i.e., intersections or refuges, and $\mathcal{E}$ is a set of edges i.e., roads. There are D refuges denoted by $\mathcal{D} = \{1, 2, \ldots, D\}$ such that $\mathcal{D} \subset \mathcal{V}$. Suppose that there are $N > 0$ evacuees, denoted by $\mathcal{N} = \{1, 2, \ldots, N\}$, and each evacuee i is initially located at vertex l_i in the target area.

To calculate the refuge assignment, we require the initial locations of the evacuees. The refuge assignment can be regarded as either pre-disaster approach or

Table 5.1. Notation.

Notation	Definition
G	Directed graph of the road network
$\mathcal{V}$	The set of vertices
$\mathcal{E}$	The set of edges
p_e	Road blockage probability of road e
$\mathcal{N}$	The set of evacuees $\{1, 2, \ldots, N\}$ [persons]
Ł	The set of initial locations of each evacuee i, $\{l_1, l_2, \ldots, l_N\}$
$\mathcal{D}$	The set of refuges $\{1, 2, \ldots, D\}$
$\mathcal{C}$	The set of refuge capacity $\{C_1, C_2, \ldots, C_D\}$ [persons]
$x_{i,j}$	Decision variable
$r_{i,j}$	Evacuee i's route to refuge j
d_e	The length of road e [m]
$f_{\mathrm{p}}(r)$	The reliability of route r
$f_{\mathrm{d}}(r)$	The length of route r [m]
f_{p}^*	The optimal route reliability
ε	The constraint on the decrease of the route reliability

post-disaster one, according to the knowledge about the initial locations of the evacuees. From the viewpoint of the pre-disaster refuge assignment, the geographical distribution of residents [129] can be used as possible initial locations of evacuees (residents). We can also adopt the time-varying geographical population distribution (e.g., People Flow Data [3]) to consider the initial locations of evacuees under human life cycle (e.g., commuting period in the morning and returning period in the evening). On the other hand, from the viewpoint of the post-disaster refuge assignment, we can collect the actual locations of the evacuees through their mobile devices at the beginning of a disaster if the terrestrial communication infrastructure (e.g., cellular networks and Wi-Fi) is working.

If the terrestrial communication infrastructures are (partly) damaged and unavailable, we can also use device to device (D2D) communication through evacuees' mobile devices [90, 147] and devices with satellite connectivity [148].

Note that such post-disaster information collection would be affected not only by communication environments but also by the penetration ratio of the proposed scheme as well as evacuees' privacy settings for their location information. If the post-disaster refuge assignment cannot obtain the actual locations of evacuees, it can also adopt the above-mentioned statistical information as in the pre-disaster one. In what follows, we mainly focus on the pre-disaster refuge assignment where the geographical distribution of residents is used as the initial locations of the evacuees.

The map matching algorithm [149] can find the nearest vertex of the internal graph from a coordinate-based location. $g : \mathcal{E} \to \mathbb{I}$ is a real-valued function that assigns road blockage probability p_e in closed unit interval $\mathbb{I} = [0, 1]$ to each edge $e \in \mathcal{E}$ in the risk map. Road blockage probability p_e is an estimated probability that road segment $e \in \mathcal{E}$ is blocked due to the collapse of building along a road under a certain earthquake [23]. The detailed definition of the road blockage probability is explained in Section 4.4.1.2 of Chapter 4.

An evacuation route r can be represented by a vector of roads. We define the length of route r as the sum of the length of each road e in r:

$$f_{\mathrm{d}}(r) = \sum_{\forall e \in r} d_e, \tag{5.1}$$

where d_e is the length of road e. In addition, we can also define the route reliability

as follows [122]:

$$f_{\mathrm{p}}(r) = \prod_{\forall e \in r} (1 - p_e), \tag{5.2}$$

which is the probability that all the roads e along the route r are passable under the assumption that the road blockage probabilities along the routes are independent. The route reliability takes a value in the range of $[0, 1]$ and a large (resp. small) value means high (resp. low) reliability. We can obtain the geographical information (e.g., the location of the refuge, the refuge capacity, and the distribution of residents) from the government and the municipalities before the disaster occurs [3, 128, 129]. Each refuge $j \in \mathcal{D}$ has a capacity of C_j persons. $\mathcal{C} = \{C_1, C_2, \ldots, C_D\}$ denotes a set of refuge capacity.

Table 5.1 summarizes notations used in this paper.

5.3.3 Overview of proposed refuge assignment scheme

In this subsection, we introduce the overview of the proposed refuge assignment scheme. Fig. 5.1 illustrates the flow chart of conducting the refuge assignment and route candidate. We first calculate the initial locations of evacuees from the geographical distribution of residents [129]. Since the geographical distribution of residents gives us the number of persons in each sub-region q, N_q, we uniformly allocate N_q evacuees to the vertices in the sub-region q. Let $\mathcal{Q}$ denote the set of sub-regions, and thus $\sum_{q \in \mathcal{Q}} N_q = N$. Considering the fact that some of the residents may stay their home or workplace even under the emergency, we further assume that β $(0 \leq \beta \leq 1)$ ratio of all the residents act as evacuees, denoted by $\mathcal{N}_\beta$. In such cases, we can regard $\mathcal{N}$ as $\mathcal{N}_\beta$.

Next, given risk map $G = (\mathcal{V}, \mathcal{E}, g)$, set of refuges $\mathcal{D}$, set of refuge capacity $\mathcal{C}$, set of evacuees $\mathcal{N}$, and initial locations of evacuees Ł, we obtain the route candidates $r_{i,j}$ between all evacuees $i \in \mathcal{N}$ and all refuges $j \in \mathcal{D}$ using Algorithm 5, which will be described in Section 5.3.5. Finally, the refuge assignment is obtained by solving ILPs, OP_{p} and/or OP_{d}, which will be desribed in Section 5.3.4.

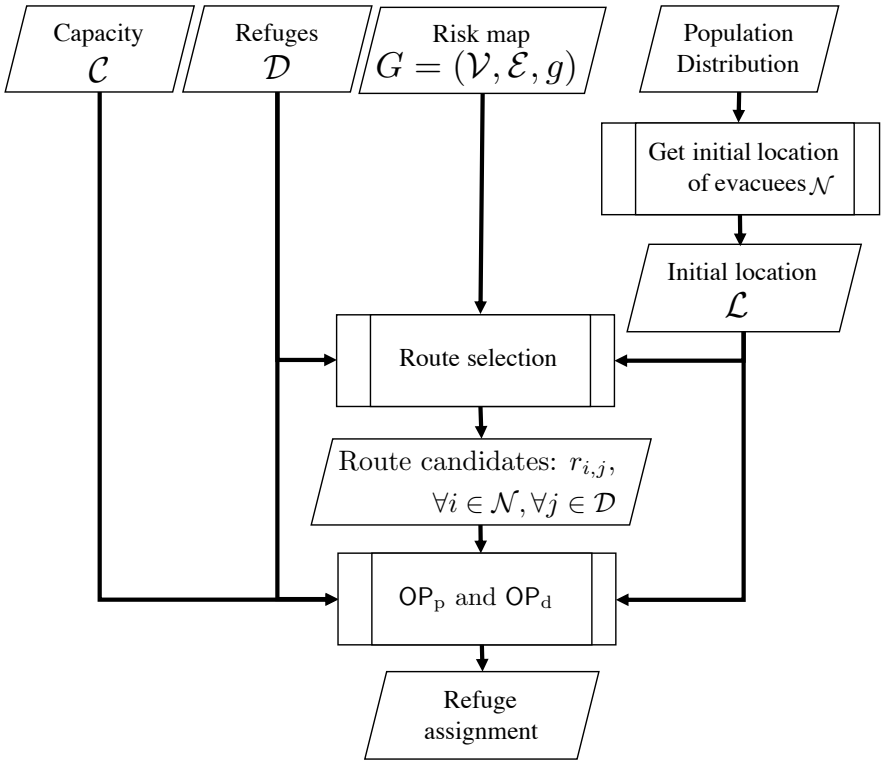

Figure 5.1. Flow chart of calculating the refuge assignment and the route candidate.

5.3.4 Two-step ILP formulation for refuge assignment

As mentioned above, the refuge assignment must be carefully designed by considering the speediness and safety of evacuation under the refuge capacity constraint. This is a kind of multi-objective optimization problems, and thus we tackle this problem in the following two-step ILP.

5.3.4.1 First step: maximization of average route reliability among evacuees under refuge capacity constraint

Given route candidates between evacuees and their possible refuges as the input data, which will be explained in Section 5.3.5, we first aim at maximizing the evacuation safety, i.e., the average route reliability among evacuees. This optimization problem can be represented by the following ILP OP_p.

$$\max \quad \frac{1}{N}\sum_{i\in\mathcal{N}}\sum_{j\in\mathcal{D}} f_{\mathrm{p}}(r_{i,j})x_{i,j}, \tag{5.3}$$

$$\text{s.t.} \quad x_{i,j} \in \{0,1\}, \quad \forall i \in \mathcal{N}, \quad \forall j \in \mathcal{D}, \tag{5.4}$$

$$\sum_{j\in\mathcal{D}} x_{i,j} = 1, \quad \forall i \in \mathcal{N}, \tag{5.5}$$

$$\sum_{i\in\mathcal{N}} x_{i,j} \leq C_j, \quad \forall j \in \mathcal{D}. \tag{5.6}$$

The objective function (5.3) is the maximization of the average road reliability among evacuees, where $r_{i,j}$ is the route candidate between evacuee i and refuge j. The calculation of $r_{i,j}$ will be described in Section 5.3.5. $x_{i,j}$ is binary decision variable given by (5.4). If evacuee i is assigned to refuge j, $x_{i,j} = 1$. Otherwise, $x_{i,j} = 0$. The constraint of (5.5) guarantees that each evacuee i must be allocated to one refuge. Since the overflow evacuees will be required to move to other refuges [150], such overflow conditions are prohibited by (5.6), which indicates that the number of evacuees assigned to each refuge does not exceed the corresponding capacity.

Since the objective function and all the constraints are linear with the binary decision variables, OP_{p} is ILP, which can be solved by the existing solver, e.g., CPLEX.

5.3.4.2 Second step: minimization of average route length among evacuees under refuge capacity constraint and average route reliability

By solving the problem OP_{p}, we can obtain the optimal value of the average route reliability f_{p}^*. The corresponding refuge assignment, however, may have some room to improve in terms of speedy evacuation. To tackle this tradeoff between the speediness and reliability, we further propose a second-step optimization as an ILP OP_{d}, which can be formulated by modifying OP_{p} as follows.

First, the objective function (5.3) is replaced with

$$\min \quad \frac{1}{N}\sum_{i\in\mathcal{N}}\sum_{j\in\mathcal{D}} f_{\mathrm{d}}(r_{i,j})x_{i,j}, \tag{5.7}$$

which is the minimization of the average route length among evacuees. In addition to the constraints of OP_p, i.e., (5.4)–(5.6), OP_d adds the following constraint:

$$\frac{1}{N}\sum_{i\in\mathcal{N}}\sum_{j\in\mathcal{D}} f_\mathrm{p}(r_{i,j})x_{i,j} \geq f_\mathrm{p}^* - \varepsilon. \tag{5.8}$$

The constraint of (5.8) guarantees a certain level of the average route availability by controlling a parameter ε ($0 \leq \varepsilon \leq f_\mathrm{p}^*$), which describes the allowable decrease of average route reliability from the optimal value f_p^*. If ε is small (resp. large), the refuge assignment is designed for reliable (speedy) evacuation. The appropriate setting for ε will be discussed in Section 5.4.2. Since the objective function and all the constraints are linear with the binary variables, OP_p is also ILP.

5.3.5 Calculation of speedy and reliable route candidates between evacuees and their possible refuges

The solution, i.e., refuge assignment, of the two-step ILP depends on its input parameters, which are the route candidates between evacuees and their possible refuges, i.e., $r_{i,j}$. We propose a speedy and reliable route selection scheme, which is an extended version of the existing route selection scheme [122].

Algorithm 4 presents a function $\mathsf{candidate\_paths}(G, i, j, k_\mathrm{max}, \delta_\mathrm{max}, \gamma_\mathrm{th})$ that enumerates at most k_max ($k_\mathrm{max} \geq 1$) shortest route candidates between evacuee i and refuge j under the constraint on route length, δ_max ($\delta_\mathrm{max} \geq 0$), and route reliability, γ_th ($0 \leq \gamma_\mathrm{th} \leq 1$). Given road network $G = (\mathcal{V}, \mathcal{E}, g)$, evacuee i, refuge j, parameters $(k_\mathrm{max}, \delta_\mathrm{max})$, and γ_th, it first initializes the set of route candidates, $\mathcal{R}_{i,j}^{k_\mathrm{max},\delta_\mathrm{max},\gamma_\mathrm{th}}$, to be empty and the shortest route length d_min to be infinity (line 1). Next, it obtains at most k_max shortest route candidates between evacuee i and refuge j, $R_{i,j}^{k_\mathrm{max}}$, by using k-$\mathsf{th\_shortest\_paths}(\cdot)$ function based on Yen's algorithm [106] (line 2). It also calculates the length of the shortest path in $R_{i,j}^{k_\mathrm{max}}$, d_min (line 3). In the next loop of lines 4–8, it extracts speedy and reliable route candidates from $R_{i,j}^{k_\mathrm{max}}$. Note that route candidates in $R_{i,j}^{k_\mathrm{max}}$ are sorted in ascending order of route length. If the length of route r is longer than that of the shortest path, i.e., d_min, at a certain level, δ_max, it stops the loop (lines 5–6). If the reliability of route r is equal or greater than a threshold γ_{th}, it adds r to $\mathcal{R}_{i,j}^{k_\mathrm{max},\delta_\mathrm{max},\gamma_\mathrm{th}}$ (line 8). Note that the existing scheme in [122] does not have this

Algorithm 4 candidate_paths$(G, i, j, k_{\max}, \delta_{\max}, \gamma_{\mathrm{th}})$: Enumeration of at most $k_{\max}$ shortest route candidates between evacuee i and refuge j under constraint on route length, $\delta_{\max}$, and route reliability, γ_{th}.

Require: $G, i, j, k_{\max}, \delta_{\max}, \gamma_{\mathrm{th}}$
Ensure: $\mathcal{R}_{i,j}^{k_{\max},\delta_{\max},\gamma_{\mathrm{th}}}$

1: $\mathcal{R}_{i,j}^{k_{\max},\delta_{\max},\gamma_{\mathrm{th}}} \leftarrow \emptyset$, $d_{\min} \leftarrow \infty$ ▷ Initialization
2: $\mathcal{R}_{i,j}^{k_{\max}} \leftarrow k$-shortest_paths$(G, i, j, k_{\max})$ ▷ Calculation of the $k_{\max}$-shortest routes
3: $d_{\min} \leftarrow \min_{r \in \mathcal{R}_{i,j}^{k_{\max}}} f_{\mathrm{d}}(r)$ ▷ Calculation of the length of the shortest route
4: **for** $r \in \mathcal{R}_{i,j}^{k_{\max}}$ **do**
5: **if** $f_{\mathrm{d}}(r) - d_{\min} > \delta_{\max}$ **then** ▷ Check on the route length condition
6: **break**
7: **if** $f_{\mathrm{p}}(r) \geq \gamma_{th}$ **then** ▷ Check on the route reliability condition
8: $\mathcal{R}_{i,j}^{k_{\max},\delta_{\max},\gamma_{\mathrm{th}}} \leftarrow \mathcal{R}_{i,j}^{k_{\max},\delta_{\max},\gamma_{\mathrm{th}}} \cup \{r\}$
9: **return** $\mathcal{R}_{i,j}^{k_{\max},\delta_{\max},\gamma_{\mathrm{th}}}$

operation, and thus the road reliability is considered in the best effort manner. After the loop, it returns $\mathcal{R}_{i,j}^{k_{\max},\delta_{\max},\gamma_{\mathrm{th}}}$ as the speedy and reliable route candidates.

The route candidates in $\mathcal{R}_{i,j}^{k_{\max},\delta_{\max},\gamma_{\mathrm{th}}}$ change depending on the parameters $k_{\max}$, $\delta_{\max}$, and γ_{th}. $k_{\max}$ and $\delta_{\max}$ controls the diversity and speediness of route candidates [122]. $k_{\max}$ can be as large as possible under the constraint on the computation overhead. $\delta_{\max}$ can also be a moderate value by considering both the speedy evacuation and reliable route discovery. On the contrary, the setting of γ_{th} tends to be difficult because the feasible route reliability between evacuee i and refuge j can change depending on the pair of i and j.

Considering these features, we propose a function speedy_reliable_path$(G, i, j, \eta, k_{\max}, \delta_{\max})$ that calculates the speedy and reliable route candidate $r_{i,j}$ between evacuee i and refuge j (Algorithm 5). Given road network $G = (\mathcal{V}, \mathcal{E}, g)$, evacuee i, refuge j, and parameters ($k_{\max}$,$\delta_{\max}$), it first initializes γ_{th} to be the maximum value, i.e., one, and $\mathcal{R}_{i,j}^{k_{\max},\delta_{\max},\gamma_{\mathrm{th}}}$ to be an empty set (line 1). In the next loop of lines 2–6, it searches for the most reliable route candidate $r_{i,j}$ between evacuee i and refuge j under the constraint on $k_{\max}$ and $\delta_{\max}$, by decreasing γ_{th} at a certain interval, η, e.g., $\eta = 0.1$. If it succeeds in finding route candidates $\mathcal{R}_{i,j}^{k_{\max},\delta_{\max},\gamma_{\mathrm{th}}}$

Algorithm 5 speedy_reliable_path$(G, i, j, \eta, k_{\max}, \delta_{\max})$: Calculation of speedy and reliable route candidate $r_{i,j}$ between evacuee i and refuge j.

Require: $G, i, j, \eta, k_{\max}, \delta_{\max}$

Ensure: $r_{i,j}$

1: $\gamma_{\mathrm{th}} \leftarrow 1$, $\mathcal{R}_{i,j}^{k_{\max},\delta_{\max},\gamma_{\mathrm{th}}} \leftarrow \emptyset$ ▷ Initialization

2: **while** $\gamma_{\mathrm{th}} \geq 0$ **do**

3: $\mathcal{R}_{i,j}^{k_{\max},\delta_{\max},\gamma_{\mathrm{th}}} \leftarrow$ candidate_paths$(G, i, j, k_{\max}, \delta_{\max}, \gamma_{\mathrm{th}})$ ▷ Calculation of the route candidates

4: **if** $\mathcal{R}_{i,j}^{k_{\max},\delta_{\max},\gamma_{\mathrm{th}}} \neq \emptyset$ **then**

5: **return** $r_{i,j}$ according to (5.9) ▷ Calculation of the speedy and reliable route candidate

6: $\gamma_{\mathrm{th}} \leftarrow \gamma_{\mathrm{th}} - \eta$ ▷ Update of γ_{th}

using candidate_paths$(\cdot)$ (line 3), it selects the most reliable one as follows (line 5):

$$r_{i,j} = \underset{r \in \mathcal{R}_{i,j}^{k_{\max},\delta_{\max},\gamma_{\mathrm{th}}}}{\arg\max} f_{\mathrm{p}}(r). \tag{5.9}$$

Otherwise, if $\mathcal{R}_{i,j}^{k_{\max},\delta_{\max},\gamma_{\mathrm{th}}}$ is empty, it continues searching for the route candidates by setting $\gamma_{\mathrm{th}} = \gamma_{\mathrm{th}} - \eta$ (line 6). As a result, Algorithm 5 provides us with speedy and reliable route candidate $r_{i,j}$ between evacuee i and refuge j.

5.4. Numerical results

In this section, we evaluate the refuge assignment obtained by solving the two-step ILP, OP_{p} and OP_{d}, using the actual information.

5.4.1 Evaluation model

For the evaluation, we select Nagoya city in Japan because it provides us with the risk map where each road is annotated by the road blockage probability [23]. There are 263 school districts, each of which is the unit of evacuation planning [127]. We select Arako district from them by considering the high average road blockage probability. The green area in Fig. 5.2 shows the risk map of

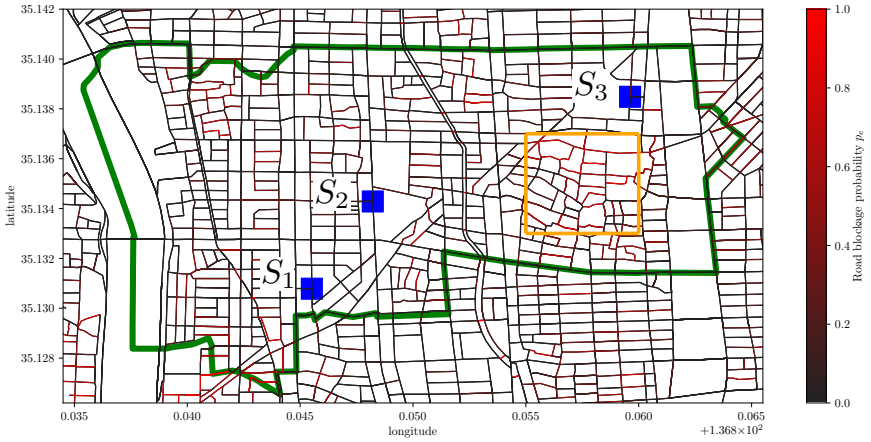

Figure 5.2. The map of Arako district covered by the green polygon (2.7 [km] × 1.9 [km]), the road blockage probability, and refuges $\mathcal{D} = \{S_1, S_2, S_3\}$. The orange area contains the roads with high road blockage probabilities.

2.7 [km] × 1.9 [km] Arako district. This map's internal graph structure is composed of 801 vertices and 1,220 edges.

As for the disaster scenario, Nagoya city provides us with the information of the road blockage probabilities for several classes depending on the degree of damages. In this thesis, we use the data of maximum class that consider Nankai megathrust earthquake. Each road in Fig. 5.2 is colored according to the road blockage probability: red (resp. black) means high (resp. low) road blockage probability. The average road blockage probability among all roads is 0.151. The orange area in Fig. 5.2 contains the roads with high road blockage probability, i.e., the average road blockage probability in this area is 0.278. We also show the three actual refuges $D = \{S_1, S_2, S_3\}$ as blue points in Fig. 5.2, according to [128]. The capacity of each refuge is given as C_{S_1} =11,500, C_{S_2} =1,964, and C_{S_3} =8,000.

There are 23,156 residents in Arako district [129] and the geographical distribution of residents is shown in Fig. 5.3. We confirm that the three refuges cannot accommodate all the residents, i.e., $\sum_{j\in\mathcal{D}} C_j$ =21,464 < 23,156. In what follows, we set β to be 0.7 as an example scenario where some of the residents stay their home or workplace even under the emergency.

For comparison purpose, we use the three schemes depending on the combi-

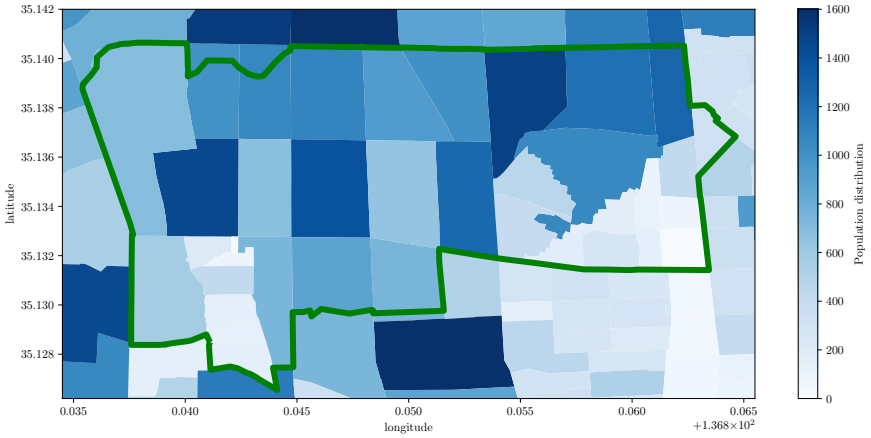

Figure 5.3. Geographical distribution of residents [persons] in Arako district covered by the green polygon (2.7 [km] × 1.9 [km]).

Table 5.2. Schemes for evaluation.

Scheme	Refuge Assignment	Route Selection
Distance-based scheme	OP_{d} without (5.8)	Shortest path selection
Proposed scheme	OP_{p} and OP_{d}	speedy_reliable_path()
Proposed scheme without capacity constraint	OP_{p} and OP_{d} without (5.6)	speedy_reliable_path()

nation of the refuge assignment and the route selection, as shown in Table 5.2. The distance-based scheme only considers the minimization of the average route length among evacuees, which can be obtained by solving a modified version of ILP OP_{d} where constraint (5.8) is removed.

We use two kinds of criteria. The first one is the average route length, $\overline{f}_{\mathrm{d}}$, to evaluate the speediness of the evacuation, which corresponds to the objective function (5.7). The second one is the average route reliability, $\overline{f}_{\mathrm{p}}$, which is related to the objective function (5.3).

$$\overline{f}_{\mathrm{d}} = N^{-1} \sum_{i \in \mathcal{N}} \sum_{j \in \mathcal{D}} f_{\mathrm{d}}(r_{i,j}) x_{i,j}, \quad \overline{f}_{\mathrm{p}} = N^{-1} \sum_{i \in \mathcal{N}} \sum_{j \in \mathcal{D}} f_{\mathrm{p}}(r_{i,j}) x_{i,j}.$$

In what follows, we show the average of ten independent numerical results, each of which has different initial locations of evacuees. Through preliminary experiments, we set the parameters for the route selection as follows: $k_{\max} = 5{,}000$, $\delta_{\max} = 300$, and $\eta = 0.1$.

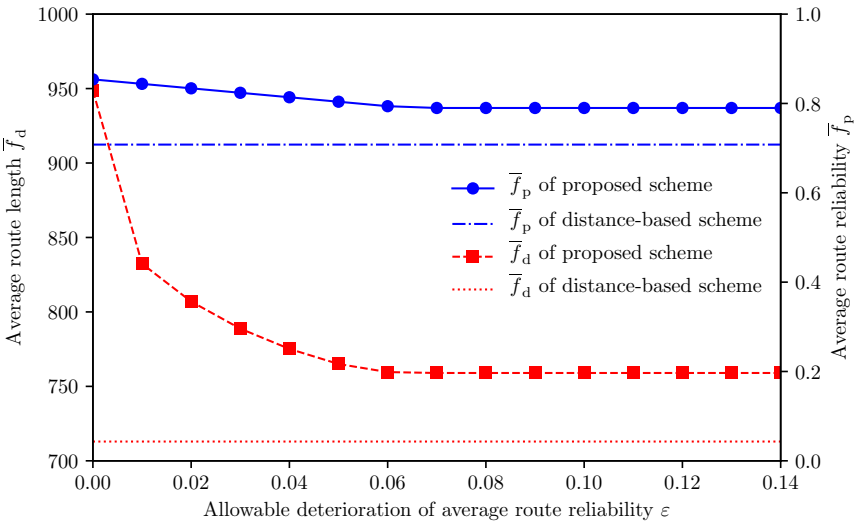

Figure 5.4. Impact of ε on $\overline{f}_{\mathrm{d}}$ and $\overline{f}_{\mathrm{p}}$ ($\beta = 0.7$).

5.4.2 Analysis of trade-off between speediness and safety under capacity constraint

In this subsection, we show the performance of the proposed scheme compared with the distance-based scheme under the capacity constraint. Fig. 5.4 illustrates how the allowable deterioration of average route reliability ε affects the average route length $\overline{f}_{\mathrm{d}}$ and average route reliability $\overline{f}_{\mathrm{p}}$ in case of relatively large evacuation demand, i.e., $\beta = 0.7$. We first focus on the performance of the proposed scheme. Since small (resp. large) ε places emphasis on the average route reliability (resp. average route length), we observe that $\overline{f}_{\mathrm{p}}$ and $\overline{f}_{\mathrm{d}}$ of the proposed scheme decrease with increase in ε. We observe that $\varepsilon = 0.05$ is one of the appropriate parameter settings in terms of both speedy and reliable evacuation. In particular, the proposed scheme can improve $\overline{f}_{\mathrm{p}}$ by 13.6% with 7.3% increase of $\overline{f}_{\mathrm{d}}$, compared with the distance-based scheme. In what follows, we set ε to be 0.05. In actual cases, the value of ε may also be affected by other factors, e.g., political judgment.

Next, we focus on the obtained refuge assignment. Figs. 5.5 and 5.6 illustrate the refuge assignment of the distance-based scheme and that of the proposed scheme, respectively. Recall that the orange area in Fig. 5.2 contains the roads

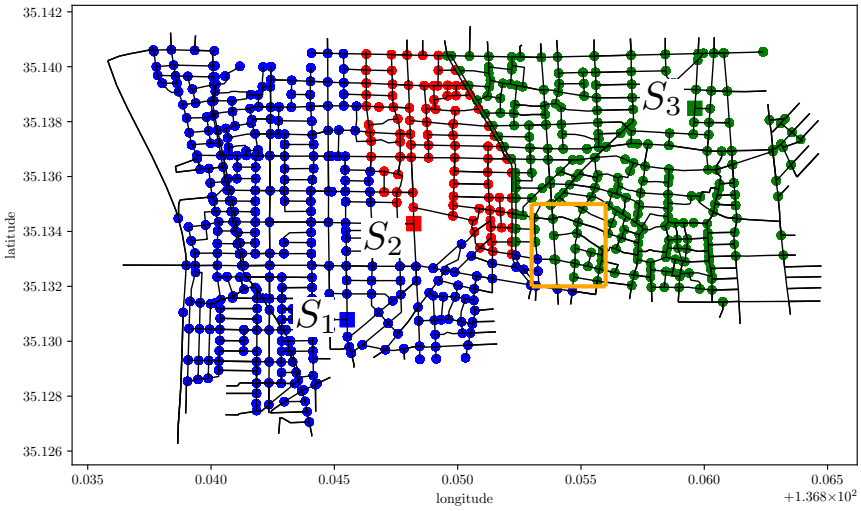

Figure 5.5. Refuge assignment of distance-based scheme ($\beta = 0.7$).

with high road blockage probability, i.e., the average road blockage probability in this area is 0.278. In the orange area of Fig. 5.5, some evacuees assigned to S_3 are forced to pass through the area with high road blockage probability. Comparing the orange areas in Figs. 5.5 and 5.6, we confirm that the proposed scheme can reduce such unsafe evacuation by assigning them to S_1.

To deeply analyze the characteristics of the proposed scheme, we further show the detailed results per refuge. Figs. 5.7 to 5.9 illustrate how ε affects the number of allocated evacuees, $\overline{f}_{\mathrm{d}}$, and $\overline{f}_{\mathrm{p}}$, per refuge, respectively. We first focus on refuge S_2. We observe that $\overline{f}_{\mathrm{d}}$ decreases with ε while keeping the number of allocated evacuees, due to the capacity limit (5.6). Specifically, we confirm that $\overline{f}_{\mathrm{d}}$ of S_2 can improve by 35.9%, i.e., 392.0 [m], by comparing the result of $\varepsilon = 0$ with that of $\varepsilon = 0.05$. This result means that evacuees near refuge S_2 are assigned to S_2 by the relaxation of the constraint (5.8). On the contrary, we observe that $\overline{f}_{\mathrm{p}}$ of S_2 increases with ε, which indicates that part of evacuees cannot be assigned to their appropriate refuges, due to the capacity limit (5.6) in case of $\varepsilon = 0$. We will describe the details of this result in Section 5.4.3.

Finally, we focus on refuges S_1 and S_3. We confirm that $\overline{f}_{\mathrm{d}}$ of S_1 and the number of allocated evacuees of S_1 decrease with ε. This phenomenon can be explained as follows. At first, evacuees distant from S_1 are assigned to S_1 in

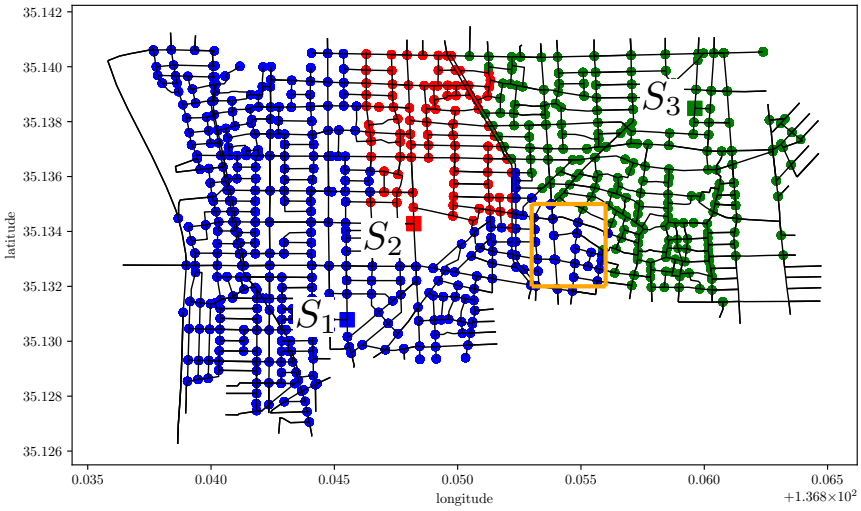

Figure 5.6. Refuge assignment of proposed scheme ($\beta = 0.7$).

case of $\varepsilon = 0$, to improve the average route reliability. By increasing ε, these evacuees can be assigned to nearer refuges, S_2 and S_3, but most of them can only be assigned to the refuge S_3, due to the limited capacity of S_2. As a result, the number of evacuees allocated to S_3 increases with ε. This forces some of them to pass through the area with high road blockage probability, and thus $\overline{f}_{\mathrm{p}}$ of S_3 decreases with ε.

5.4.3 Impact of capacity limit on speedy and reliable evacuation

In this subsection, we examine the appropriate design for the refuge capacity by comparing the proposed scheme and that without the capacity constraint, which can be regarded as an ideal case.

Fig. 5.10 presents the refuge assignment of the proposed scheme without the capacity constraint when $\beta = 0.7$. Comparing Fig. 5.6 with Fig. 5.10, we first confirm that the proposed scheme without the capacity constraint assigns more evacuees to refuge S_2. This result indicates that the demand for the refuge S_2 significantly exceeds the current refuge capacity C_{S_2}.

Fig. 5.11 illustrates how the impact of β on $\overline{f}_{\mathrm{d}}$ and $\overline{f}_{\mathrm{p}}$ changes between the

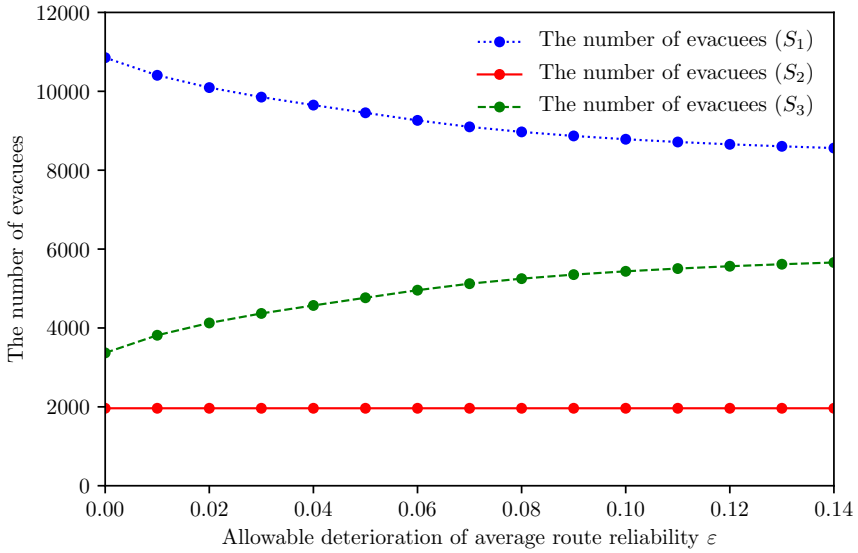

Figure 5.7. Relationship between ε and the number of allocated evacuees per refuge ($\beta = 0.7$).

proposed scheme and that without the capacity constraint. Fig. 5.12 shows the corresponding result per refuge. We observe that the proposed scheme increases $\overline{f}_{\mathrm{d}}$ by 6.5% compared with the proposed scheme without (5.6) when $\beta = 0.7$. This is because the capacity of refuge S_2 lacks 4,118 of the actual demand as shown in Fig. 5.12. In the proposed scheme, the overflow evacuees tend to be assigned to S_1, which has sufficient capacity and is located at relatively safe region. In Fig. 5.11, we also confirm that the proposed scheme keeps $\overline{f}_{\mathrm{p}}$ regardless of β, compared with the proposed scheme without the capacity constraint.

These results indicate that the current setting for refuge capacity should be reconsidered especially for refuge S_2. In other words, the proposed scheme can be used to a tool to calculate the required capacity of each refuge for speedy and reliable evacuation.

5.4.4 Discussion

At the last of this section, we briefly discuss the limit of the proposed scheme from the viewpoint of implementation in real-world context. The refuge assign-

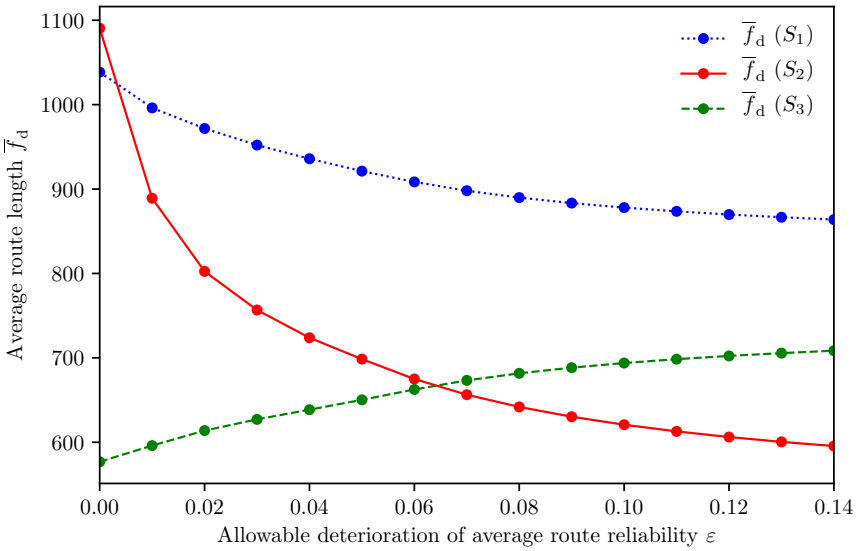

Figure 5.8. Relationship between ε and $\overline{f}_{\mathrm{d}}$ per refuge ($\beta = 0.7$).

ment based on the proposed scheme should be announced/advertised to evacuees before their evacuations. We expect that the cooperation with the mobile-cloud collaborative automatic evacuation guiding system [24] is one possible way. In this system, the mobile application of an evacuee can automatically estimate the actual road state (i.e., passable or blocked) during the evacuation, with the help of the implicit interactions with its owner. The estimated information will be shared with other mobile devices (evacuees) and cloud through the terrestrial communication networks (e.g., cellular networks and Wi-Fi) and/or D2D communication. These dynamically obtained information can be used to update the refuge assignment.

5.5. Summary

When a large-scale disaster occurs, each evacuee should move to an appropriate refuge in a speedy and safe manner. This can be achieved by the combination of both pre-disaster and post-disaster approaches. In this thesis, we have considered an earthquake case study and proposed a refuge assignment scheme that can support speedy and reliable evacuation under the refuge capacity constraint.

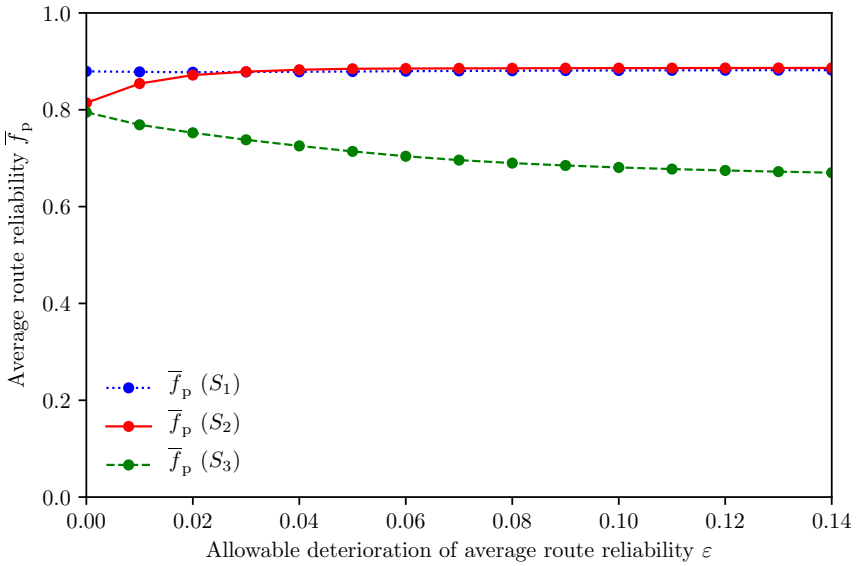

Figure 5.9. Relationship between ε and $\overline{f}_{\mathrm{p}}$ per refuge ($\beta = 0.7$).

Given route candidates between evacuees and their possible refuges, we have first formulated the refuge assignment problem as the two-step ILP, which minimizes the average route length while guaranteeing a certain level of the average route reliability under the constraint on the refuge capacity. As for the route candidates, we have further proposed a speedy and reliable route selection scheme that generates the input of the two-step ILP, i.e., route candidates between evacuees and their possible refuges.

Through numerical results using the actual data of Arako district of Nagoya city in Japan, representative results have shown that (1) the proposed scheme can control the balance between the evacuation speediness and reliability under the refuge capacity constraint by adjusting a control parameter and (2) the proposed scheme with the appropriate parameter setting can improve the average route reliability by 13.6% while suppressing the increase of the average route length by 7.3%, compared with the distance-based scheme. In addition, we have also revealed that the proposed scheme can be used as a tool to reconsider the current settings for the refuge capacity. In particular, we have demonstrated that the capacity of a certain refuge lacks 4,118 of the actual demands, which increases the average route length by 6.5%. In future work, we plan to conduct a comprehensive

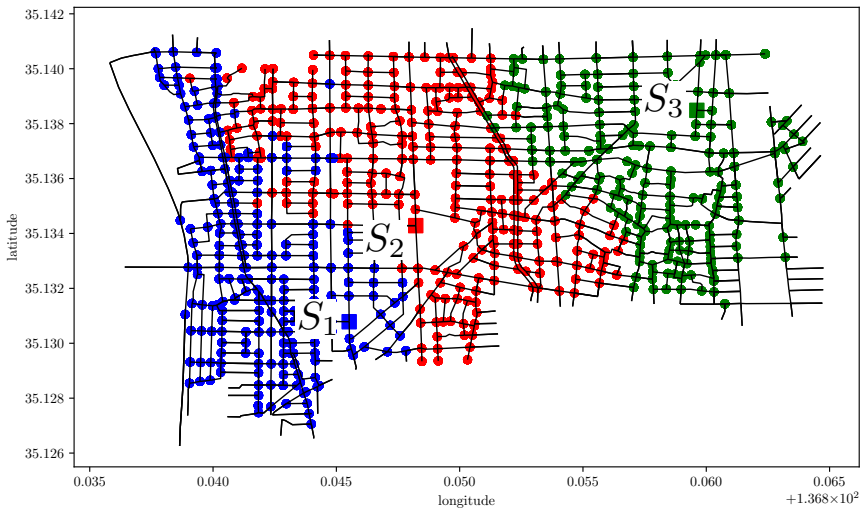

Figure 5.10. Refuge assignment of proposed scheme without capacity constraint.

survey of the potential risks in other districts of Nagoya city.

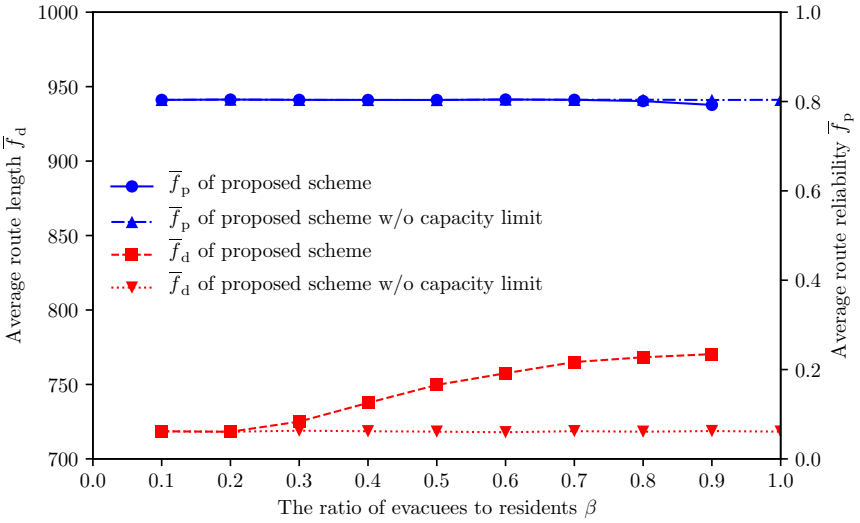

Figure 5.11. Impact of β on $\overline{f}_{\mathrm{d}}$ and $\overline{f}_{\mathrm{p}}$ (proposed scheme vs. proposed scheme without capacity limit).

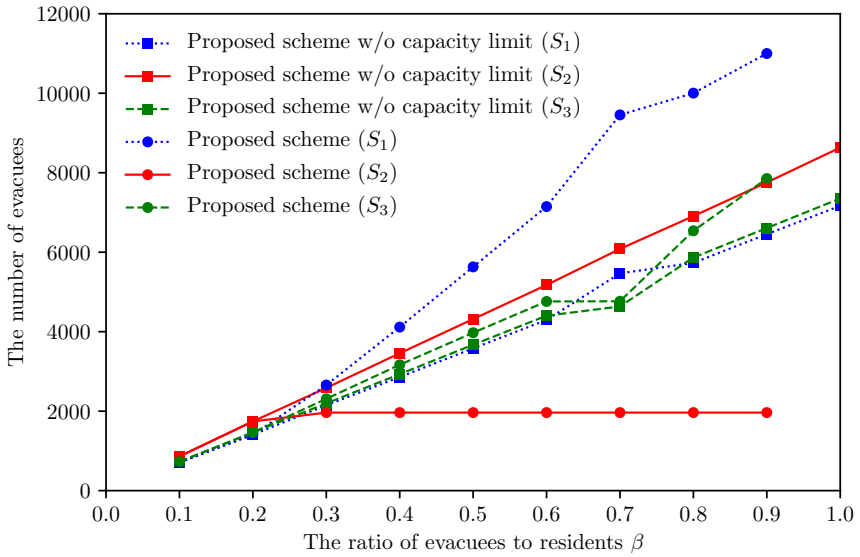

Figure 5.12. Impact of β on the number of allocated evacuees per refuge (proposed scheme vs. proposed scheme without capacity limit).

Chapter 6

Conclusion

6.1. Summary

In this thesis, focusing on the impact of the travel risk information on the user behavior, we have addressed the multi-agent routing leveraging the travel risk information to achieve the optimal crowd guidance under the ordinary or emergency situations, respectively.

Chapter 2 and Chapter 3 have focusd on the ordinary situations. In Chapter 2, we have focused on the travel congestion caused by the individual selfish routing in the ordinary situations. We have proposed the selfish yet optimal routing, which leads users to conduct the optimal routing under the rational decision making by internalizing the marginal cost into their perceiving information. Fundamental results through the numerical experiments under the grid-like road network have shown that (1) the proposed scheme exhibits almost the same performance as the optimal routing and (2) it improves the average travel time of 82% users by 0.77 [min] compared with the notification of the actual traffic information. In addition, we also have evaluated the practicality and scalability of the proposed scheme under the local-level and city-level road network. We have demonstrated that the proposed scheme improves the average travel time by 19.1% (resp. 7.4%), compared with the notification of the actual traffic information, in case of the local-level (resp. city-level) road network with 1,197 (resp. 10,004) users.

In Chapter 3, we have provided the multi-agent distributed route selection under the consideration of time-dependency among agents' road usage. Through

the numerical and simulation results, we have shown that the proposed scheme can estimate the travel time more accurately. Compared with the existing scheme, the proposed scheme can improve the actual travel time by 5.1% with help of the more accurate estimation under the consideration of time-dependency among agents while keeping the exponential convergence property.

Chapter 4 and Chapter 5 have focused on the evacuation under a large-scale disaster situation. In Chapter 4, we have proposed the geographical risk analysis based path selection scheme for the existing automatic evacuation guidance to achieve the speedy and reliable evacuation. Through simulation experiments, we have shown that the proposed scheme can improve the evacuation safety by 28.2% while keeping the evacuation time even under the severe communication environment. In addition, we have demonstrated how the proactive and reactive information affects the evacuation movement under the various communication environments. Specifically, the improvement of the evacuation safety is almost saturated when the coverage ratio of the communication infrastructure is only 30%.

Chapter 5 has presented the capacitated refuge assignment to achieve the speedy and reliable evacuation. We have considered the earthquake case study and formulated the refuge assignment problem as the two-step ILP, which minimizes the average route length while guaranteeing a certain level of the average route reliability under the constraint on the refuge capacity. As for the route candidates, we have further proposed a speedy and reliable route selection scheme that generates the input of the two-step ILP. Through numerical results using the actual data of Arako district of Nagoya city in Japan, we have shown that the proposed scheme can improve the average route reliability by 13.6% while suppressing the increase of the average route length by 7.3%, compared with the distance-based scheme. Furthermore, we have revealed the potential risks of mismatch between the geographical population distribution and the locations and capacities of refuges. Specifically, we have shown that the capacity of a certain refuge lacks 4,118 of the actual demands, which increases the average route length by 6.5%.

6.2. Future Perspective

6.2.1 Consideration of Uncertainty of Users' Decision Making

In Chapter 2, we have proposed the selfish yet optimal routing, which achieves the social optimum under the selfish/rational decision making of individual users. This scheme assumes that each user believes the traffic information notified by the server but some users might doubt whether the perceived traffic information is tweaked and defect the proposed system. This phenomenon tends to stem from the users' experiential information (EI).

In future work, we plan to extend the selfish yet optimal routing, which can cope with such uncertainty of users' decision making.

6.2.2 Robustness against Unexpected Evacuees' Behavior

In Chapter 4, we have shown the contribution of the reactive and proactive information to the evacuation movement. Recall that the reactive information, i.e., road state (passable/blocked), is automatically estimated by the evacuee's trajectory and its difference from the recommended route. This approach implicitly assumes that evacuees always follow the system guidance. Some evacuees, however, might (temporarily) defect from the guidance for their own purpose, e.g., visiting home/office. Such unexpected evacuees' behavior will result in misestimation of road state and dissemination of the wrong information might disturb evacuation guidance.

In future work, we first plan to investigate the impact of the existence of outlier evacuees on the system performance under the various communication environments. Furthermore, we will propose a scheme to detect outliers by analyzing the features of trajectories.

6.2.3 Personalized Guiding Considering Users' Attributes

In this thesis, we have basically assumed that all users are homogeneous. In actual situations, users can be distinguished according to their heterogeneous

attributes and route (and refuge) selection should be carefully considered according to their attributes. For example, healthy persons can select a route including stairs and/or slopes while elder and/or handicapped persons may have to search for a route as flat as possible. From the viewpoint of travel distance, such elder and/or handicapped persons may also have to find a refuge as near as possible in the evacuation situations. The attributes may also be related to the relationship with others. For instance, persons tend to move together with their family, friends, or colleagues. Since giving different route selection to the same group may cause confusion, group-based guidance will be required. These attributes can be registered to the proposed application in advance under the consideration of their privacy. In future work, we will extend the proposed schemes to support the personalized guiding.

Acknowledgements

Upon the the completion of this doctoral thesis, I would like to express my utmost gratitude to important people.

I would like to express my deepest appreciation to Prof. Shoji Kasahara, who is my supervisor, for his guidance and encouragement throughout my research period. I would like to extend my deepest gratitude to Associate Prof. Masahiro Sasabe, who is also my supervisor, for his guidance and encouragement during the whole period of my PhD course in Nara Institute of Science and Technology (NAIST). I have learnt a lot of important things from him including academic thinking, technical writing, how to proceed with a research project, and education. Their kindness and academic ability encourage me not only in my study but also in my future work.

I would like to express my appreciation to Associate Prof. Jun Kawahara from Kyoto University and Assistant Prof. Yuanyu Zhang. I would like to grateful to the laboratory secretary, Ms. Yoko Hashimoto, who support my research and work in the laboratory during my research period. I would also like to thank Ms. Hideko Hayashi who is a secretary of intelligent system control laboratory, for their various supports. I would also like to thank all the member of Large-Scale Systems Management Laboratory.

I would like to thank my parents for their kind support.

This research was partly supported by Grant-in-Aid for the JSPS Research Fellow under Grant JP20J11108.

The part of Chapter 4 is reprinted by permission from Springer Nature Customer Service Centre GmbH: Springer, Journal of Ambient Intelligence and Humanized Computing, "Geographical Risk Analysis Based Path Selection for Automatic, Speedy, and Reliable Evacuation Guiding Using Evacuees' Mobile Devices," T. Hara, M. Sasabe, and S. Kasahara, 2019, and Springer, Lecture Notes in Computer Science, "Short and Reliable Path Selection for Automatic Evacuation Guiding Based on Interactions Between Evacuees and Their Mobile Devices," T. Hara, M. Sasabe, and S. Kasahara, 2017.

List of Publication

Journal Papers

- M. Sasabe and T. Hara. "Capacitated Shortest Path Tour Problem Based Integer Linear Programming for Service Chaining and Function Placement in NFV Networks," to appear in IEEE Transactions on Network and Service Management, pp.1-14, March 2021.
- T. Hara, M. Sasabe, and S. Kasahara, "Selfish yet Optimal Routing by Adjusting Perceived Traffic Information of Road Networks," IEEE Open Journal of Intelligent Transportation Systems, vol. 1, pp. 120–133, 2020.
- T. Hara, M. Sasabe, T. Matsuda, and S. Kasahara, "Capacitated Refuge Assignment for Speedy and Reliable Evacuation," ISPRS International Journal of Geo-Information, vol. 9, no. 7, p. 442: 1–19, Jul. 2020.
- T. Hara, M. Sasabe, and S. Kasahara, "Geographical Risk Analysis Based Path Selection for Automatic, Speedy, and Reliable Evacuation Guiding Using Evacuees' Mobile Devices," Journal of Ambient Intelligence and Humanized Computing, vol. 10, no. 6, pp. 2291–2300, Jun. 2019.

Conference Papers

- T. Hara, M. Sasabe, and S. Kasahara, "Distributed Route Selection under Consideration of Time Dependency among Agents' Road Usage for Vehicular Networks," in Proc. of the International Conference on Emerging Technologies for Communications, Dec. 2020, pp. 1–4.
- H. Shimizu, T. Hara, T. Iwata, "Deep Reinforcement Learning for Pedestrian Guidance", in Proc. of the 23rd International Conference on Principles and Practice of Multi-Agent Systems (PRIMA 2020), Nov. 2020, pp 1–8.
- M. Sasabe and T. Hara, "Shortest Path Tour Problem Based Integer Linear Programming for Service Chaining in NFV Networks", in Proc. of 6th IEEE Conference on Network Softwarization (NetSoft), June 2020, pp. 114–121.

- T. Hara, M. Sasabe, and S. Kasahara, "Short and Reliable Path Selection for Automatic Evacuation Guiding Based on Interactions Between Evacuees and Their Mobile Devices," in Proc. of Mobile Web and Intelligent Information Systems, ser. Lecture Notes in Computer Science, M. Younas, I. Awan, and I. Holubova, Eds. Cham: Springer International Publishing, Aug. 2017, pp. 33–44.

Domestic Conference

- 大谷珠有, 原崇徳, 笹部昌弘, 笠原正治, "距離制約付き迂回可能性を含む経路の到達可能性に関する検討," 信学技報, vol. 120, no. 258, CQ2020-49, pp. 10-15, 2020 年 11 月.
- 原崇徳, 笹部昌弘, 笠原正治, "地理リスク情報を考慮した自動避難誘導アプリケーションの設計・実装," 信学技報, vol. 119, no. 367, CQ2019-113, pp. 35-40, 2020 年 1 月.
- 原崇徳, 笹部昌弘, 笠原正治, "道路網におけるトラヒック情報制御による利己的最適ルーティング (Invited Lecture)," 信学技報 RISING 研究会, 2019 年 11 月. (ポスター発表)
- 原崇徳, 清水仁, 岩田具治, "人流誘導のための深層強化学習の報酬設計", 第 22 回情報論的学習理論ワークショップ, 2019.11. (ポスター発表)
- 松田大樹, 原崇徳, 笹部昌弘, 笠原正治, "モバイル・エッジ連携型自動避難誘導における迅速性・安全性・避難所容量を考慮した避難所選択方式," 信学技報, vol. 118, no. 395, CQ2018-86, pp. 59-64, 2019 年 1 月.
- 原崇徳, 笹部昌弘, 笠原正治, "道路網におけるユーザの利己性を考慮した最適ルーティングのためのトラヒック情報制御方式 (Encouragement Talk)," 信学技報, vol. 118, no. 371, NS2018-160, pp. 23-28, 2018 年 12 月. (若手研究奨励賞)
- 原崇徳, 笹部昌弘, 笠原正治, "道路網におけるユーザの寛容性と情報共有が分散型経路選択方式に与える影響," 信学技報, vol. 118, no. 38, NS2018-26, pp. 63-68, 2018 年 5 月.

- 原崇徳, 笹部昌弘, 笠原正治, “道路網におけるユーザの利己的行動と情報共有が分散型経路選択方式に与える影響,” 信学技報, vol. 118, no. 8, CQ2018-11, pp. 59-64, 2018 年 4 月.
- 原崇徳, 笹部昌弘, 笠原正治, “道路網におけるユーザの利己的行動と通信環境が分散型経路選択方式に与える影響 (Poster Presentation),” 第 5 回コミュニケーションクオリティ基礎講座ワークショップ, 2018 年 1 月. (ポスター発表, 最優秀研究賞)
- 原崇徳, 笹部昌弘, 笠原正治, “避難者・モバイル端末間連携型自動避難誘導における経路の長さと信頼性を考慮した避難経路選択方式に関する一検討,” 信学技報, vol. 116, no. 484, NS2016-247, pp. 517-522, 2017 年 3 月.
- 大谷珠有, 原崇徳, 笹部昌弘, 笠原正治, “距離制約付き迂回路を含む経路の到達可能性に関する一検討” 電子情報通信学会ソサイエティ大会, 2020.9.
- 松田大樹, 原崇徳, 笹部昌弘, 笠原正治, “モバイル・エッジ連携型自動避難誘導における迅速性・安全性・避難所容量を考慮した避難所選択方式に関する一検討,” 電子情報通信学会ソサイエティ大会, 2018.9.
- 原崇徳, 笹部昌弘, 笠原正治, “道路網における情報共有とユーザの利己的行動が分散型経路選択方式に与える影響に関する一検討,” 電子情報通信学会総合大会, 2018.3.
- 原崇徳, 笹部昌弘, 笠原正治, “避難者・モバイル端末間連携型自動避難誘導における避難経路選択方式に関する一検討,” 電子情報通信学会総合大会, 2017.3.

Awards

- ICETC, Best Paper Award, 2020
- NS 研究会, 若手研究奨励賞, 2018
- 第 5 回コミュニケーションクオリティ基礎講座ワークショップ 最優秀研究賞, 2018

References

[1] Japan Digital Road Map Association, "DRM–JAPAN DIGITAL ROAD MAP ASSOCIATION," http://www.drm.jp/english/drm/e_index.htm, Accessed 14 Jan. 2021.

[2] University of Tokyo Center for Spatial Information Science People Flow Project, "People Flow Project," http://pflow.csis.u-tokyo.ac.jp/home/, Accessed 14 Jan. 2021.

[3] Y. Sekimoto, R. Shibasaki, H. Kanasugi, T. Usui, and Y. Shimazaki, "PFlow: Reconstructing People Flow Recycling Large-Scale Social Survey Data," *IEEE Pervasive Computing*, vol. 10, no. 4, pp. 27–35, Apr. 2011.

[4] A. Maimaris and G. Papageorgiou, "A Review of Intelligent Transportation Systems from a Communications Technology Perspective," in *Proc. of 2016 IEEE 19th International Conference on Intelligent Transportation Systems (ITSC)*, Nov. 2016, pp. 54–59.

[5] L. Zhu, F. R. Yu, Y. Wang, B. Ning, and T. Tang, "Big Data Analytics in Intelligent Transportation Systems: A Survey," *IEEE Transactions on Intelligent Transportation Systems*, vol. 20, no. 1, pp. 383–398, Jan. 2019.

[6] E. Avineri and J. N. Prashker, "The Impact of Travel Time Information on Travelers' Learning under Uncertainty," *Transportation*, vol. 33, no. 4, pp. 393–408, Jul. 2006.

[7] E. Ben-Elia, I. Erev, and Y. Shiftan, "The Combined Effect of Information and Experience on Drivers' Route-Choice Behavior," *Transportation*, vol. 35, no. 2, pp. 165–177, Mar. 2008.

[8] E. Ben-Elia and Y. Shiftan, "Which Road Do I Take? A Learning-Based Model of Route-Choice Behavior with Real-Time Information," *Transportation Research Part A: Policy and Practice*, vol. 44, no. 4, pp. 249–264, May 2010.

[9] E. Ben-Elia and E. Avineri, "Response to Travel Information: A Behavioural Review," *Transport Reviews*, vol. 35, no. 3, pp. 352–377, May 2015.

[10] T. Roughgarden and É. Tardos, "How Bad is Selfish Routing?" *J. ACM*, vol. 49, no. 2, pp. 236–259, Mar. 2002.

[11] D. R. Parisi and C. O. Dorso, "Microscopic Dynamics of Pedestrian Evacuation," *Physica A: Statistical Mechanics and its Applications*, vol. 354, pp. 606–618, Aug. 2005.

[12] ——, "Morphological and Dynamical Aspects of the Room Evacuation Process," *Physica A: Statistical Mechanics and its Applications*, vol. 385, no. 1, pp. 343–355, Nov. 2007.

[13] A. Desmet and E. Gelenbe, "Reactive and Proactive Congestion Management for Emergency Building Evacuation," in *Proc. of Annual IEEE Conference on Local Computer Networks*, Oct. 2013, pp. 727–730.

[14] Google, "Google Maps," http://maps.google.co.jp, Accessed 14 Jan. 2021.

[15] Ministry of Land, Infrastructure and Transport, "System Overview of VICS (in Japanese)," http://www.mlit.go.jp/road/vics/vics/index.html, Accessed 2 July. 2018.

[16] B. Chen and H. H. Cheng, "A Review of the Applications of Agent Technology in Traffic and Transportation Systems," *IEEE Transactions on Intelligent Transportation Systems*, vol. 11, no. 2, pp. 485–497, Jun. 2010.

[17] F.-Y. Wang, "Parallel Control and Management for Intelligent Transportation Systems: Concepts, Architectures, and Applications," *IEEE Transactions on Intelligent Transportation Systems*, vol. 11, no. 3, pp. 630–638, Sep. 2010.

[18] A. L. C. Bazzan and F. Klügl, "A Review on Agent-Based Technology for Traffic and Transportation," *The Knowledge Engineering Review*, vol. 29, no. 3, pp. 375–403, Jun. 2014.

[19] J. Zhang, F.-Y. Wang, K. Wang, W.-H. Lin, X. Xu, and C. Chen, "Data-Driven Intelligent Transportation Systems: A Survey," *IEEE Transactions on Intelligent Transportation Systems*, vol. 12, no. 4, pp. 1624–1639, Dec. 2011.

[20] R. H. Thaler and C. R. Sunstein, *Nudge: Improving Decisions about Health, Wealth, and Happiness*. New Haven, Conn: Yale University Press, 2008.

[21] D. Kahneman, *Thinking, Fast and Slow*. New York: Farrar, Straus and Giroux, 2011.

[22] S. Lim and D. Rus, "Congestion-Aware Multi-Agent Path Planning: Distributed Algorithm and Applications," *The Computer Journal*, vol. 57, no. 6, pp. 825–839, Jun. 2014.

[23] City of Nagoya, "Earthquake-Resistance City Development Policy (in Japanese)," http://www.city.nagoya.jp/jutakutoshi/cmsfiles/contents/0000002/2717/honpen.pdf, 2015, Accessed 14 Jan. 2021.

[24] N. Komatsu, M. Sasabe, J. Kawahara, and S. Kasahara, "Automatic Evacuation Guiding Scheme Based on Implicit Interactions between Evacuees and Their Mobile Nodes," *GeoInformatica*, vol. 22, no. 1, pp. 127–141, Jan. 2018.

[25] Road Bureau, Ministry of Land, Infrastructure, Transport and Tourism in Japan, "Performance Management of Road Administration in Japan (in Japanese)," http://www.mlit.go.jp/road/ir/ir-perform/h18/07.pdf, Accessed 14 Jan. 2021.

[26] Centre for Economics and Business Research, "The Future Economic and Environmental Costs of Gridlock in 2030," https://cebr.com/reports/the-future-economic-and-environmental-costs-of-gridlock/, Accessed 14 Jan. 2021.

[27] R. Johari and J. Tsitsiklis, "Network Resource Allocation and a Congestion Game: The Single Link Case," in *Proc. of IEEE International Conference on Decision and Control (IEEE Cat. No.03CH37475)*, vol. 3, Dec. 2003, pp. 2112–2117 Vol.3.

[28] J. G. Wardrop, "Some Theoretical Aspects of Road Traffic Research," *Proceedings of the Institution of Civil Engineers*, vol. 1, no. 3, pp. 325–362, May 1952.

[29] J. Zheng and D. Boyce, "Comparison of User-Equilibrium and System-Optimal Route Flow Solutions Under Increasing Traffic Congestion," in *Proc. of Transportation Research Board 90th Annual MeetingTransportation Research Board*, Washington, DC, USA,, 2011, pp. 1–16.

[30] E. Koutsoupias and C. Papadimitriou, "Worst-Case Equilibria," in *Proc. of STACS 99*, ser. Lecture Notes in Computer Science, C. Meinel and S. Tison, Eds. Berlin, Heidelberg: Springer, 1999, pp. 404–413.

[31] J. Aslam, S. Lim, and D. Rus, "Congestion-Aware Traffic Routing System Using Sensor Data," in *Proc. of International IEEE Conference on Intelligent Transportation Systems*. Anchorage, AK, USA: IEEE, Sep. 2012, pp. 1006–1013.

[32] E. Altman, T. Boulogne, R. El-Azouzi, T. Jiménez, and L. Wynter, "A Survey on Networking Games in Telecommunications," *Computers & Operations Research*, vol. 33, no. 2, pp. 286–311, Feb. 2006.

[33] Y. Korilis, A. Lazar, and A. Orda, "Achieving Network Optima Using Stackelberg Routing Strategies," *IEEE/ACM Transactions on Networking*, vol. 5, no. 1, pp. 161–173, Feb./1997.

[34] T. Roughgarden, "Stackelberg Scheduling Strategies," in *Proc. of Annual ACM Symposium on Theory of Computing*, ser. STOC '01. New York, NY, USA: Association for Computing Machinery, Jul. 2001, pp. 104–113.

[35] H. Yang, X. Zhang, and Q. Meng, "Stackelberg Games and Multiple Equilibrium Behaviors on Networks," *Transportation Research Part B: Methodological*, vol. 41, no. 8, pp. 841–861, Oct. 2007.

[36] N. Groot, B. De Schutter, and H. Hellendoorn, "Dynamic Optimal Routing Based on a Reverse Stackelberg Game Approach," in *Proc. of International IEEE Conference on Intelligent Transportation Systems*, Sep. 2012, pp. 782–787.

[37] A. de Palma and R. Lindsey, "Traffic Congestion Pricing Methodologies and Technologies," *Transportation Research Part C: Emerging Technologies*, vol. 19, no. 6, pp. 1377–1399, Dec. 2011.

[38] R. Cole, Y. Dodis, and T. Roughgarden, "Pricing Network Edges for Heterogeneous Selfish Users," in *Proc. of Annual ACM Symposium on Theory of Computing*, ser. STOC '03. New York, NY, USA: Association for Computing Machinery, Jun. 2003, pp. 521–530.

[39] T. Litman, *London Congestion Pricing – Implications for Other Cities.* Victoria, BC, Canada.: Victoria Transport Policy Institute, 2005.

[40] F. H. Administration, "Lessons Learned From International Experience in Congestion Pricing," https://ops.fhwa.dot.gov/publications/fhwahop08047/02summ.htm, Accessed 14 Jan. 2021.

[41] J. Eliasson, "The Stockholm Congestion Charges: An Overview," Tech. Rep., 2014.

[42] K. Staňková, G. J. Olsder, and M. C. J. Bliemer, "Comparison of Different Toll Policies in the Dynamic Second-Best Optimal Toll Design Problem: Case study on a Three-Link Network," *European Journal of Transport and Infrastructure Research*, vol. 9, no. 4, Sep. 2009.

[43] D. Joksimovic, M. Bliemer, P. Bovy, and Z. Verwater-Lukszo, "Dynamic Road Pricing for Optimizing Network Performance with Heterogeneous Users," in *Proc. of IEEE Networking, Sensing and Control, 2005.*, Mar. 2005, pp. 407–412.

[44] A. L. C. Bazzan and R. Junges, "Congestion Tolls as Utility Alignment between Agent and System Optimum," in *Proc. of International Joint Conference on Autonomous Agents and Multiagent Systems*, ser. AAMAS '06. Hakodate, Japan: Association for Computing Machinery, May 2006, pp. 126–128.

[45] B. Schaller, "New York City's Congestion Pricing Experience and Implications for Road Pricing Acceptance in the United States," *Transport Policy*, vol. 17, no. 4, pp. 266–273, Aug. 2010.

[46] J. Eliasson, "Lessons from the Stockholm Congestion Charging Trial," *Transport Policy*, vol. 15, no. 6, pp. 395–404, Nov. 2008.

[47] E. Ben-Elia, R. Di Pace, G. N. Bifulco, and Y. Shiftan, "The Impact of Travel Information's Accuracy on Route-Choice," *Transportation Research Part C: Emerging Technologies*, vol. 26, pp. 146–159, Jan. 2013.

[48] S. Wang, S. Djahel, Z. Zhang, and J. McManis, "Next Road Rerouting: A Multiagent System for Mitigating Unexpected Urban Traffic Congestion," *IEEE Transactions on Intelligent Transportation Systems*, vol. 17, no. 10, pp. 2888–2899, Oct. 2016.

[49] G. J. Olsder, "Phenomena in Inverse Stackelberg Games, Part 1: Static Problems," *Journal of Optimization Theory and Applications*, vol. 143, no. 3, pp. 589—-600, May 2009.

[50] Y.-C. Ho, P. B. Luh, and G. J. Olsder, "A Control-Theoretic View on Incentives," *Automatica*, vol. 18, no. 2, pp. 167–179, Mar. 1982.

[51] L. Bu, F. Wang, X. Zhou, and C. Yin, "Managed Gating Control Strategy for Emergency Evacuation," *Transportmetrica A: Transport Science*, vol. 15, no. 2, pp. 963–992, Nov. 2019.

[52] O. Jahn, R. H. Möhring, A. S. Schulz, and N. E. Stier-Moses, "System-Optimal Routing of Traffic Flows with User Constraints in Networks with Congestion," *Operations Research*, vol. 53, no. 4, pp. 600–616, Aug. 2005.

[53] E. Angelelli, V. Morandi, M. Savelsbergh, and M. G. Speranza, "System Optimal Routing of Traffic Flows with User Constraints Using Linear Programming," pp. 1–19, 2016.

[54] E. Angelelli, I. Arsik, V. Morandi, M. Savelsbergh, and M. Speranza, "Proactive Route Guidance to Avoid Congestion," *Transportation Research Part B: Methodological*, vol. 94, pp. 1–21, Dec. 2016.

[55] M. van Essen, T. Thomas, E. van Berkum, and C. Chorus, "From User Equilibrium to System Optimum: A Literature Review on the Role of

Travel Information, Bounded Rationality and Non-Selfish Behaviour at the Network and Individual Levels," *Transport Reviews*, vol. 36, no. 4, pp. 527–548, Jul. 2016.

[56] M. R. Hasan, A. L. C. Bazzan, E. Friedman, and A. Raja, "A Multiagent Solution to Overcome Selfish Routing in Transportation Networks," in *Proc. of International Conference on Intelligent Transportation Systems (ITSC)*, Nov. 2016, pp. 1850–1855.

[57] E. Ben-Elia, R. Ishaq, and Y. Shiftan, ""If only I Had Taken the Other Road...": Regret, Risk and Reinforced Learning in Informed Route-Choice," *Transportation*, vol. 40, no. 2, pp. 269–293, Feb. 2013.

[58] G. d. O. Ramos, A. L. Bazzan, and B. C. da Silva, "Analysing the Impact of Travel Information for Minimising the Regret of Route Choice," *Transportation Research Part C: Emerging Technologies*, vol. 88, pp. 257–271, Mar. 2018.

[59] N. Nisan, Ed., *Algorithmic Game Theory*, repr., [nachdr.] ed. Cambridge: Cambridge Univ. Press, 2008.

[60] S. Devarajan, "A Note of Network Equilibrium and Noncooperative Games," *Transportation Research Part B: Methodological*, vol. 15, no. 6, pp. 421–426, Dec. 1981.

[61] A. Orda, R. Rom, and N. Shimkin, "Competitive Routing in Multi-User Communication Networks," in *Proc. of IEEE INFOCOM '93 The Conference on Computer Communications*, Mar. 1993, pp. 964–971 vol.3.

[62] H. Bar-Gera and A. Luzon, "Differences among Route Flow Solutions for the User-Equilibrium Traffic Assignment Problem," *Journal of Transportation Engineering*, vol. 133, no. 4, pp. 232–239, Apr. 2007.

[63] Y. Sheffi, *Urban Transportation Networks: Equilibrium Analysis with Mathematical Programming Methods*. Englewood Cliffs, N.J: Prentice-Hall, 1984.

[64] Y. Sheffi and W. Powell, "A Comparison of Stochastic and Deterministic Traffic Assignment over Congested Networks," *Transportation Research Part B: Methodological*, vol. 15, no. 1, pp. 53–64, Feb. 1981.

[65] A. S. Schulz and N. E. Stier-Moses, "Efficiency and Fairness of System-Optimal Routing with User Constraints," *Networks*, vol. 48, no. 4, pp. 223–234, Dec. 2006.

[66] C. F. Daganzo, "Some Statistical Problems in Connection with Traffic Assignment," *Transportation Research*, vol. 11, no. 6, pp. 385–389, Dec. 1977.

[67] D. Watling, "A Second Order Stochastic Network Equilibrium Model, I: Theoretical Foundation," *Transportation Science*, vol. 36, no. 2, pp. 149–166, May 2002.

[68] C. F. Daganzo, "Stochastic Network Equilibrium with Multiple Vehicle Types and Asymmetric, Indefinite Link Cost Jacobians," *Transportation Science*, vol. 17, no. 3, pp. 282–300, Aug. 1983.

[69] H. Konishi, "Uniqueness of User Equilibrium in Transportation Networks with Heterogeneous Commuters," *Transportation Science*, vol. 38, no. 3, pp. 315–330, Aug. 2004.

[70] Roads, Bureau of Public, "Traffic Assignment Manual," US Department of Commerce, Washington, DC, 1964.

[71] J. R. Hauser, "Consideration-Set Heuristics," *Journal of Business Research*, vol. 67, no. 8, pp. 1688–1699, Aug. 2014.

[72] C. G. Prato and S. Bekhor, "Applying Branch-and-Bound Technique to Route Choice Set Generation," *Transportation Research Record*, vol. 1985, no. 1, pp. 19–28, Jan. 2006.

[73] P. H. L. Bovy, "On Modelling Route Choice Sets in Transportation Networks: A Synthesis," *Transport Reviews*, vol. 29, no. 1, pp. 43–68, Jan. 2009.

[74] S. Shelat, O. Cats, N. van Oort, and H. van Lint, "Calibrating Route Choice Sets for an Urban Public Transport Network using Smart Card Data," in *Proc. of International Conference on Models and Technologies for Intelligent Transportation Systems (MT-ITS)*, Jun. 2019, pp. 1–8.

[75] R. W. Rosenthal, "A Class of Games Possessing Pure-Strategy Nash Equilibria," *International Journal of Game Theory*, vol. 2, no. 1, pp. 65–67, Dec. 1973.

[76] L. R. Ford and D. R. Fulkerson, "Constructing Maximal Dynamic Flows from Static Flows," *Operations Research*, vol. 6, no. 3, pp. 419–433, Jun. 1958.

[77] L. R. Ford, *Flows in networks*. Princeton, N.J. Woodstock: Princeton University Press, 2010.

[78] L. Fleischer and M. Skutella, "Quickest Flows Over Time," *SIAM Journal on Computing*, vol. 36, no. 6, pp. 1600–1630, Jan. 2007.

[79] E. Köhler, K. Langkau, and M. Skutella, "Time-Expanded Graphs for Flow-Dependent Transit Times," in *Proc. of Algorithms — ESA 2002*, ser. Lecture Notes in Computer Science, R. Möhring and R. Raman, Eds. Springer Berlin Heidelberg, 2002, pp. 599–611.

[80] E. Anshelevich and S. Ukkusuri, "Equilibria in Dynamic Selfish Routing," in *Proc. of International Symposium on Algorithmic Game Theory*, ser. Lecture Notes in Computer Science, M. Mavronicolas and V. G. Papadopoulou, Eds. Berlin, Heidelberg: Springer, 2009, pp. 171–182.

[81] R. Koch and M. Skutella, "Nash Equilibria and the Price of Anarchy for Flows over Time," *Theory of Computing Systems*, vol. 49, no. 1, pp. 71–97, Jul. 2011.

[82] M. Hoefer, V. S. Mirrokni, H. Röglin, and S.-H. Teng, "Competitive Routing Over Time," *Theoretical Computer Science*, vol. 412, no. 39, pp. 5420–5432, Sep. 2011.

[83] M. Macko, K. Larson, and Ľ. Steskal, "Braess's Paradox for Flows over Time," *Theory of Computing Systems*, vol. 53, no. 1, pp. 86–106, Jul. 2013.

[84] U. Bhaskar, L. Fleischer, and E. Anshelevich, "A Stackelberg Strategy for Routing Flow Over Time," *Games and Economic Behavior*, vol. 92, pp. 232–247, Jul. 2015.

[85] X. Kong, Z. Xu, G. Shen, J. Wang, Q. Yang, and B. Zhang, "Urban Traffic Congestion Estimation and Prediction Based on Floating Car Trajectory Data," *Future Generation Computer Systems*, vol. 61, pp. 97–107, Aug. 2016.

[86] M. Fouladgar, M. Parchami, R. Elmasri, and A. Ghaderi, "Scalable Deep Traffic Flow Neural Networks for Urban Traffic Congestion Prediction," in *Proc. of International Joint Conference on Neural Networks (IJCNN)*, May 2017, pp. 2251–2258.

[87] B. Afshar-Nadjafi and A. Afshar-Nadjafi, "A Constructive Heuristic for Time-Dependent Multi-Depot Vehicle Routing Problem with Time-Windows and Heterogeneous Fleet," *Journal of King Saud University - Engineering Sciences*, vol. 29, no. 1, pp. 29–34, Jan. 2017.

[88] F. Rossi, R. Zhang, Y. Hindy, and M. Pavone, "Routing Autonomous Vehicles in Congested Transportation Networks: Structural Properties and Coordination Algorithms," *Autonomous Robots*, vol. 42, no. 7, pp. 1427–1442, Oct. 2018.

[89] Ministry of Internal Affairs and Communications, "2011 WHITE PAPER Information and Communications in Japan," http://www.soumu.go.jp/johotsusintokei/whitepaper/eng/WP2011/2011-index.html, 2011, Accessed 14 Jan. 2021.

[90] K. Fall, "A Delay-Tolerant Network Architecture for Challenged Internets," in *Proc. of the Conference on Applications, Technologies, Architectures, and Protocols for Computer Communications*. Association for Computing Machinery, 2003, pp. 27–34.

[91] Y. Iizuka, K. Yoshida, and K. Iizuka, "An Effective Disaster Evacuation Assist System Utilized by an Ad-Hoc Network," in *Proc. of HCI International 2011 – Posters' Extended Abstracts*, ser. Communications in Computer and Information Science, C. Stephanidis, Ed. Berlin, Heidelberg: Springer, 2011, pp. 31–35.

[92] A. Fujihara and H. Miwa, "Disaster Evacuation Guidance Using Opportunistic Communication: The Potential for Opportunity-Based Service," in *Big Data and Internet of Things: A Roadmap for Smart Environments*, ser. Studies in Computational Intelligence, N. Bessis and C. Dobre, Eds. Cham: Springer International Publishing, 2014, pp. 425–446.

[93] M. Zhou, H. Dong, P. A. Ioannou, Y. Zhao, and F.-Y. Wang, "Guided Crowd Evacuation: Approaches and Challenges," *IEEE/CAA Journal of Automatica Sinica*, vol. 6, no. 5, pp. 1081–1094, Sep. 2019.

[94] R. L. Church and T. J. Cova, "Mapping Evacuation Risk on Transportation Networks Using a Spatial Optimization Model," *Transportation Research Part C: Emerging Technologies*, vol. 8, no. 1, pp. 321–336, Feb. 2000.

[95] X. Chen, M.-P. Kwan, Q. Li, and J. Chen, "A Model for Evacuation Risk Assessment with Consideration of Pre- and Post-Disaster Factors," *Computers, Environment and Urban Systems*, vol. 36, no. 3, pp. 207–217, May 2012.

[96] Y. Iida, "Basic Concepts and Future Directions of Road Network Reliability Analysis," *Journal of Advanced Transportation*, vol. 33, no. 2, pp. 125–134, 1999.

[97] A. Chen, H. Yang, H. K. Lo, and W. H. Tang, "Capacity Reliability of a Road Network: An Assessment Methodology and Numerical Results," *Transportation Research Part B: Methodological*, vol. 36, no. 3, pp. 225–252, Mar. 2002.

[98] R. K. Ahuja, *Network Flows: Theory, Algorithms, and Applications*, 1st ed. Pearson Education, 2017.

[99] Q. Lu, B. George, and S. Shekhar, "Capacity Constrained Routing Algorithms for Evacuation Planning: A Summary of Results," in *Proc. of Advances in Spatial and Temporal Databases*, ser. Lecture Notes in Computer Science, C. Bauzer Medeiros, M. J. Egenhofer, and E. Bertino, Eds. Berlin, Heidelberg: Springer, 2005, pp. 291–307.

[100] Y. Yuan and D. Wang, "Path Selection Model and Algorithm for Emergency Logistics Management," *Computers & Industrial Engineering*, vol. 56, no. 3, pp. 1081–1094, Apr. 2009.

[101] M. Saadatseresht, A. Mansourian, and M. Taleai, "Evacuation Planning Using Multiobjective Evolutionary Optimization Approach," *European Journal of Operational Research*, vol. 198, no. 1, pp. 305–314, Oct. 2009.

[102] M. Dorigo, M. Birattari, and T. Stutzle, "Ant Colony Optimization," *IEEE Computational Intelligence Magazine*, vol. 1, no. 4, pp. 28–39, Nov. 2006.

[103] M. Haklay and P. Weber, "OpenStreetMap: User-Generated Street Maps," *IEEE Pervasive Computing*, vol. 7, no. 4, pp. 12–18, Oct. 2008.

[104] Ministry of Land, Infrastructure and Transport, "Cites Conducted the Person Trip Survey (PT) - Japan," http://www.mlit.go.jp/crd/tosiko/pt/map_e.html, Accessed 14 Jan. 2021.

[105] Y. Kasai, M. Sasabe, and S. Kasahara, "Congestion-Aware Route Selection in Automatic Evacuation Guiding based on Cooperation Between Evacuees and Their Mobile Nodes," *EURASIP Journal on Wireless Communications and Networking*, vol. 2017, no. 1, pp. 1–11, Oct. 2017.

[106] J. Y. Yen, "Finding the K Shortest Loopless Paths in a Network," *Management Science*, vol. 17, no. 11,, pp. 712–716, 1971.

[107] T. Akiba, T. Hayashi, N. Nori, Y. Iwata, and Y. Yoshida, "Efficient Top-k Shortest-Path Distance Queries on Large Networks by Pruned Landmark Labeling," in *Proc. of AAAI Conference on Artificial Intelligence*, ser. AAAI'15. Austin, Texas: AAAI Press, Jan. 2015, pp. 2–8.

[108] A. Keränen, J. Ott, and T. Kärkkäinen, "The ONE Simulator for DTN Protocol Evaluation," in *Proc. of International Conference on Simulation Tools and Techniques*, ser. Simutools '09. Rome, Italy: ICST (Institute for Computer Sciences, Social-Informatics and Telecommunications Engineering), Mar. 2009, pp. 1–10.

[109] S. Kongsomsaksakul, C. Yang, and A. Chen, "Shelter Location-Allocation Model for Flood Evacuation Planning," *Journal of the Eastern Asia Society for Transportation Studies*, vol. 6, pp. 4237–4252, 2005.

[110] J. Coutinho-Rodrigues, L. Tralhão, and L. Alçada-Almeida, "Solving a Location-Routing Problem with a Multiobjective Approach: The Design of Urban Evacuation Plans," *Journal of Transport Geography*, vol. 22, pp. 206–218, May 2012.

[111] J. Coutinho-Rodrigues, N. Sousa, and E. Natividade-Jesus, "Design of Evacuation Plans for Densely Urbanised City Centres," in *Proc. of the Institution of Civil Engineers - Municipal Engineer*, vol. 169, Sep. 2016, pp. 160–172.

[112] V. Bayram, B. Ç. Tansel, and H. Yaman, "Compromising System and User Interests in Shelter Location and Evacuation Planning," *Transportation Research Part B: Methodological*, vol. 72, pp. 146–163, Feb. 2015.

[113] F. Kılcı, B. Y. Kara, and B. Bozkaya, "Locating Temporary Shelter Areas after an Earthquake: A Case for Turkey," *European Journal of Operational Research*, vol. 243, no. 1, pp. 323–332, May 2015.

[114] J. Xu, X. Yin, D. Chen, J. An, and G. Nie, "Multi-Criteria Location Model of Earthquake Evacuation Shelters to Aid in Urban Planning," *International Journal of Disaster Risk Reduction*, vol. 20, pp. 51–62, Dec. 2016.

[115] M. Ng, J. Park, and S. T. Waller, "A Hybrid Bilevel Model for the Optimal Shelter Assignment in Emergency Evacuations," *Computer-Aided Civil and Infrastructure Engineering*, vol. 25, no. 8, pp. 547–556, Nov. 2010.

[116] V. Bayram, "Optimization Models for Large Scale Network Evacuation Planning and Management: A Literature Review," *Surveys in Operations Research and Management Science*, vol. 21, no. 2, pp. 63–84, Dec. 2016.

[117] M. Yusoff, J. Ariffin, and A. Mohamed, "Optimization Approaches for Macroscopic Emergency Evacuation Planning: A Survey," in *Proc. of International Symposium on Information Technology*, vol. 3, Aug. 2008, pp. 1–7.

[118] Y.-J. Zheng, S.-Y. Chen, and H.-F. Ling, "Evolutionary Optimization for Disaster Relief Operations: A Survey," *Applied Soft Computing*, vol. 27, pp. 553–566, Feb. 2015.

[119] D. Larsson, "Developing the Structure of a Fire Risk Index Method for Timber-frame Multistorey Apartment Buildings." *(2000)*, 2000.

[120] M. Sasabe, K. Fujii, and S. Kasahara, "Road Network Risk Analysis Considering People Flow Under Ordinary and Evacuation Situations," *Environment and Planning B: Urban Analytics and City Science*, pp. 759–774, Oct. 2018.

[121] Italian technical commission for seismic micro-zoning, *Handbook of analysis of emergency conditions in urban scenarios (manuale per l'analisi della condizione limite del- l'emergenza dell'insediamento urbano (CLE)).* Roma: CNR, Dipartimento sistemi di produzione, 2014.

[122] T. Hara, M. Sasabe, and S. Kasahara, "Geographical Risk Analysis Based Path Selection for Automatic, Speedy, and Reliable Evacuation Guiding Using Evacuees' Mobile Devices," *Journal of Ambient Intelligence and Humanized Computing*, vol. 10, no. 6, pp. 2291–2300, Jun. 2019.

[123] E. R. Galea, X. H, and P. J. Lawrence, "Experimental and Survey Studies on the Effectiveness of Dynamic Signage Systems," *Fire Safety Science*, vol. 11, pp. 1129–1143, 2014.

[124] H. Xie, L. Filippidis, E. R. Galea, D. Blackshields, and P. J. Lawrence, "Experimental Analysis of the Effectiveness of Emergency Signage and Its

Implementation in Evacuation Simulation," *Fire and Materials*, vol. 36, no. 5-6, pp. 367–382, 2012.

[125] R. Zhu, J. Lin, B. Becerik-Gerber, and N. Li, "Human-Building-Emergency Interactions and Their Impact on Emergency Response Performance: A Review of the State of the Art," *Safety Science*, vol. 127, pp. 1–19, Jul. 2020.

[126] ILOG, "IBM ILOG CPLEX Optimizer," https://www.ibm.com/products/ilog-cplex-optimization-studio, 2019, Accessed 14 Jan. 2021.

[127] MILT of Japan, "National Land Numerical Information Download Service: School District Data (in Japanese)," http://nlftp.mlit.go.jp/ksj/gml/datalist/KsjTmplt-A27-v2_1.html, 2010, Accessed 14 Jan. 2021.

[128] Aichi Prefecture, " Aichi Prefecture Regional Disaster Prevention Plan Annex (in Japanese) ," http://www.pref.aichi.jp/bousai/boukei/list-fuzoku.htm, 2017, Accessed 14 Jan. 2021.

[129] MIC of Japan, "e-Stat Portal Site of Official Statistics of Japan," https://www.e-stat.go.jp/en, 2008, Accessed 14 Jan. 2021.

[130] J. Fruin, *Designing for Pedestrians: A Level of Service Concept.* Polytechnic University of Brooklyn, 1970.

[131] A. Seyfried, B. Steffen, and T. Lippert, "Basics of Modelling the Pedestrian Flow," *Physica A: Statistical Mechanics and its Applications*, vol. 368, no. 1, pp. 232–238, Aug. 2006.

[132] M.-P. Kwan and D. M. Ransberger, "LiDAR Assisted Emergency Response: Detection of Transport Network Obstructions Caused by Major Disasters," *Computers, Environment and Urban Systems*, vol. 34, no. 3, pp. 179–188, May 2010.

[133] S. Santarelli, G. Bernardini, and E. Quagliarini, "Earthquake Building Debris Estimation in Historic City Centres: From Real World Data to Experimental-Based Criteria," *International Journal of Disaster Risk Reduction*, vol. 31, pp. 281–291, Oct. 2018.

[134] S. Santarelli, G. Bernardini, E. Quagliarini, and M. D'Orazio, "New Indices for the Existing City-Centers Streets Network Reliability and Availability Assessment in Earthquake Emergency," *International Journal of Architectural Heritage*, vol. 12, no. 2, pp. 153–168, Feb. 2018.

[135] E. Quagliarini, G. Bernardini, S. Santarelli, and M. Lucesoli, "Evacuation Paths in Historic City Centres: A Holistic Methodology for Assessing their Seismic Risk," *International Journal of Disaster Risk Reduction*, vol. 31, pp. 698–710, Oct. 2018.

[136] G. Bernardini, E. Quagliarini, and M. D'Orazio, "Towards Creating a Combined Database for Earthquake Pedestrians' Evacuation Models," *Safety Science*, vol. 82, pp. 77–94, Feb. 2016.

[137] H. Liu, B. Xu, D. Lu, and G. Zhang, "A Path Planning Approach for Crowd Evacuation in Buildings Based on Improved Artificial Bee Colony Algorithm," *Applied Soft Computing*, vol. 68, pp. 360–376, Jul. 2018.

[138] G. Bernardini, S. Santarelli, E. Quagliarini, and M. D'Orazio, "Dynamic Guidance Tool for a Safer Earthquake Pedestrian Evacuation in Urban Systems," *Computers, Environment and Urban Systems*, vol. 65, pp. 150–161, Sep. 2017.

[139] T. Sugiman and J. Misumi, "Development of a New Evacuation Method for Emergencies: Control of Collective Behavior by Emergent Small Groups," *Journal of Applied Psychology*, vol. 73, no. 1, pp. 3–10, 1988.

[140] Y. Ma, R. K. K. Yuen, and E. W. M. Lee, "Effective Leadership for Crowd Evacuation," *Physica A: Statistical Mechanics and its Applications*, vol. 450, pp. 333–341, May 2016.

[141] M. Ehrgott, *Multicriteria Optimization*. Springer Science & Business Media, 2005, vol. 491.

[142] V. Chankong and Y. Y. Haimes, *Multiobjective Decision Making: Theory and Methodology*. Courier Dover Publications, 2008.

[143] Y. H. YV, L. S. Lasdon, and D. A. Da Wismer, "On a Bicriterion Formulation of the Problems of Integrated System Identification and System Optimization," *IEEE Transactions on Systems, Man and Cybernetics*, no. 3, pp. 296–297, 1971.

[144] G. Mavrotas, "Effective implementation of the ϵ-constraint method in Multi-Objective Mathematical Programming problems," *Applied Mathematics and Computation*, vol. 213, no. 2, pp. 455–465, Jul. 2009.

[145] G. Mavrotas and K. Florios, "An Improved Version of the Augmented ϵ-constraint Method (AUGMECON2) for Finding the Exact Pareto Set in Multi-Objective Integer Programming Problems," *Applied Mathematics and Computation*, vol. 219, no. 18, pp. 9652–9669, May 2013.

[146] The Government of Japan, "Disaster Countermeasures Basic Act," http://www.japaneselawtranslation.go.jp/law/detail_main?re=02&vm=&id=3092, 1961, Accessed 25 Apr. 2019.

[147] R. I. Ansari, C. Chrysostomou, S. A. Hassan, M. Guizani, S. Mumtaz, J. Rodriguez, and J. J. P. C. Rodrigues, "5G D2D Networks: Techniques, Challenges, and Future Prospects," *IEEE Systems Journal*, vol. 12, no. 4, pp. 3970–3984, Dec. 2018.

[148] R. Santos, D. Mosse, T. Znati, and L. Comfort, "Design and Implementation of a Witness Unit for Opportunistic Routing in Tsunami Alert Scenarios," *Safety Science*, vol. 90, pp. 75–83, Dec. 2016.

[149] M. A. Quddus, W. Y. Ochieng, L. Zhao, and R. B. Noland, "A General Map Matching Algorithm for Transport Telematics Applications," *GPS Solutions*, vol. 7, no. 3, pp. 157–167, Dec. 2003.

[150] F. Usman, K. Murakami, A. D. Wicaksono, and E. Setiawan, "Application of Agent-Based Model Simulation for Tsunami Evacuation in Pacitan, Indonesia," *MATEC Web of Conferences*, vol. 97, pp. 1–16, 2017.